Function of constitutive IκB Kinase 2 activation in the intestinal epithelium of mice

Inaugural-Dissertation
zur
Erlangung des Doktorgrades
der Mathematisch-Naturwissenschaftlichen Fakultät
der Universität zu Köln

vorgelegt von
Katerina Vlantis
aus Mönchengladbach

Köln, 2010

Berichterstatter: Prof. Dr. Manolis Pasparakis
Prof. Dr. Thomas Langer

Tag der mündlichen Prüfung: 28.01.2011

Zusammenfassung

Die NF-κB Signalkaskade stellt eine Verbindung zwischen Entzündungsprozessen und Krebs dar. Der NF-κB Signalweg wird durch Stress-assoziierte Reize wie Pathogen-assoziierte Molekulare Muster (PAMPs), inflammatorische Zytokine und UV-Licht initiiert. Da die Aktivierung dieses Signalweges zur Expression von anti-apoptotischen Molekülen, inflammatorischen Signalkomponenten, sowie anti-bakteriellen Peptiden führt, stellt NF-κB einen zentralen Regulator von entzündlichen Prozessen dar. Darüber hinaus weisen verschiedene Krebsarten eine erhöhte NF-κB Aktivität auf, die sich nicht nur auf Tumor-infiltrierende Immunzellen beschränkt, sondern auch in den Krebszellen selber aufzufinden ist. Es wird vermutet, dass die Wirkung von NF-κB in Tumorzellen den Zelltod verhindert und die Zellproliferation fördert. Dahingegen induziert NF-κB in Zellen des Immunsystems die Sekretion von Zytokinen und Wachstumsfaktoren, wodurch Tumorwachstum und Angiogenese gefördert werden. Allerdings ist bisher nicht geklärt worden, ob die Aktivierung von NF-κB die Entstehung von Tumoren durch zellinterne Tumor-fördernde Wirkungen in nicht transformierten Zellen zu initiieren vermag. In dieser Arbeit wird gezeigt, dass die Expression einer konstitutiv aktiven Form der zur Aktivierung des kanonischen NF-κB Signalwegs notwendigen zentralen Kinase IKK2 (IKK2ca) in intestinalen Epithelzellen von Mäusen zu einer spontanen Entzündung sowohl des Dick- als auch des Dünndarms führte. Die konstitutive Aktivierung von IKK2/NF-κB im Darmepithel resultierte in einer Rekrutierung und Aktivierung von Immunzellen und Fibroblasten. Darüber hinaus erhöhte die Expression von IKK2ca im Darmepithel die Sensitivität gegenüber DSS-induzierter Colitis und steigerte die Tumorrate in chemisch- sowie Apc-Mutation-initiiertem Darmkrebs. Intestinale Epithelzellen, die konstitutiv aktive IKK2 exprimierten, zeigten eine erhöhte Proliferationsrate, eine Stabilisierung von β-catenin und eine verstärkte Transkription von Stammzell-assoziierten Faktoren. Hierbei ist zu betonen, dass die Expression von IKK2ca im Darmepithel von Mäusen zur spontanen Entwicklung von Colon- und Dünndarmtumoren führte. Die in dieser Dissertation vorgelegten Daten implizieren, dass die konstitutive Aktivierung von IKK2/NF-κB im Darmepithel ausreichend ist um sowohl durch zellinterne Faktoren, als auch durch die Erzeugung eines Tumor-förderlichen, entzündlichen Milieus, eine Tumorgenese nicht nur zu unterstützten, sondern auch zu induzieren.

Abstract

The NF-κB pathway has been proposed to provide a link between inflammation and carcinogenesis. NF-κB signalling is activated by various stress-associated stimuli such as pathogen associated molecular patterns (PAMPs), inflammatory cytokines and UV-light. Since NF-κB activation induces the expression of anti-apoptotic molecules, proinflammatory mediators and anti-microbial peptides, it is a central regulator of inflammatory processes. Moreover, various cancers exhibit increased activation of NF-κB, not only in tumour infiltrating immune cells, but also in cancer cells themselves. In tumour cells NF-κB is believed to act mainly to prevent tumour cell death and promote proliferation, whereas in immune cells NF-κB functions to induce secretion of cytokines and growth factors to sustain tumour growth and angiogenesis. However, so far it has not been addressed whether activation of NF-κB signalling is sufficient to initiate tumour development through cell-intrinsic tumour-promoting effects in pre-malignant cells. Here we show that expression of constitutively active IKK2, the central kinase inducing canonical NF-κB activation, specifically in intestinal epithelial cells of mice results in spontaneous inflammation of the colon and the small intestine. Constitutive activation of IKK2/NF-κB in the intestinal epithelium induced recruitment and activation of inflammatory cells and stromal fibroblasts. Furthermore, expression of IKK2ca in the intestinal epithelium rendered mice more susceptible to DSS-mediated colitis and strongly enhanced tumour development in chemically induced and Apc-mutation mediated tumourigenesis. IKK2ca-expressing IECs exhibited increased proliferative activity, stabilisation of β-catenin and elevated expression levels of stem cell associated factors. Importantly, expression of IKK2ca in intestinal epithelial cells was sufficient for spontaneous tumour development, both in the colon and the small intestine of aged mice.

Therefore results presented in this thesis imply that constitutive activation of IKK2/NF-κB in the intestinal epithelium is sufficient to promote and induce intestinal tumourigenesis through cell-intrinsic mechanisms, as well as through creating a tumour-promoting, inflammatory microenvironment.

Contents

Abbreviations

ABC	Avidin-Biotin-Complex
AOM	Azoxymethane
APC	Adenomatous Polyposis Coli
Ascl2	Achaete scute like 2
Bmi-1	polycomb ring finger oncogene
BSA	Bovine Serum Albumin
CAC	Colitis Associated Cancer
CD	Crohn´s Disease
cDNA	complementary DNA
CRC	Colorectal Cancer
Cre	Causes recombination
DAB	Diaminobenzidine
DAPI	4'-6-Diamidino-2-phenylindole
DLK1	Drosophila homolog delta like 1
DMEM	Dulbecco´s Modified Eagle Medium
DNA	Desoxyribonucleic acid
dNTPs	desoxyribonucleotides
DSS	Dextrane Sulfate Sodium
DTT	Dithiothreithol
ECL	Enhanced Chemiluminescence
EDTA	Ethylene Diamine Tetraacetate
eGFP	enhanced GFP
EMSA	Electrophoretic Mobility Shift Assay
FCS	Fetal Calf Serum
GFP	Green Fluorescent Protein
GI	Gastrointestinal Tract
H&E	Hematoxylin and Eosin
het	heterozygous
hom	homozygous
HRP	Horseradish peroxidase
IBD	Inflammatory Bowel Disease
IEC	Intestinal Epithelial Cell
IF	immunofluorescent

IHC	immunohistochemistry
I.p.	intraperitoneal
iκBα	Inhibitor of NF-κB alpha
IKK2	Inhibitor of κB Kinase 2
IKK2ca	Inhibitor of κB Kinase 2 constitutively active
IL	Interleukin
IRES	Internal Ribosomal Entry Site
IVC	Individual Ventilated Cages
l	liter
Lgr5	Leucine rich G-protein coupled receptor 5
LoxP	Locus of X-over P1
MEFs	Murine Embryonic Fiboblasts
MEICS	Mean Endoscopic Index of Colitis Severity
ml	milliliter
µl	microliter
MMP	Matrix Metalloprotease
mRNA	messenger RNA
NEMO	Nuclear Factor-kappa B essential modulator
NF-κB	Nuclear Factor-kappa B
NGS	Normal Goat Serum
NP-40	Nonident P40
Olfm4	Olfactomedin 4
PCR	Polymerase chain reaction
PBS	Phosphate-buffered saline
PFA	Paraformaldehyde
RNA	Ribonucleic Acid
ROS	Reactive Oxygen Species
rpm	rounds per minute
RT-PCR	Real-Time PCR
SDS	Sodium Dodecyl Sulfate
SI	Small Intestine
sFL	loxP flanked Stop cassette
α-SMA	alpha Smooth Muscle Actin
TA	Transit Amplifying
TBE	Tris Boric acid EDTA buffer

TBS	Tris buffered saline
TE	Tris EDTA buffer
Tg	transgenic
TLR	Toll-Like Receptor
TNF	Tumour Necrosis Factor
TNFR1	TNF Receptor 1 (p55)
TnfRsF19	TNF Receptor superfamily member 19
UC	Ulcerative colitis
v/v	volume per volume
vil	villin
WT	wild-type
w/v	weight per volume

1. Introduction

1.1 NF-κB signalling

The Rel/NF-κB family of transcription factors in mammals consists of five members: RelA or p65, RelB, c-Rel, p50 (NF-κB1) and p52 (NF-κB2) (Hayden and Ghosh, 2008). NF-κB molecules consist of a Rel-homology domain (RHD) situated at the N-terminus that is essential for formation of homo- and heterodimers and is required for DNA binding (Hayden and Ghosh, 2008). Nuclear NF-κB dimers bind to specific DNA consensus sites in the promoter regions of NF-κB target genes. p65, RelB and c-Rel posses a transcription activation domain (TAD) located in the C-terminal part of the protein and therefore homo- and heterodimers containing one of these family members can mediate transcriptional activation of NF-κB target genes (Hayden and Ghosh, 2008). In contrast, homodimers of p50 or p52 or dimers composed of a p50 and a p52 subunit are not able to activate transcription of NF-κB target genes and have instead been suggested to suppress target gene expression.

In unstimulated cells NF-κB target gene expression is prevented by proteins of the inhibitor of NF-κB (IκB) family consisting of IκBα, IκBβ and IκBε, BCL3, and IκBζ or IκBNS, as well as p100 and p105, which are precursor forms of p52 and p50, respectively (Hayden and Ghosh, 2008). Ankyrin repeats of IκBs mediate binding to NF-κB molecules, which masks the nuclear localisation signals (NLS) of NF-κB. This way, the IκBs prevent nuclear accumulation of NF-κB. In addition, IκBα contains a nuclear export signal (NES) that exports IκB-NF-κB complexes back into the cytoplasm (Hayden and Ghosh, 2008).

For NF-κB activation, IκBs have to be degraded to release NF-κB dimers and allow their nuclear accumulation. The activation of NF-κB is under control of the so-called IKK-complex, which is composed of two kinases, IκB kinase 1 (IKK1 or IKKα) and IκB kinase 2 (IKK2 or IKKβ) and the regulatory subunit NF-κB essential modulator (NEMO or IKKγ) (Hayden and Ghosh, 2008). The latter is devoid of kinase activity, but nevertheless is essential for the activation of the IKK-complex. IKKs phosphorylate IκBα on two particular serine residues, Ser32 and Ser36. This phosphorylation pattern generates a phospho-degron signal that marks IκBα for K48-linked polyubiquitination by the βTrCP-SCF complex and is followed by its proteasomal degradation (Hayden and Ghosh, 2008). Free NF-κB dimers are then

able to translocate to the nucleus, where they can induce transcription of NF-κB target genes.

Two distinct pathways for the activation of NF-κB have been described. The classical or canonical NF-κB pathway is triggered by inflammatory cytokines such as TNF and IL-1, by bacterial and viral products through Toll-like receptors (TLRs) and intracellular nucleotide-binding and oligomerization domain (NOD) like receptors (NLRs), by irradiation, reactive oxygen species (ROS) and other stress factors. The canonical pathway leads to nuclear translocation of NF-κB dimers mainly consisting of p65, p50 and c-Rel and subsequent activation of genes coding for proinflammatory cytokines and chemokines, adhesion molecules and anti-apoptotic proteins. The non-canonical or alternative NF-κB pathway induces the processing of p100 to p52 (Hayden and Ghosh, 2008). Alternative NF-κB signalling is mainly induced upon ligation of receptors belonging to the TNF receptor superfamily, such as the receptor for BAFF (B-cell activating factor belonging to the TNF family, Tnfsf13b) or lymphotoxin-β receptor (Vallabhapurapu and Karin, 2009). Induction of the alternative pathway also results in transcriptional upregulation of cytokines and chemokines but additionally controls the organisation of lymphoid tissues and the development and survival of lymphoid cells. Processing of p100 is induced by phosphorylation of two particular serine residues, Ser866 and Ser870, in the C-terminal part of the molecule. This processing of p100 requires NIK-mediated activation of IKK1 and occurs independently of IKK2 or NEMO (Hayden and Ghosh, 2008).

The generation of mice lacking specific subunits of the IKK-complex allowed investigation of the distinct functions of each individual IKK subunit (Pasparakis et al., 2006; Xiao et al., 2001). Studies with cells lacking NEMO showed that NEMO is indispensable for canonical NF-κB signalling and in the absence of this subunit no canonical NF-κB activation takes place. Similar experiments revealed that IKK2 is mainly responsible for activating NF-κB in the canonical pathway, though deletion of IKK2 does not completely block NF-κB activation. Residual NF-κB activity is mediated by IKK1, since the deletion of both kinases leads to complete blockade of NF-κB function, as it is the case in the absence of NEMO. IKK1 was shown to mediate phosphorylation of p100 at two particular serine residues in the C-terminal part of the protein, leading to its partial proteolysis, which gives rise to p52 (Xiao et al., 2001). Thus, while canonical NF-κB activation mainly depends on IKK2, non-canonical NF-κB activation depends solely on IKK1.

Depending on the NF-κB activating signal, different pathways are triggered and different upstream molecules are in charge for activating the IKK complex. IKK activation downstream of TNF stimulation will be described in further detail as an example of a signal transduction pathway leading to NF-κB activation. Upon ligation of TNF to TNFR1 the latter induces intracellular signalling cascades triggering programmed cell death (apoptosis) on the one hand but also the induction of the NF-κB pathway and the mitogen activated protein kinase (MAPK) pathways leading to activation of JNK, p38 and ERK on the other hand.

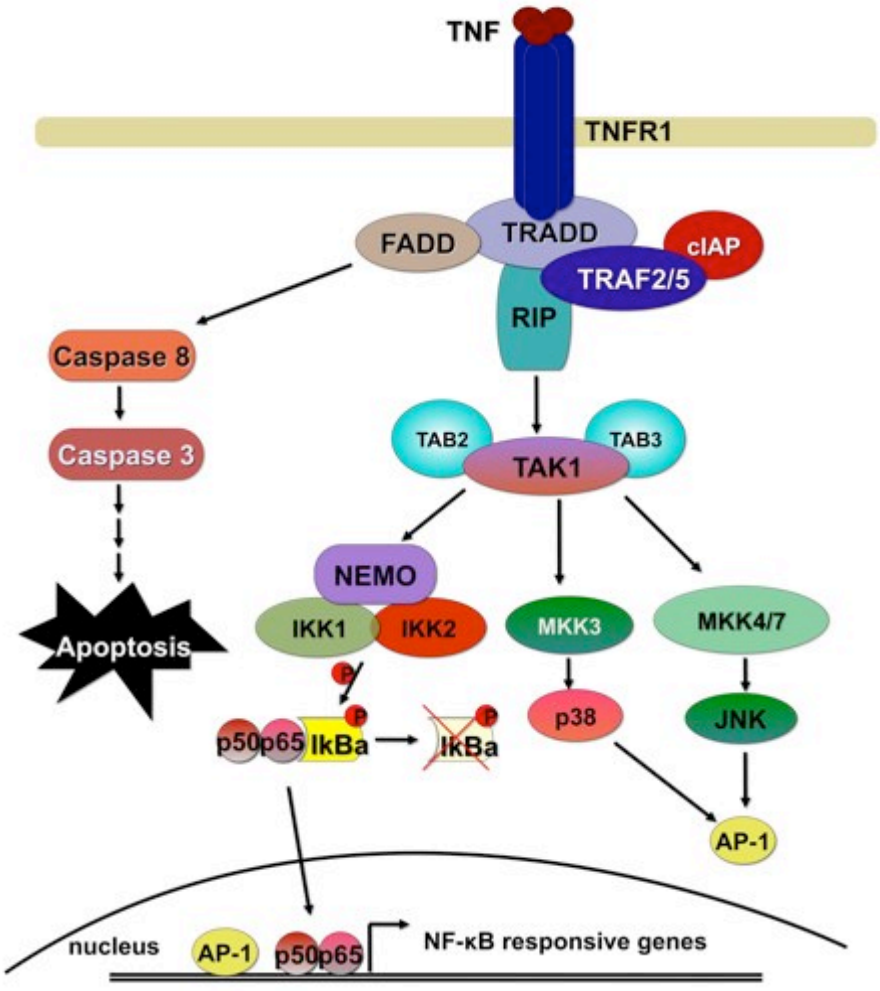

Figure 1 Activation of the NF-κB signalling cascade downstream of TNFR1
Upon ligation of TNF to TNFR1 adapter molecules are recruited to the cytoplasmic part of the receptor. Various ubiquitination and phosphorylation events result in activation of NF-κB and MAPK signalling and the subsequent upregulation of pro-inflammatory and anti-apoptotic molecules. In the absence of NF-κB and MAPK activation, TNF signalling results in apoptosis. For details see text.

Upon binding of TNF to TNFR1, a number of proteins required for the activation of the TNF-induced signalling cascade are recruited to the plasma membrane. Through its cytoplasmic protein-protein interaction domain named death domain (DD), the central adapter TNFR1-associated death domain (TRADD) protein is bound to the

receptor. Furthermore receptor interacting protein 1 (RIP1) kinase, TNF receptor associated factors TRAF2 and TRAF5, which are both endowed with ubiquitin ligase activity, as well as the cellular inhibitors of apoptosis cIAP1 and cIAP2 become part of this receptor-proximal signalling complex (Varfolomeev and Vucic, 2008; Vlantis and Pasparakis, 2010). Through the generation of knockout cells for these components of the TNF-signalling cascade it has been shown that TRADD, RIP1 and TRAF2/5 are important for robust activation of NF-κB downstream of TNFR1 (Ea et al., 2006; Ermolaeva et al., 2008; Tada et al., 2001).

Ligation of TNFR1 by TNF results in polyubiquitination of RIP1, establishing a platform for the recruitment and activation of kinase molecules required for the induction of NF-κB and MAPK pathways. Analysis of knockout cells has revealed that polyubiquitination of RIP1 depends on the ubiquitin ligases TRAF2 and TRAF5 (Tada et al., 2001). Furthermore cIAP1 and cIAP2 were shown to be important for signalling through TNFR1 (Varfolomeev et al., 2008). K63-linked polyubiquitination of RIP1 has turned out to be of major importance for the activation of TNF-induced signalling and the downstream activation of NF-κB and MAPK signalling (Adhikari et al., 2007; Ea et al., 2006). It has been suggested that these K63-linked polyubiquitin chains on RIP1 form a docking site for the so called TAK1 signalling complex composed of Transforming growth factor-β-activated kinase1 (TAK1) and the TAK binding proteins TAB1 and TAB2 (Ea et al., 2006). TAB1 and TAB2 are considered to be responsible for binding to ubiquitin chains of RIP1. Furthermore recruitment of the IKK-complex is also mediated by ubiquitinated RIP1 (Ea et al., 2006). TAK1 has been proposed to be responsible for phosphorylation and therefore activation of IKKs and upstream kinases of the MAPK pathway (Wang et al., 2001).

Though the described signalling model had found wide acceptance, a recent study showed that the lack of RIP1 did not prevent activation of NF-κB downstream of TNFR1, suggesting that RIP1 is not required for the activation of NF-κB (Wong et al., 2010). This raises the possibility that either the role of RIP1 is cell type specific or that other molecules can compensate for the loss of RIP1 and activate the downstream pathway.

1.2 The gastrointestinal tract and anatomy of the intestinal epithelium

The intestinal tract consists of the small intestine, composed of (from cranial to caudal) the duodenum, jejunum and ileum and is followed by the further distally located large intestine or colon. The main function of the small intestine is digestion of food and absorption of nutrients. In the colon, in addition to the nutrient absorption, water is reabsorbed from the faeces. Furthermore the intestine harbours a large number of immune cells and therefore represents a major part of the immune system.

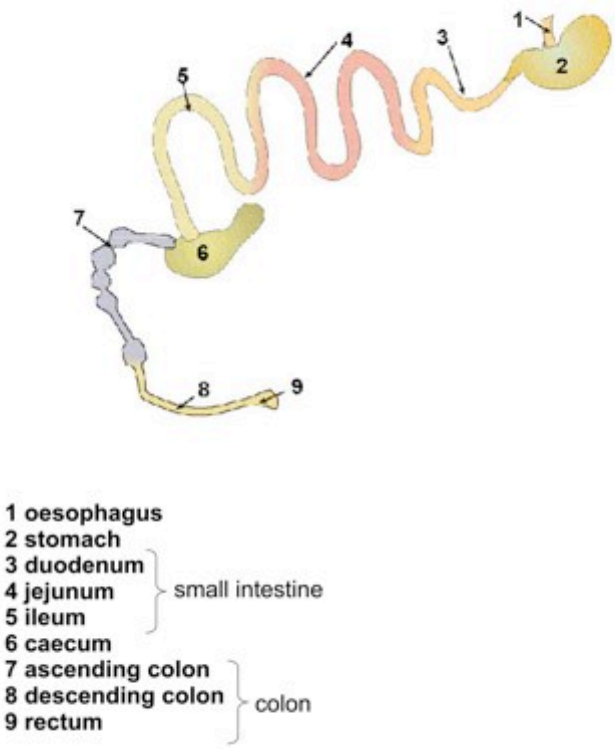

Figure 2 Gastrointestinal tract of mice
Schematic representation of the gastrointestinal tract of mice. Figure adapted from NIAID.com

A cross section through the intestine reveals the following structures from the outside to the inside. The outer part of the intestine is formed by two muscle layers, the inner circular muscle and the outer longitudinal muscle layer, which together are responsible for peristalsis, regulated tissue contractions that propagate the intestinal contents further distally. The muscle layers are followed by the submucosa, which harbours big blood and lymphatic vessels as well as nerves embedded in an irregular connective tissue. The innermost layer, the mucosa, can be separated into three parts: the intestinal epithelium that lines the intestinal lumen, the lamina propria harbours the immune cells of the digestive tract in a loose connective tissue and the muscularis mucosa, a thin smooth muscle layer that separates the mucosa from the submucosa.

The intestinal epithelium forms a single cell layered barrier that separates cells in the lamina propria from luminal contents. This barrier prevents the contact of mucosal immune cells by commensal bacteria and various antigens residing in the lumen. Disturbance of epithelial integrity leads to an encounter of immune cells with immune reactive components of the intestinal lumen, resulting in an inflammatory response that impairs intestinal immune homoeostasis. Indeed, patients suffering from inflammatory bowel disease (IBD) such as Ulcerative Colitis (UC) or Crohn's Disease (CD) display a disturbance in the intestinal epithelial barrier function (McGuckin et al., 2009; Roda et al., 2010). Therefore, maintaining intestinal epithelial integrity is essential for the health of an individual.

Although the intestinal tract is lined by a single cell-layered epithelium composed of intestinal epithelial cells (IECs), the epithelium of the small intestine and the colon each display a characteristic architecture and are composed of various kinds of specialised epithelial cells. The mucosa of the small intestine is organised into protrusions that project into the lumen, the villi, and mucosal invaginations called the crypts of Lieberkühn (see Fig. 3) (Reya and Clevers, 2005). The presence of villi enlarges the surface area where absorption of nutrients takes place. Crypts harbour the proliferating epithelial compartment that consists of stem cells and the transit amplifying (TA) cells that fuel the villi with new IECs. In contrast to the small intestine, the surface of the colonic mucosa is flat and does not possess villi (Fig. 3) (Reya and Clevers, 2005). However, also the colonic epithelium is organised in crypts with the stem cell compartment at the crypt bottom and the adjacent TA region. The intestinal epithelium is one of the most actively regenerating tissues of the mammalian body, in which the whole epithelium is renewed every 3 to 5 days (Brittan and Wright, 2004; Radtke and Clevers, 2005). New IECs derive from stem cells at the crypt bottom that divide only once per day and give rise to new stem cells and TA cells. The TA cells undergo cell divisions more frequently (every 12-16 hours) and are responsible for replenishment of the epithelium (Marshman et al., 2002). TA cells remain in the crypt for about two days and divide four to five times before they undergo cell cycle arrest and migrate towards the apical part of the crypt (van der Flier and Clevers, 2009). During this migratory phase epithelial precursors start differentiating into one of the four intestinal epithelial cell types, namely the absorptive enterocytes and three secretory cell types: goblet cells, enteroendocrine cells and in the small intestine also Paneth cells (van der Flier and Clevers, 2009). Enterocytes or columnar epithelial

cells are the most abundant cell type in the epithelium and make up more than 80% of all IECs (van der Flier and Clevers, 2009). Enterocytes possess a brush border at the apical side and are responsible for the uptake of nutrients. Goblet cells are the most frequent cell type of the secretory lineage. Goblet cells secrete mucins and trefoil factors and thus produce the protective mucus layer that prevents tissue damage from luminal contents and hinders bacteria to get into direct contact with IECs (McGuckin et al., 2009; van der Flier and Clevers, 2009). Enteroendocrine (or neuroendocrine) cells can be found throughout the intestinal tract and these cells coordinate intestinal functions by secreting peptide hormones such as gastrin, secretin, serotonin and substance P, which regulate secretion of digestive juices and contraction of intestinal muscles.

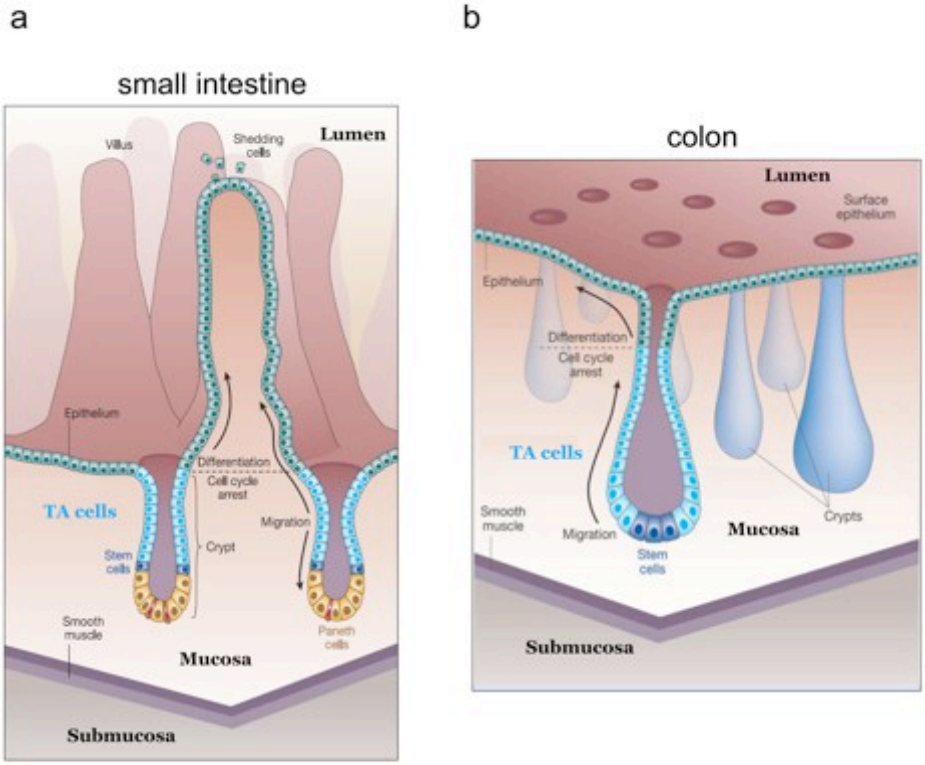

Figure 3 Tissue architecture of the small intestine and colon.
a. The surface area of the small intestinal mucosa is increased due to formation of protrusions, called villi. A single cell-layered epithelium separates the mucosa from the intestinal lumen. Stem cells and proliferating precursors (TA cells) of intestinal epithelial cells (IECs) are located in epithelial invaginations, the crypts of Lieberkühn. Paneth cells are located at the crypt bases in between stem cells (stem cells depicted in blue and red).
b. The mucosal surface of the colon is flat, though crypts are arranged in the same way as in the small intestine and harbour stem cells and TA cells but are devoid of Paneth cells.
Figure adapted from Reya and Clevers, 2005

Paneth cells reside at the base of small intestinal crypts and with a life expectancy of more than three weeks they are the most long-lived cells of the epithelium after stem cells (Bjerknes and Cheng, 1981). Paneth cells play an important role in the

regulation of the bacterial outgrowth in the intestinal tract by producing antimicrobial peptides such as lysozyme and defensins (Wehkamp and Stange, 2006).

In contrast to Paneth cells, which upon differentiation migrate towards the crypt base, differentiating IECs move towards the apical part of the mucosa (Reya and Clevers, 2005). When terminally differentiated IECs have reached the tip of small intestinal villi or the apical part of the colonic mucosa, they are shed off into the lumen. This is regulated through a specific form of cell death, termed anoikis, which is initiated by detachment from the basal membrane (Gilmore, 2005).

Although it was known that the stem cells of the intestinal epithelium are located at the lower part of the crypts in both the colon and the small intestine, the exact position and identity of this cell type remained elusive for a long time due to the lack of specific markers reliably labelling epithelial stem cells. However, recent reports have provided evidence that intestinal crypts harbour two types of stem cells with different kinetics in cell division and different localisation (Li and Clevers, 2010). Stem cells at the base of the crypt, also known as crypt-base columnar cells, are actively cycling with a dividing frequency of about once per day (Barker et al., 2007). These cells produce Ki67 and express Lgr5 and Ascl2, two molecules proposed to label this stem cell compartment (Barker et al., 2007; van der Flier et al., 2009). The second population of stem cells is located further towards the lumen of crypts at the +4 position (4^{th} cell from the crypt bottom) and is negative for Lgr5 or Ascl2 (Barker et al., 2007; van der Flier et al., 2009). These cells are cycling very rarely, they do not produce Ki67 and they are referred to as quiescent stem cells. Quiescent stem cells have been identified to exist also in other tissues, such as the hair follicle and the bone marrow (Li and Clevers, 2010). This quiescent stem cell compartment is thought to function as a backup system that only replicates under stress conditions, such as extensive epithelial damage upon irradiation, and under these circumstances gives rise to new actively cycling crypt base columnar cells (Li and Clevers, 2010; Scoville et al., 2008). Although some molecules have been proposed, thus far no marker has been identified that exclusively labels the quiescent stem cell compartment. For instance, Bmi-1 is a chromatin associated factor expressed in +4 stem cells in the small intestine (Li and Clevers, 2010), but also Lgr5 positive base columnar cells were shown to express this protein (van der Flier et al., 2009). Currently it is not clear, whether Lgr5 positive and Bmi-1-expressing cells represent fully overlapping cell populations. Importantly, the base columnar and quiescent stem

cell compartments were reported to function independently of each other. Indeed, deletion of Bmi-1 did not affect Ascl2 positive stem cells at the crypt base (van der Flier et al., 2009).

1.3 Wnt signalling pathway

It is well established that Wnt signalling is crucial for proper development and maintenance of the intestinal epithelium (Fevr et al., 2007; Korinek et al., 1998). The Wnt pathway is responsible for differentiation and proliferation of the intestinal epithelium, as well as for proper positioning of the different intestinal epithelial cell types along the crypt-villus axis through regulating the expression of the EphB/ephrin-B system (Batlle et al., 2002). In addition, the Wnt pathway is essential for maintaining intestinal epithelial stem cells, since deletion of Tcf4 leads to depletion of the stem cell compartment and early postnatal death in mice (Korinek et al., 1998). Induced deletion of β-catenin in the intestinal epithelium of adult mice disrupted intestinal homoeostasis and resulted in loss of intestinal functions due to loss of proliferating cells and stem cells (Fevr et al., 2007).

Along the basal-apical axis of the intestinal epithelium, Wnt signalling is highest at the stem cell containing crypt base and gradually decreases towards the luminal part of the mucosa. This is not only reflected in a declining expression of Wnt target genes, but also in a decrease of the ratio of cytoplasmic versus nuclear β-catenin abundance when IECs move towards the apical part of the crypt. These observations clearly show that the main driving force behind proliferation of IECs and maintenance of stem cells is the Wnt signalling pathway. This signalling cascade shows a high degree of conservation throughout the animal kingdom underscoring the importance of this pathway in developmental processes (Klaus and Birchmeier, 2008).

Activation of the transcription factor β-catenin is the central outcome of the Wnt signalling pathway (see Fig. 4). If not membrane-bound to adherens junctions via its association with E-cadherin, cytoplasmic β-catenin is targeted for proteasomal degradation at the so-called “destruction complex”. The destruction complex is composed of the scaffolding proteins adenomatous polyposis coli (APC) and Axin2/Conductin, which bind β-catenin and expose particular N-terminal serine and threonine residues of β-catenin for phosphorylation. Through phosphorylation of these target sites by casein kinase I (CK1) and glycogen synthase kinase 3β (Gsk3β), β-catenin is targeted to the β-TrCP-SCF complex, which in turn is

responsible for polyubiquitination and proteasomal degradation of the molecule (Clevers, 2006). When a Wnt-ligand binds to the cognate receptor complex, composed of a Frizzled (Frz)-receptor and the low-density lipoprotein receptor-related protein 5/6 (LRP5/6) co-receptor, the destruction complex is reorganized due to relocalisation of Dishevelled (a protein acting upstream of β-catenin and GSK3β) and Axin to the phosphorylated receptor complex at the cell membrane. Therefore, β-catenin is not phosphorylated at its N-terminus and thus accumulates in the cytoplasm and translocates to the nucleus, where it binds to transcription factors of the T cell factor/lymphocyte enhancer factor (TCF/LEF) family (Clevers, 2006). These dimers can induce transcription of Wnt target genes, which encode proteins involved in proliferation such as c-myc and Cyclin D1, but also proteins involved in tissue remodelling (matrix metalloprotease 7, MMP7) or cell positioning (EphB receptors), as well as proteins produced in stem cells (Lgr5/Gpr49, Ascl2, Sox9) (Batlle et al., 2002; Brabletz et al., 1999; Crawford et al., 1999; He et al., 1998; Shtutman et al., 1999; Tetsu and McCormick, 1999; van der Flier et al., 2009).

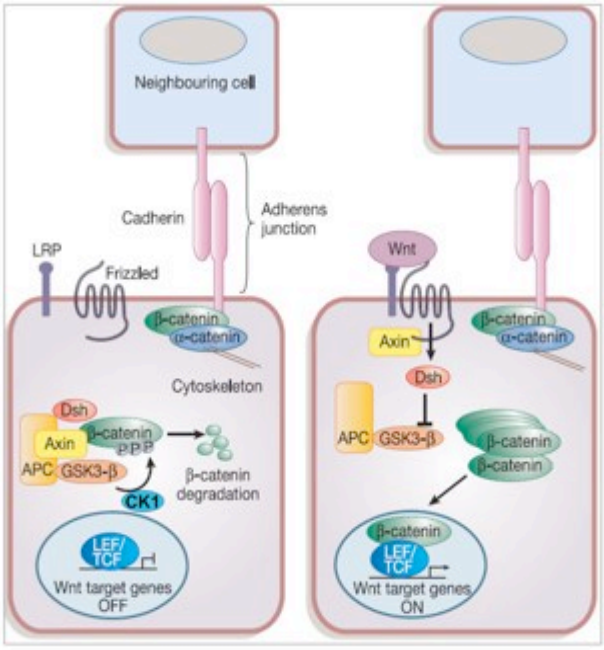

.

Figure 4 Wnt-signalling pathway
The Wnt-pathway is activated upon ligation of a Wnt-ligand to the cognate Frizzled-receptor complex. This leads to recruitment of dishevelled and Axin2 to the receptor complex and thus to inactivation of the so-called destruction complex, comprising the tumour suppressor Apc, as well as Axin2 and the kinases CK1 and GSK3β. When Wnt is present β-catenin can accumulate, translocate to the nucleus and activate TCF/LEF transcription factors and thereby induce expression of Wnt target genes. In the absence of Wnt signal cytoplasmic β-catenin is marked for ubiquitin-mediated degradation through phosphorylation by CK1 and GSK3β and thereby its accumulation and the transcription of target genes are prevented. Figure adapted from Reya and Clevers, 2005

Because of the obvious role for β-catenin activation in the differentiation and proliferation of IECs, it is clear that deregulation of this pathway might have deleterious consequences for intestinal homoeostasis. Indeed, both in humans and in mice mutations associated with intestinal carcinogenesis often affect components of the Wnt signalling cascade, leading to an enhancement of cytoplasmic and nuclear accumulation of β-catenin and thus uncontrolled production of Wnt target genes. Mutations leading to activation of the Wnt pathway often affect APC, resulting in the formation of a non-functional APC molecule that cannot exert its functions and ensure degradation of cytoplasmic β-catenin (Fodde et al., 2001). Mutations in Apc are very common in both hereditary cancer syndromes like familial adenomatous polyposis coli (FAP), in which over 95% of FAP patients were shown to carry Apc mutations and in spontaneous intestinal cancers, with more than 80% of spontaneous colon cancers harbouring mutant forms of Apc (Laken et al., 1999). The function of APC as a true tumour suppressor protein was proven in mice lacking APC in IECs or carrying a mutated Apc allele, as such mice spontaneously develop intestinal tumours (see further). These observations indicate that deregulation of the Wnt pathway might be an early event in intestinal tumour formation and underscore the need for controlling Wnt signalling for the maintenance of intestinal homoeostasis and to prevent tumour development (Bjerknes and Cheng, 1981; Fodde et al., 2001).

1.4 Murine models of colitis and intestinal cancer

Various colitis models have been established in mice that mimic human IBD. Apart from genetic disease models such as IL-10 knockout mice or TNFΔARE animals that develop spontaneous intestinal disease, chemically inducible inflammatory models have been established (Kontoyiannis et al., 1999; Kuhn et al., 1993; Rennick et al., 1995). For instance, supplying mice with dextran sulfate sodium (DSS) in the drinking water results in inflammation of the distal colon that is similar to disease characteristics in UC patients (Cooper et al., 1993; Okayasu et al., 1990). So far the exact mechanisms through which DSS induces colonic inflammation are not completely understood. DSS acts as an irritant on the colonic epithelium, resulting in mucosal ulceration and translocation of luminal contents into the mucosa, triggering an inflammatory response. Disease severity induced by DSS ingestion has been shown to depend on the bacterial microflora. Mice held under germ-free conditions show enhanced sensitivity to DSS colitis, implying that bacteria exert a protective role in this epithelial erosion based colitis model (Kitajima et al., 2001).

DSS can be administered following an intraperitoneal injection with the pro-carcinogen Azoxymethane (AOM) in order to induce colonic tumour formation. AOM is hydroxylated in the liver by cytochromes P450 to an intermediate compound (methylazoxymethanol, MAM) and then transported in bile to the intestine. Factors derived from commensal bacteria are required for the generation of the alkylating methyldiazonium that induces DNA mutations through alkylation of Guanine residues at the O6 position (Greten et al., 2004; Neufert et al., 2007). Therefore, AOM induces DNA damage specifically in the intestinal epithelium of the colon (Neufert et al., 2007; Tanaka et al., 2003). In order to accelerate proliferation of cells with AOM-induced mutations, multiple cycles of DSS are administered to the mice interrupted by a regeneration phase, in which mice receive normal drinking water. In this way, DSS invokes a chronic colitis associated with damage to the mucosal epithelium and regenerative proliferation of intestinal epithelial cells (Suzuki et al., 2006).

To study AOM-induced tumour formation that does not depend on inflammation-mediated tumour promotion, AOM is repetitively applied in weekly doses without the following DSS administration and tumour formation is assessed usually 30 weeks after the first AOM injection (Neufert et al., 2007).

In addition to chemically induced cancer models, also genetic mouse models for intestinal carcinogenesis have been established. For instance, mouse models

carrying mutations that occur in human colorectal cancer patients such as mutations in the Apc tumour suppressor gene were generated.

In this respect, Apc^{min} mice carry a point mutation in codon 850 in the Apc gene that leads to production of a truncated Apc polypeptide (Moser et al., 1990; Su et al., 1992). Apc^{min} mice develop multiple small intestinal polyps mimicking intestinal polyposis in FAP patients. Apc^{min} animals exhibit a very aggressive phenotype with 100-200 polyps growing in their small intestines and therefore exhibit a reduced life expectancy (Moser et al., 1990). A different Apc mutation in Apc1638N mice results in a milder disease manifestation (Fodde et al., 1994). In these mice a truncated version of the molecule, comprising the amino-terminal 1638 amino acids of Apc is produced, which is achieved through interruption of the coding sequence by a NEO-cassette (Fodde et al., 1994). Apc1638N mice only develop four to six small intestinal polyps in the very proximal part of the small intestine (duodenum and jejunum) at an age of about five to nine months (Fodde et al., 1994). When mice are left to age for one year, they were reported to show lesions also in the colon and the stomach (Fodde et al., 1994). In all mouse APC-models lesions occur only upon loss of heterozygocity for the wild-type Apc allele in tumour initiating epithelial cells.

In the AOM/DSS tumour protocol mutations affecting β-catenin that render the molecule resistant to degradation are very frequent (Takahashi et al., 2000; Takahashi and Wakabayashi, 2004). Therefore mutations leading to activation of Wnt signalling are involved in different intestinal tumour models, indicating that perturbations of the Wnt pathway are an early event in intestinal tumourigenesis.

1.5 NF-κB in intestinal disease

A number of recent studies have demonstrated the importance of functional NF-κB signalling in the intestinal epithelium for maintaining tissue homoeostasis. Deletion of NEMO specifically in intestinal epithelial cells ($NEMO^{IEC\text{-}KO}$) triggers spontaneous development of chronic colitis in mice (Nenci et al., 2007). $NEMO^{IEC\text{-}KO}$ mice display scattered apoptotic events in the epithelium already at young age, which may result in a disturbance of the intestinal epithelial barrier leading to colonic inflammation. This hypothesis is supported by the observed translocation of commensal bacteria into the colonic mucosa, associated with recruitment of immune cells that secrete various cytokines and chemokines. Mice lacking either TAK1 or p65 specifically in IECs confirmed the essential role for NF-κB activation in the intestinal epithelium as

demonstrated by NEMO^{IEC-KO} mice. TAK1^{IEC-KO} mice exhibited severe intestinal disease affecting the colon and the small intestine and resulted in death within the first day after birth (Kajino-Sakamoto et al., 2008). Already during embryogenesis (at embryonic day 18), though the intestinal morphology still appeared normal, TAK1^{IEC-KO} mice displayed increased apoptosis of IECs and transcription levels of inflammatory mediators were elevated. Since deletion of TAK1 blocks activation of NF-κB and MAPK signalling, it is not surprising that TAK1^{IEC-KO} mice display a more severe phenotype than NEMO^{IEC-KO} mice. While NEMO^{IEC-KO} mice only lack canonical NF-κB activity and can induce production of anti-apoptotic and pro-inflammatory molecules through activation of MAPK signalling, TAK1^{IEC-KO} mice cannot.

Furthermore, 10-15% of mice lacking the NF-κB subunit p65 specifically in the intestinal epithelium developed intestinal bleeding few days after birth and died shortly after weaning age (Steinbrecher et al., 2008). However, 85-90% of p65^{IEC-KO} mice remained disease free throughout adulthood and did not display histological abnormalities in the intestinal tract. This milder phenotype of p65^{IEC-KO} mice compared to NEMO^{IEC-KO} animals most probably can be explained by the remaining activity of other NF-κB transcription factors in IECs. Indeed, whereas deletion of NEMO completely blocks activation of canonical NF-κB signalling, loss of p65 in the intestinal epithelium only partially impairs NF-κB dependent gene transcription. However, when challenged with DSS, p65^{IEC-KO} animals exhibited more severe colitis development than control littermates (Steinbrecher et al., 2008). This observation underscores the importance of NF-κB signalling in IECs for maintaining intestinal homoeostasis under stress conditions.

In accordance with the idea that partial inhibition of NF-κB signalling does not result in impaired intestinal homoeostasis under basal conditions, mice lacking IKK2 in IECs (IKK2^{IEC-KO} mice) did not exhibit a spontaneous phenotype (Greten et al., 2004). Only IKK2^{IEC-KO} mice with an additional deletion of IKK1 in IECs (IKK2, IKK1^{IEC-KO}) developed a colonic disease similar to NEMO^{IEC-KO} animals (Nenci et al., 2007), indicating that under basal conditions residual NF-κB activation in IECs mediated by IKK1 is sufficient to maintain intestinal homoeostasis. However, IKK2^{IEC-KO} mice were more sensitive to high doses of DSS-administration, arguing that full NF-κB signalling capacity in IECs is necessary to respond appropriately during DSS-triggered colitis (Greten et al., 2004).

Together, these above described studies show that NF-κB signalling in IECs is essential for maintaining epithelial integrity under steady state levels, during which low levels of NF-κB activity appear to suffice for IEC maintenance. However, to control colitis severity in chemically induced colitis high levels of epithelial NF-κB activation are necessary.

Apart from studying the role of NF-κB activation during intestinal inflammation, mice carrying conditional alleles of IKK2 have also been used to investigate the role of NF-κB activation in intestinal tumourigenesis. In the AOM/DSS-induced model of colon cancer, $IKK2^{IEC\text{-}KO}$ mice exhibited reduced colorectal carcinogenesis. Since the lack of IKK2 in the intestinal epithelium led to increased IEC apoptosis upon DSS treatment, the authors suggested that cells carrying AOM-induced carcinogenic mutations were eliminated and therefore could not give rise to tumours (Greten et al., 2004). Thus, epithelial IKK2 activity was suggested to contribute to AOM/DSS-induced cancer development through its anti-apoptotic effect in early initiated tumour cells. In contrast to $IKK2^{IEC\text{-}KO}$ mice, mice lacking IKK2 in myeloid cells ($IKK2^{myeloid\text{-}KO}$) did not reveal a differential tumour incidence but instead harboured significantly smaller colonic tumours than control animals. This indicates that IKK2 in myeloid cells promotes tumour growth rather then tumour initiation (Greten et al., 2004). Lack of IKK2 in myeloid cells reduced the production of cytokines and chemokines during AOM/DSS treatment. Since cytokines and chemokines are thought to act as growth factors for tumour cells (Coussens and Werb, 2002), this observation suggests that shortage of these inflammatory factors in $IKK2^{myeloid\text{-}KO}$ mice impairs tumour growth (Greten et al., 2004).

1.6 Cre/LoxP conditional gene targeting

Conditional gene targeting by Cre/LoxP mediated recombination allows cell type specific analysis of gene function in mice. In addition, the Cre/LoxP technique permits to investigate the function of genes that are essential for mouse development and of which the corresponding conventional full body knockout mouse does not reach adulthood (Rajewsky et al., 1996; Sauer and Henderson, 1988). To generate a cell type specific knockout of a particular allele, this allele is flanked by specific 34 bp sequences, the so-called LoxP-sites, in the same orientation. Alleles with these LoxP-flanked sequences are referred to as 'floxed' alleles. Mice carrying these floxed alleles are then crossed to mice expressing a bacteriophage P1-derived Cre recombinase transgene under the control of a cell type specific promoter. This Cre recombinase binds to and mediates recombination between the LoxP sites, resulting in excision of the DNA flanked by the LoxP sites specifically in the cell type producing Cre.

The Cre-LoxP system can also be used in order to induce the expression of a transgene only in a specific cell type. This is achieved when the coding sequence of this transgene is preceded by a stop-signal that is flanked by LoxP-sites, thereby preventing its expression. Cre-mediated recombination between the LoxP-sequences removes the Stop-signal and allows expression of the transgene specifically in the cell type in which Cre is present.

1.7 Project description

Genetic mouse models, in which NF-κB signalling was impaired specifically in the intestinal epithelium, have shown that activation of NF-κB in intestinal epithelial cells protects the intestine during inflammatory processes (Greten et al., 2004; Nenci et al., 2007; Steinbrecher et al., 2008; Vallabhapurapu and Karin, 2009). A complete blockade of canonical NF-κB activity in intestinal epithelial cells resulted in severe chronic colitis, demonstrating that basal levels of functional NF-κB signalling are required to preserve intestinal immune homoeostasis (Nenci et al., 2007). Partial inhibition of NF-κB signalling by deletion of either IKK2 or p65 in IECs rendered mice more sensitive to DSS-induced colitis (Greten et al., 2004; Steinbrecher et al., 2008), indicating that NF-κB activity in IECs is essential to cope with inflammation associated tissue damage. Indeed, IKK2-deficient IECs displayed increased apoptosis upon DSS treatment, suggesting a cytoprotective effect of NF-κB activation in IECs under inflammatory conditions. On the other hand, the anti-apoptotic effect of

NF-κB activation in IECs promotes intestinal tumour development, as lack of IKK2 in intestinal epithelial cells reduced tumour incidence in AOM/DSS-induced cancer experiments due to enhanced cell death of carcinogen exposed IECs (Greten et al., 2004). These loss-of-function approaches in mice indicate that though NF-κB activation in IECs preserves intestinal homoeostasis and therefore is protective during excessive intestinal inflammation, at the same time it acts as a tumour promoter in intestinal tumourigenesis.

Considering these findings we decided to use a gain-of-function approach to investigate *in vivo* the outcome of increased NF-κB activity in intestinal epithelial cells. Therefore, we applied Cre/LoxP mediated recombination to generate mice that express a constitutively active IKK2 molecule selectively in intestinal epithelial cells. With this mouse model we wanted to address the role of constitutive IKK2/NF-κB activation specifically in the intestinal epithelium in mucosal homoeostasis, inflammatory disease and intestinal tumourigenesis.

2. Material and Methods

2.1 Material

2.1.1 Chemicals

Chemicals and compounds were purchased from Sigma & Aldrich, AppliChem, Merck, Roth, MP, VWR, Bayer, Ratiopharm, Dako, Vector Laboratories, GE Healthcare, Thermo Scientific, Li-Cor Biosciences

2.1.2 Material for mouse work

High resolution mini-endoscope, *Coloview* with Xenon light source, Karl-Storz (Tuttlingen, Germany)
Ketamin 10 mg/ml, Ratiopharm
Rompun 2%, Bayer Healthcare
Azoxymethane (AOM), Sigma
Dextran Sulfate Sodium (DSS), MW 36000-50000, MP
Haemoccult sensa, Beckmann Coulter
Syringes, Braun and Injection Needles, Terumo and Braun

2.1.3 Material for Histology

Tissue retriever 2100, PickCell
Tissue processor, Leica TP1020
Rotary Microtome, Leica RM2255
Modular tissue embedding center, Leica EG1150 and Leica EG1150 C
Fluorescent microscope, Leica DM5500
ABC Kit Vectastain Elite (Vector, PK 6100)
Avidin/Biotin Blocking Kit (Vector, no. SP-2001)
Liquid DAB Substrate Chromogen System (DakoCytomation, Code K3466)
Fluoromount-G, SouthernBiotech
Glas slides, Menzel

2.1.4 Material for Biochemistry

Homogenizer Precellys 24, PeqLab
2 ml tubes for homogenisation, Peqlab
1,4 mm Zirconium oxide beads for tissue homogenisation, Peqlab

Gel casting system and SDS-Page system, Biorad

Powersupply, Biorad

Protease Inhibitor Cocktail complete mini EDTA free, Roche

PhosphoStop, phosphatase inhibitor, Roche

Bradford reagent, Biorad

Protein Marker PeqGold Protein Marker V, PeqLab

PVDF membranes Immobilon-P, Millipore

Films Hyperfilm ECL, Amersham

Odyssey detection system

2.1.5 Molecular Biology Reagents and Equipment

Trizol reagent, Invitrogen

RNA extraction RNeasy mini kit, Qiagen

RNase-free DNase set, Qiagen

SuperScriptIII cDNA synthesis Kit, Invitrogen

RT Cycler ABI HT 7900 Cycler, Applied Biosystems

Power SYBR® Green PCR Master Mix, Applied Biosystems

TaqMan® Gene Expression Master Mix, Applied Biosystems

MicroAmp® Optical Adhesive Film, Applied Biosystems

MicroAmp™ Optical 384-Well Reaction Plate, Applied Biosystems

2.1.6 Laboratory equipment

Centrifuges, Eppendorf and Haereus

Thermomixer, Eppendorf

PCR-cyclers, Biorad DNA Engine, Biometra and Eppendorf

DNA ladder, Peqlab

Primers, Invitrogen and Metabion

Bio Photometer, Eppendorf

NanoDrop ND8100, PeqLab

QIAfilter plasmid purification kit, Qiagen

2.1.7 Cell culture

DMEM (Gibco)

TrypLE™ Express (Gibco)

100x Penicillin (10000 U/ml)/Streptomycin (10000 µg/ml) (Gibco)

100x L-Glutamine (200 mM) (Gibco)

100x Sodiumpyruvate (100 mM) (Gibco)

Fetal Calf Serum (PAN)

PBS (without Ca^{2+} and Mg^{2+}) (Gibco)

Lipofectamine Reagent 2000 (Invitrogen)

Plastic ware for cell culture from BD Falcon, Millipore, TPP, Corning Tubes

Eppendorf 1,5 ml and 2 ml reaction tubes

8 x 0,2 ml tube stripes Biozym

2.1.8 Software

Photoshop CS3, Leica microscopy Software Leica application suite, Prism Graph, Microsoft Office, OpenOffice Sun Microsystems, EndnoteX2

2.1.2 Buffers and Solutions

2.1.2.1 Washing buffers

PBS (1x) pH 7,3

NaCl	137 mM
KCl	2,7 mM
$Na_2HPO_4 \_ 7H_2O$	4,3 mM
KH_2PO_4	1,4 mM

TBS (1x) pH 7,5

Tris-Base	24,2 g
NaCl	80 g

2.1.2.2 Buffers and solutions for immunostainings

Endogenous peroxidase blocking buffer (for IHC)

NaCitrate	0,04 M
Na_2HPO_4	0,121 M
NaN_3	0,03M
H_2O_2	3 % (v/v)

TEX Protease K buffer pH 8.0 (for protease mediated antigen retrieval)

Tris-base	50 mM
EDTA	1 mM
Triton X-100	0,5% (v/v)

2.1.2.3 Preparation of protein extracts

High salt RIPA lysis buffer (for preparation of total cell extracts)

HEPES (pH 7,6)	20 mM
NaCl	350 mM
$MgCl_2$	1 mM
EDTA	0,5 mM
EGTA	0,1 mM
Glycerol	20% (v/v)

1% Nonident P-40, Protease inhibitor and Phosphatase inhibitors were added prior to use.

Cytoplasmic and nuclear protein extraction buffers

Buffer A (hypotonic lysis buffer)

HEPES (pH 7.6)	10 mM
KCl	10 mM
$MgCl_2$	2 mM
EDTA	0.1 mM

After the swelling step 0,8% (v/v) Nonident P-40 was added.

Protease inhibitor and Phosphatase inhibitors were added prior to use

Buffer C (high salt nuclear lysis buffer)

HEPES (pH 7.8)	50 mM
KCl	50 mM
NaCl	300 mM
EDTA	0.1 mM
Glycerol	10 % (v/v)

Protease inhibitor and Phosphatase inhibitors were added prior to use

2.1.2.4 Buffers and solutions used for Western Blot analysis

Tris-glycine electrophoresis buffer

Tris-Base	25 mM
Glycine	250 mM
SDS	0,1% (w/v)

SDS-polyacrylamid gel

10% resolving gel (for 20 ml)

H_2O	7,9 ml
30% acrylamide mix	6,7 ml
1,5 M Tris (pH 8,8)	5,0 ml
10% (w/v) SDS	0,2 ml
10% (w/v) APS	0,2 ml
TEMED	0,012 ml

5% stacking gel (for 10 ml)

H_2O	6,8 ml
30% acrylamide mix	1,7 ml
1 M Tris (pH 6,8)	1,25 ml
10% (w/v) SDS	0,1 ml
10% (w/v) APS	0,1 ml
TEMED	0,01 ml

Transfer Buffer (for semidry transfer)

Tris-Base	25 mM	
Glycine	192 mM	
Methanol	20% (v/v)	pH 8,3-8,5

Blocking buffer

PBS + 0,1% (v/v) Tween-20 + 5% (w/v) nonfat dry milk

primary antibody dilution buffer

TBS + 0,1% (v/v) Tween-20 + 5% (w/v) BSA or 5% (w/v) nonfat dry milk

5x Laemmli loading buffer

Tris-HCl (pH 6,8)	250 mM
SDS	10% (w/v)
Glycerol	50% (v/v)
Bromphenolblue	0,01% (w/v)
β-Mercaptoethanol	10% (v/v) (can be added prior to use)

Home made ECL solution

Stock solutions

Tris-HCl (pH 8,5)	100 mM
Luminol	250 mM (in DMSO)
Paracoumaric acid (PCA)	90 mM (in DMSO)
H_2O_2	30% (v/v)

Solution 1

10 ml of 10 mM Tris-HCl (pH 8,5) with 2,5 mM Luminol (100 µl of stock) and 400 µM PCA (44 µl of stock).

Solution 2

10 ml of 10 mM Tris-HCl (pH 8,5) with 7 µl 30% (v/v) H_2O_2 (5,4 mM).

The two solutions were mixed and applied on the membrane.

2.1.2.5 Buffers and solutions used for EMSA

1x TBE

Tris-base	89 mM
Boric acid	89 mM
EDTA	2 mM

Nondenaturing gels (for 25 ml)

H_2O	19,25 ml
10x TBE	1,25 ml
30% Acrylamide/Bisacrylamide mix	4,14 ml
10% (w/v) APS	315 µl
TEMED	40 µl

10x EMSA binding buffer

Tris-HCl (pH 7,5)	100 mM
NaCl	500 mM
DTT	10 mM

2.1.2.6 Buffers used for DNA extraction and genotyping PCRs

Tail lysis Buffer

Tris-HCl (pH 8,5)	100 mM
EDTA	5 mM
NaCl	200 mM
SDS	0,2 % (w/v)

0,1 mg Proteinase K (10mg/ml in 50 mM Tris, pH 8.0) per 500 µl lysis buffer was added prior to use.

TE buffer

Tris-HCl (pH 8)	10 mM
EDTA (pH 8)	1 mM

10x TAG buffer

Tris-base (pH 8,5)	200 mM
KCl	500 mM

TAE Buffer (25x) for 10 l

Tris-Base	1210 g
EDTA (pH 8.0)	500 ml of 0,5 M solution
Acteic acid	285.5 ml

DNA loading buffer

15 % (w/v) Ficoll 400 was resolved in distilled water at ~50 °C. Orange G was added till the colour turned red

2.2 Methods

2.2.1 Animal handling and mouse experiments

2.2.1.1 Mouse maintenance

Mice were housed in individually ventilated cages (IVC) in a specific pathogen free (SPF) mouse facility and in a conventional animal facility in the Institute for Genetics at the University of Cologne. Mice had permanent access to regular chow diet (Teklad Global Rodent 2018, Harlan) and acidified water. Animals were kept at a regular 12 hours light and 12 hours dark cycle.

For breeding male and female mice were set together at a minimum age of 6 weeks. Litters were weaned at 3 weeks of age and marked with an eartag. Tail biopsies were taken at the same time for isolation of genomic DNA and genotyping

Care of all mice was within institutional animal care committee guidelines. All animal procedures were conducted in accordance with European, national and institutional guidelines and protocols and were approved by local government authorities (Bezirksregierung Köln, Cologne, NRW, Germany).

2.2.1.2 Generation of conditional mice

To generate mice that express constitutively active IKK2 specifically in the intestinal epithelium R26IKK2ca^{sFL} (Sasaki et al., 2006) mice were bred with villin Cre transgenics (Madison et al., 2002) (R26IKK2ca sFL; villin Cre mice). To generate double mutant mice Apc1638N (Fodde et al., 1994) were crossed to R26IKK2ca sFL; villin Cre mice. All mice were maintained in a C57BL/6 background.
For all experiments littermates only carrying loxP-flanked alleles served as control mice.

2.2.1.3 Endoscopy

Mice were anaesthetized by intraperitoneal injection of 200 µl per 20 g bodyweight a Ketamine/Rampun mixture. The distal colon was analysed with a high-resolution mouse mini-endoscope, denoted Coloview, from Karl Storz. For imaging of the distal colon area the endoscope was gently inserted into the anus. Constant airflow induced dilation of the intestine and allowed an unperturbed view on the colonic mucosa. Disease index determined via endoscopy was composed of 5 scoring

features indicative for intestinal disease severity, each of which was scored ranging from 0 to 3 with 0 being healthy and 3 indicating severe inflammation, as has been described before (Becker et al., 2005). The sum of the following parameter scores results in murine endoscopic index of colitis severity (MEICS), an index between 0 and 15, allowing the evaluation of disease severity. The characteristics scored during examination were stool consistency, vascularisation pattern, fibrin abundance, thickening of the bowel wall and surface appearance of the mucosa. Furthermore the existence of tumours, ulcers and other intestinal lesions could be assessed through endoscopic examination.

After endoscopy mice were allowed to recover from anaesthesia or were immediately killed.

2.2.1.4 Dextran sulfate sodium (DSS)-induced colitis

In order to induce colonic inflammation resembling UC in human IBD patients, a well-established protocol of Dextran sulfate sodium (DSS) feeding was conducted (Cooper et al., 1993; Okayasu et al., 1990). Mice were fed DSS ad libidum in the drinking water. DSS (1,5% w/v or 2% w/v) was dissolved in millipore water and autoclaved prior administration. During the course of DSS experiments mice were monitored on a daily basis to assess bodyweight, stool consistency and intestinal bleeding. In order to monitor intestinal inflammation and damage of the colonic mucosa, stool samples of each animal were collected every day. Fresh stool pellets were spread on Heamoccult test sheets (Beckmann Coulter) in order to visualize occult blood. Blood scores from 0 to 4 were determined as follows: no blood in stool: score 0, occult blood visualized with Haemoccult kit: score 1, blood in stool visible in stool when spread: score 2, stool pellet covered by blood: score 3, gross bleeding from anus: score 4. Stool consistency scores from 0 to 4 were determined by the following scoring criteria: regularly formed stool pellets: score 0, still formed but softer stool pellets: score 1, enlarged, soft stool pellets: score 2, spread unformed stool: score 3, heavy diarrhoea with stool spread around the anus: score 4. The sum of blood score and stool consistency scores results in the total stool score.

2.2.1.5 AOM/DSS-induced colorectal cancer protocol

To induce colorectal colitis associated cancer (CAC), mice were undertaken an established chemically induced inflammation dependent cancer protocol (Neufert et al., 2007; Tanaka et al., 2003). On day zero of the treatment mice received an

intraperitoneal injection with 10 mg/kg bodyweight Azoxymethane (AOM) diluted in sterile PBS. In order to induce acute intestinal inflammation, on the same day, drinking water was replaced by water supplemented with DSS. During the first 2 weeks of the experiment mice were weighed daily and stool was analysed for diarrhoea and occult blood as described for DSS treatment. During the course of the treatment and at the end of the experiment mice were endoscopised in order to monitor disease and tumour development *in vivo*. Mice were sacrificed 9 weeks after the AOM injection and tissue samples were processed for histological evaluation.

2.2.1.6 AOM-induced tumour protocol

To induce colorectal cancer independently of inflammation driven tumour promotion, mice were repetitively injected with AOM without additional DSS feeding (Neufert et al., 2007). Mice received 10 mg/kg bodyweight AOM diluted in sterile PBS i.p. once per week for 5 consecutive weeks. Mice were monitored regularly to monitor health status.

2.2.1.7 Sacrifice of mice

Mice were euthanized by cervical dislocation.

2.2.1.8 Tissue processing

After cervical dislocation the abdominal cavity was opened by a longitudinal incision. The large and small intestines were removed by cutting out the colon in close proximity to the anus and the small intestine was cut after the pylorus. The intestines were placed into PBS and cleaned from mesentery and fat. The intestinal contents were carefully squeezed out with scissors and pieces of the gastrointestinal tract were taken for histological examination and RNA extraction.

For examination of bigger parts of intestinal tissue the “swiss-roll technique” was applied. For this the whole colon was opened longitudinally and the contents were removed. The tissue was then placed with the mucosa facing down on a dish. With the help of injection needles the tissue was rolled up lengthwise to form a so-called “swiss-roll” with the muscle tissue facing to the inside of the roll and the mucosa outwards. Small intestine of adult mice was cut into three pieces and individual rolls were prepared from these segments. About 3 to 5 mm long pieces of intestinal tissue were used for preparation of cross sections.

2.2.2 Histology

2.2.2.1 Preparation of intestinal tissue for histological evaluation

For histological examination tissue was fixed in histology cassettes over night at 4°C in 4% (w/v) phosphate buffered paraformaldehyde. The samples were passed through an increasing concentrations of ethanol for tissue dehydration (for 2 h each in 30% (v/v), 50% (v/v), 70% (v/v), 96% (v/v) and 2x in 100% (v/v) ethanol), were kept for two times 2 h each in xylol and then transferred to paraffin in order to be embedded in paraffin blocks. Intestinal tissue was sectioned with a microtome at 3 to 4 µm thickness and stained with haematoxylin and eosin for histological evaluation.

2.2.2.2 Haematoxylin and Eosin staining of intestinal tissue sections

To de-wax tissue sections, glass slides were placed in xylol for 20 min, then put for 2 min in each of the following ethanol-solutions for tissue rehydration: 100% (v/v) ethanol (or 100% (v/v) isopropanol), 95% (v/v) ethanol, 75% (v/v) ethanol and then in PBS for 5 min. Slides were washed in tap water for 1 min and placed into Meyers' Haematoxylin for 2 min. After being kept in tepid tap water for maximally 20 s the slides were incubated in tap water for another 15 min at room temperature to blue, followed by a short incubation in deionised water. Samples were placed in Eosin staining solution for 1 min and the excessive staining removed by washing the slides for 6 to 7 times in tap water. Samples were placed for 2 min in each 75% (v/v), 96% (v/v) and 100% (v/v) ethanol to dehydrate and were subsequently cleared in xylol. Coverslips were mounted with Entellan.

2.2.2.3 Immunostainings

For immunofluorescent and immunohistochemical (IHC) staining, slides were de-waxed in xylol and transferred through an ascending series of ethanol solutions as described under H&E staining procedure. After washing twice for 5 min in tap water for IHC endogenous peroxidase activity was blocked for 15 min at room temperature in endogenous peroxidase blocking buffer. Thereafter slides were washed three times for 5 min in tap water and antigen unmasking in form of heat induced epitope retrieval was performed, either in a pressure steam cooking device, where samples were heated for 20 min to 120°C or over night at 80°C in citrate buffer, pH 6 supplemented with 0,05% (v/v) Tween-20. Alternatively (for cytoplasmic and nuclear visualisation of β-catenin) retrieval was performed in TE pH 9 (10 mM Tris, 1 mM

EDTA). Antigen unmasking by Proteinase K digestion was performed for F4/80 immunostainings. In this case, tissue was covered with 20 µg/ml Proteinase K in TEX buffer for 20 min at room temperature. After washing the slides in PBS unspecific background was blocked in PBS with 10% (v/v) normal goat serum, 0,3% (v/v) Triton-X-100 and Avidin (Avidin was only added in case of IHC). Primary antibodies were incubated on slides over nigh at 4°C diluted in PBS, 0,2 % (v/v) cold fish skin gelatine and Biotin in case of IHC and in PBS supplemented with 0,2 % (v/v) cold fish skin gelatine in case of IF. After washing three times in PBS with 0,05% (v/v) Tween-20 the secondary antibody diluted in PBS with 10% (v/v) normal goat serum was applied for one hour at room temperature, followed by three 5 min washes in PBS with 0,05% (v/v) Tween-20. For IF nuclei were counterstained with DAPI and cover slides mounted with Fluoromount. In case of IHC after the secondary antibody an Avidin-Biotin-HRP complex (ABC Kit) was incubated on the samples for 30 min at room temperature and after washing staining was developed with DAB chromogen. Precipitate formation was followed under a microscope and the reaction stopped after sufficient staining intensity was reached by immersing the slides in PBS. To ensure equal staining conditions all samples were incubated with DAB staining solution for the same time. Nuclei were counterstained in Meyers' Haematoxylin for 1 min, when immunostainings for nuclear antigens were performed, and for 2 min in case of cytoplasmic and cell surface epitopes. Tissue was mounted with Kaisers' gelatine after a short wash in PBS or dehydrated in descending series of ethanol solutions, cleared in Xylol and mounted with Entellan.

Table 1: Primary antibodies and conditions for immunostainings:

Antigen	Host	Company	Clone	Dilution	Retrieval
B220	rat	home made	RA3 6B2	1:1000	10 mM Citrate, pH 6
β-catenin	mouse	BD	Clone 14	1:5000	10 mM Tris, 1mM EDTA, pH 9
CD3	rabbit	Abcam	Ab 5690	1:200	10 mM Citrate, pH 6
F4/80	rat	home made	A3-1	1:100	Protease K digestion
FLAG	rabbit	Sigma	F7425	1:500	10 mM Citrate, pH 6
Gr1	rat	BD Pharmingen	1A8	1:500	10 mM Citrate, pH 6
γH2A.X	mouse	Millipore	JBW301	1:1000	10 mM Citrate, pH 6
Ki67	rat	Dako	TEC-3	1:1000	10 mM Citrate, pH 6
αSMA	mouse	Sigma	1A4	1:2000	10 mM Citrate, pH 6
Sox9	rabbit	Millipore	AB5535	1:1000	10 mM Citrate, pH 6

Table 2: Secondary antibodies and conditions used for immunostainings

Antigen	Antibody modification	Host	Company	Clone	Dilution
mouse IgG	biotinylated	goat	Biozol	BA-9200	1:1000
rabbit IgG	biotinylated	goat	Perkin Elmer	NEF813	1:500
rat IgG	biotinylated	rabbit	DAKO	E0468	1:1000
rabbit IgG	Alexa488	goat	Invitrogen	A11008	1:1000
rat IgG	Alexa488	goat	Invitrogen	A11006	1:1000

2.2.3 Biochemical analysis

2.2.3.1 Isolation of intestinal epithelial cells (IECs) from colon and small intestine

After euthanasia the peritoneal cavity was opened, the intestines removed and transferred into cold PBS. IECs were isolated according to the published protocol (Ukena et al., 2007). The colon and the small intestine were cut open longitudinally and the intestinal contents were removed by washing in cold PBS. Colons/small intestines were placed into separate 50 ml Falcon tubes with pre-warmed PBS supplemented with 1 mM DTT and shaken for 10 min at 180 rpm and 37°C to remove mucus and debris. The tissue was shortly washed in PBS, transferred into new tubes and incubated in HANK's salt solution (HBSS) supplemented with 1,5 mM EDTA for 15 min at 37°C and 180 rpm. For efficient detachment of epithelial cells and crypts, tubes were vortexed vigorously at full speed for about 1 minute. Colon/SI tissue was removed with forceps and IECs were pelleted by centrifugation for 10 min at 1200 rpm. Pellets of colon and SI IECs were resuspended in 1 ml and 3 ml PBS respectively and transferred into eppendorf tubes. After another centrifugation for 5 min at 5000 rpm pellets were either shock frozen in liquid Nitrogen, or processed for protein extraction or RNA preparation.

2.2.3.2 Preparation of IEC protein extracts

For total extracts of colonic or small intestinal IECs, cells were lysed in an appropriate amount of high salt RIPA lysis buffer (depending on the size of IEC pellets, lysis buffer volumes ranging from 50 µl to 800 µl were used) supplemented with protease- and phosphatase inhibitors. For lysis the cells were kept on ice for 30 min and during this incubation period tubes were inverted repetitively. The lysis step was followed by 20 min centrifugation at 4°C and full speed to pellet cell debris. The supernatant containing cytoplasmic and nuclear proteins was harvested.

2.2.3.3 Preparation of cytoplasmic and nuclear protein extracts

For separation of cytoplasmic and nuclear proteins, IEC pellets were resuspended in buffer A and kept on ice for 5 min for hypotonic swelling of cells. Addition of NP-40 to a final concentration of 0,8% (v/v) and incubation for 10 min on ice allowed cell lysis without opening the nuclei. Nuclei were separated from the cytoplasmic protein fraction by centrifugation at full speed for 1 min at 4°C. Supernatant containing the cytoplasmic protein fraction was transferred to a fresh tube and frozen away. The procedure was repeated in order to lyse cells that were not lysed during the first lysis step. To remove remaining cytoplasmic extracts nuclei were washed twice in buffer A without NP-40. Afterwards the whitish nuclear pellet was resuspended in an appropriate amount of high salt buffer C. Nuclear lysis was performed on ice for 20 min and the extracts were isolated by a centrifugation step at full speed and 4°C for 10 min. The supernatant containing the nuclear protein fraction was transferred into a fresh tube and frozen away.

2.2.3.4 Assessment of protein concentration by Bradford assay

To determine the protein concentration, samples were diluted 1:10 in lysis buffer and 2 µl were added to 1 ml of Bradford solution. To generate a protein concentration standard curve 0,5 µg, 1 µg, 2 µg, 5 µg and 10 µg BSA each were diluted in 1 ml of Bradford solution and incubated at RT for 10 min. Protein concentrations were measured with a spectrophotometer at an absorbance of 595 nm. For calculation of protein concentrations the BSA-standard curve was applied.

2.2.3.5 Western Blot analysis

To reduce disulfide bonds and denature proteins prior to loading, samples were boiled in 1x Laemmli loading buffer for 10 min.

Equal amounts of protein as determined by Bradford analysis were separated according to size by electrophoresis on 10% SDS-polyacrylamid gels (SDS-PAGE). Gels were run under denaturing conditions in Tris-Glycine electrophoresis buffer until sufficient separation of protein bands at the molecular weight of interest was reached.

Proteins were transferred to PVDF membranes via semidry electrotransfer. First PVDF membranes were activated by incubation in 100% (v/v) methanol for 2 to 3 minutes and were then placed in transfer buffer. Prior to transfer SDS gels were equilibrated and 3 mm thick Whatman paper was soaked in semi dry transfer buffer.

From bottom to top the following assembly was built up to allow transfer of proteins from SDS gels to the membranes. A piece of Whatman paper was covered by the PVDF nitrocellulose membrane, followed by the gel and another sheet of Whatman paper. Per cm^2 membrane 1 mA current was applied for 90 to 120 minutes to assure efficient transfer of proteins. After protein blotting, membranes were washed in PBS and, to reduce unspecific binding of antibodies, membranes were blocked in PBS with 0,1 % (v/v) Tween-20 and 5% (w/v) non-fat dry milk under agitation. Primary antibodies were applied either over night at 4°C or for 1 to 3 hours at room temperature and were diluted either in PBS with 0,1 % (v/v) Tween-20 and 5% (w/v) milk or TBS with 0,1% Tween-20 and 5% (w/v) BSA. Excessive antibodies were removed by washing in PBS with 0,1 % Tween-20. Membranes were incubated with HRP-conjugated secondary antibodies raised against mouse, rabbit or goat immunoglobulins were diluted in PBS with 0,1 % (v/v) Tween-20 and 5% (w/v) non fat dry milk for 1 h at room temperature under agitation.

After washing in PBS with 0,1 % (v/v) Tween-20 and depending on signal intensity, protein bands were visualized either with homemade ECL solution, commercial ECL, ECL plus or with ECL Femto. For signal development membranes were soaked with the corresponding ECL solution for at least 1 min. Chemiluminescent films were placed on the membranes in cassettes and were exposed for various time points. Exposed films were first developed in AGFA developer solution and fixed in AGFA Fixer solution.

Loading differences of proteins were identified by comparison of the β-actin or α-tubilin levels.

Table 3: Primary antibodies used for WB analysis

Antigen	Host	Company	Clone	Dilution
β-actin	goat polyclonal	Santa Cruz	I19	1:1000
Ascl2	rabbit polyclonal	abcam	ab74499	1:1000
Active β-catenin	mouse monoclonal	Millipore	8E7	1:1000
β-catenin	mouse monoclonal	BD	14	1:2000
IκBα	rabbit polyclonal	Santa Cruz	C-21	1:1000
IKK2	rabbbit monoclonal	Cell Signaling	2C8	1:1000
Lamin A/C	goat polyclonal	Santa Cruz	N-18	1:1000
α-tubulin	mouse monoclonal	Sigma	B-5-1-2	1:5000

Table 4: Secondary antibodies used for WB analysis

Antigen	Host	Company	Clone	Dilution
mouse IgG	sheep	Amesham Pharmacia	NA9310V	1:3000
rabbit IgG	donkey	Amesham Pharmacia	NA934V	1:5000
goat IgG	donkey	Jackson ImmunoResearch	705-035-033	1:3000

2.2.4. Molecular Biology

2.2.4.1 Electrophoretic mobility shift assay (EMSA)

In order to determine DNA-binding activity of nuclear NF-κB, we performed NF-κB-DNA binding assays with nuclear protein extracts prepared form IECs.

To allow binding of NF-κB transcription factors to a consensus NF-κB site in a DNA probe, the following reaction was set up and incubated at room temperature in the dark for 40 min. 2 µl 10x EMSA binding buffer, 1 µl of poly dIdC (1-2 µg/µl), 1 µl of 25 mM DTT, 2,5% (v/v) Tween-20, 1 µl of NF-κB probe labelled with IR Dye 781 and the corresponding volume of 5 to 10 µg nuclear protein extract. The final volume was adjusted to 20 µl with nuclease-free water. After the binding reaction 2 µl of orange loading dye were added.

NF-κB probe sequence

5'AGT TGA GGG GAC TTT CCC AGG C 3'

5'G CCT GGG AAA GTC CCC TCA ACT 3'

Both oligonucleotides were labelled with IR Dye 781 at the 5' end.

During the binding reaction of the probes the nondenaturing gel was pre-run in 0,5x TBE buffer at 9 V per cm of gel. EMSA was run at 9 V per cm of gel protected from light. The result was visualized with Odyssey detection system.

2.2.4.2 Extraction of RNA

For extraction of RNA from IECs or whole colon tissue, samples were homogenised in 1 ml of Trizol reagent (Invitrogen). Samples were left for 20 min at room temperature to allow complete lysis of nuclei. Centrifugation for 10 min at full speed pelleted cell debris and membranes. The supernatant was transferred into a new eppendorf cup and incubated at room temperature for another 5 min. 200 µl chloroform per 1 ml of Trizol were added to the homogenate and the tubes shaken vigorously by hand for about 15 s to extract nucleic acids, followed by a 5 min incubation step at room temperature. To separate the organic and aqueous phases, samples were centrifuged for 15 min at full speed. The clear upper aqueous phase

was transferred into a fresh tube, an equal volume of 70% (v/v) ethanol was added and the solution was mixed gently by pipetting. Up to 700 µl of this mix were loaded on a Qiagen RNAeasy column. Columns were centrifuged for 1 min at 9000 g and the process repeated with the remaining extracts. The column filter was thereafter washed with washing buffer (provided by the manufacturer), which was removed by centrifugation (15 s at 9000 g). To perform on column genomic DNA digestion, the column was equilibrated with equilibration buffer (provided by the manufacturer), the buffer removed by centrifugation and then the DNA digestion performed for 15 to 20 min at room temperature with RNase-free DNase in RDD buffer (provided by the manufacturer). Digestion of genomic DNA was followed by two washing steps and filter bound RNA was then eluted in nuclease free water. Until further use RNA was stored at -80°C.

1 µl of RNA solution was run on an agarose gel to asses RNA quality. Furthermore a PCR for β-actin was performed with RNA to check for contamination with genomic DNA.

Concentration and purity of RNA were assessed by photometric analysis.

2.2.4.3 cDNA synthesis

1 µg RNA was used for in vitro cDNA synthesis with Superscript lll kit (Invitrogen) according to the manufacturers instructions. In a final reaction volume of 10 µl 1 µg of RNA was mixed with 1 µl of 10 mM dNTPs and 1 µl random hexamer primers (50 ng/µl). This reaction was incubated for 5 min at 65°C to allow annealing of primers to RNA. Then 10 µl of the cDNA-Synthesis mix consisting of 2 µl 10x RT-reaction buffer, 4 µl 25 mM $MgCl_2$, 2 µl of 0,1 M DTT, 1 µl RNase OUT (40 U/µl) and 1 µl of SuperScript lll polymerase (200U/µl) (all provided by the manufacturer) were added to the annealing mix after the latter was incubated on ice for a few minutes. For reverse transcription the following reaction was carried out on a PCR Cycler: 10 min at 25°C, 50 min at 50°C for cDNA synthesis and finally 85°C for 5 min for termination of the reaction. RNA was digested by addition of 1 µl of RNase H and incubation for 20 min at 37°C. The resulting reaction volume was diluted 10-fold with nuclease-free H_2O and 2 µl of this cDNA solution were used for quantitative real time PCR.

To assure proper synthesis of cDNA in all samples, 2 µl of cDNA solution were subjected to an actin-PCR.

2.2.4.4 Quantitative real time PCR

For quantitative real time PCRs samples were run in duplicates. Probe-based Taqman quantitative RT-PCR reactions were performed in a final volume of 12 µl. 2 µl of cDNA were mixed with 6 µl of 2x Mastermix (Applied Biosystems), 0,6 µl of primer-probe mix (Applied Biosystems) and 3,4 µl of water in 384-well plates. All Taqman probes were purchased from Applied Biosystems

The PCR programme applied was suggested by the manufacturer (Applied Biosystems) and was composed of an activation step for 10 min at 95 °C, followed by 40 cycles of 10 s at 95°C and 1 min at 60 °C.

For Sybr-Green based quantitative RT-PCRs 2 µl of cDNA were added to 1,2 µl of 20 µM primer mix, 6 µl of 2x reaction buffer (Applied Biosystems) and 2,8 µl of water. The PCR programme applied was suggested by the manufacturer: after 10 min at 95°C, 40 cycles of 95°C for 10 s, annealing at 60°C for 20 s and an elongation step of 40 s at 72°C were used. After these 40 cycles the PCR-amplicons were subjected to a dissociation stage.

Primers for Sybr-Green quantitative RT-PCR were purchased from Invitrogen and primer sequences were obtained from http://pga.mgh.harvard.edu/primerbank/.

RNA expression levels were determined according to the comparative ΔΔCT method. Therefore, the Ct value (which corresponds to the cycle number when the amplification plot crosses the fixed threshold) for each gene and sample was substracted from the Ct value of an endogenous control (the reference gene; villin, Gapdh or TATA box binding protein) to generate the ΔCT value. Relative quantification was performed by using the ΔΔCT.

Table 5: Taqman probes used for quantitative RT-PCR analysis

Gene	Taqman probe
Cxcl-1 = KC	Mm00433859_m1
Cxcl-10 = IP-10	Mm00445235_m1
Cxcl-16	Mm00469712_m1
Ccl20	Mm00444228_m1
IL-1b	Mm00434228_m1
IL-6	Mm00446190_m1
IL-12a, p35	Mm00434165_m1
IL-23, p19	Mm00518984_m1
IL-12b, p40	Mm99999067_m1
IL-17A	Mm00439619_m1

Table 5 (continued): Taqman probes used for quantitative RT-PCR analysis

Gene	Taqman probe
TNF	Mm00443258_m1
TGF-b1	Mm03024053_m1
Tslp	Mm00498739_m1
Ascl2	Mm01268891_g1
Olfm4	Mm01320260_m1
Lgr5	Mm00438890_m1
Prominin-1 = CD133	Mm00477115_m1
DLK1	Mm00494477_m1
MMP7	Mm01168420_m1
Ptgs2 = Cox2	Mm00478374_m1
Gapdh	Mm99999915_g1
Tbp = TATA box binding protein	Mm00446973_m1

Table 6: Primer-sequences for Sybr-Green based quantitative RT-PCR

Gene	forward (5'→ 3')	reverse (5'→ 3')
Tnfrsf19	ATTCTCTTCCTACTCCACCTG	CATAGCCGAAGCCACATTC
Bmi-1	TATAACTGATGATGAGATAATAAGC	CTGGAAAGTATTGGGTATGTC
Cyclin D1	GCGTACCCTGACACCAATCTC	CTCCTCTTCGCACTTCTGCTC
β-catenin	ATGGAGCCGGACAGAAAAGC	CTTGCCACTCAGGGAAGGA
Axin-2/conductin	TGACTCTCCTTCCAGATCCCA	TGCCCACACTAGGCTGACA
Tcf4 = Tcf7L2	GCACACATCGTTCAGAGCC	GGGTGTAGAAGTGCGGACA
Tcf1 = Tcf7	AGCTTTCTCCACTCTACGAACA	AATCCAGAGAGATCGGGGGTC
CD44	TCTGCCATCTAGCACTAAGAGC	GTCTGGGTATTGAAAGGTGTAGC
ITF-2 = SEM2	CAGCACTGCCGACTACAACA	CCATAGCCCGGCTGATTCAT
Id-2	ATGAAAGCCTTCAGTCCGGTG	AGCAGACTCATCGGGTCGT
c-myc	ATGCCCCTCAACGTGAACTTC	CGCAACATAGGATGGAGAGCA
IKK1	GTCAGGACCGTGTTCTCAAGG	GCTTCTTTGATGTTACTGAGGGC
IKK2	CTGAAGATCGCCTGTAGCAAA	TCCATCTGTAACCAGCTCCAG
L1CAM	AAAGGTGCAAGGGTGACATTC	TCCCCACGTTCCTGTAGGT
Lamg2 = laminin γ2	CAGACACGGGAGATTGCTACT	CCACGTTCCCCAAAGGGAT
Ccl6	GCTGGCCTCATACAAGAAATGG	GCTTAGGCACCTCTGAACTCTC
Ccl11	GAATCACCAACAACAGATGCAC	ATCCTGGACCCACTTCTTCTT
Ccl20	GCCTCTCGTACATACAGACGC	CCAGTTCTGCTTTGGATCAGC
Ccl25	TTACCAGCACAGGATCAAATGG	CGGAAGTAGAATCTCACAGCAC
Ccl28	GTGTGTGGCTTTTCAAACCTCA	TGCATGAACTCACTCTTTCCAG
Cxcl5	TGCGTTGTGTTTGCTTAACCG	AGCTATGACTTCCACCGTAGG
RegIIIγ	TTCCTGTCCTCCATGATCAAAA	CATCCACCTCTGTTGGGTTCA

Table 6 (continued): Primer-sequences for Sybr-Green based quantitative RT-PCR

Gene	forward (5'→ 3')	reverse (5'→ 3')
IL-11	TGTTCTCCTAACCCGATCCCT	CAGGAAGCTGCAAAGATCCCA
villin	TCAAAGGCTCTCTCAACATCAC	AGCAGTCACCATCGAAGAAGC
Gapdh	CATGTTCCAGTATGACTCCACTC	GGCCTCACCCCATTTGATGT

2.2.4.5 Preparation of genomic DNA from tail biopsies

Tail biopsies were placed in 500 µl of tail lysis buffer supplemented with Proteinase K (10 mg/ml). Tails were lysed for a minimum of 2 h at 56°C under agitation or over night at 56°C with or without agitation to digest the tissue. Undissolved material (hair, cartilage and bone) was pelleted by centrifugation for 10 min at full speed. The supernatant was transferred into a new tube containing 500 µl isopropanol and the tube was inverted several times to precipitate DNA. Genomic DNA was collected at the bottom of the tube by 5 min centrifugation at full speed and followed by a washing step with 200 µl 70% (v/v) ethanol after discarding the supernatant. After another 5 min of centrifugation at full speed the pellet was air-dried and then suspended in 100-200 µl Tris-EDTA buffer. Genomic DNA was used for genotyping PCRs.

2.2.4.6 Genotyping PCRs

For PCR-based genotyping 2 µl of genomic tail DNA were used per reaction. The PCR-reaction mix was composed of 3 µl 10x TAG buffer, 3 µl of 2 mM dNTPs, 3 µl of 3 µM primer mix, 1,8 µl 25 mM $MgCl_2$, 1,8 µl DNA loading dye, 0,5 µl home made Taq-enzyme and 17 µl of H_2O in a final volume of 30 µl. Adequate annealing and elongation times were used for each typing protocol. To assess PCR results 10 µl PCR reaction were run on agarose gels.

Table 7: Primer-sequences for genotyping PCRs and PCR-amplified fragment sizes:

typing for	Primer sequences (5'→3')	bands
Apc1638N	TCAGCCATGCCAACAAAGTCA	**WT 200 bp Tg 400 bp**
	GGAAAAGTTTATAGGTGTCCCTTCT	
R26 knock-in	AAAGTCGCTCTGAGTTGTTATC	**WT 570 bp sFL 450 bp**
	GATATGAAGTACTGGGCTCTT	
	GCATCGCCTTCTATCGCCT	
villin Cre	ACAGGCACTAAGGGAGCCAATG	**WT 900 bp Tg 350 bp**
	ATTGCAGGTCAGAAAGAGGTCACAG	
	GTTCTTGCGAACCTCATCACTC	

Table 8: PCR-programmes for genotyping PCRs

typing for	PCR program		cycles
Apc1638N	94°C	5 min	
	94°C	60 sec	35
	55°C	45 sec	
	72°C	45 sec	
	72°C	5 min	
R26 knock-in	94°C	3 min	
	94°C	30 sec	35
	56°C	30 sec	
	72°C	30 sec	
	72°C	5 min	
villin Cre	94°C	3 min	
	94°C	1 min	35
	67°C	1 min	
	72°C	1 min	
	72°C	5 min	

2.2.4.7 Agarose gel electrophoresis

PCR-amplified DNA fragments were separated according to size by agarose gel electrophoresis. Depending on fragment size, 1 to 2 % (w/v) agarose were boiled in 1x TAE buffer and supplemented with 0,5 mg/ml Ethidiumbromide. Gels were run in 1x TAE electrophoresis buffer.

2.2.5 Cell Biology

2.2.5.1 Culture of human colon cancer cell lines

HCT116 human colon cancer cells were cultured in DMEM supplemented with 10% (v/v) FCS, Penicillin/Streptomycin, Pyruvate and Glutamine. Cells were grown to confluency in 15 cm Petri dishes and incubated at 37°C and 5% (v/v) CO_2. Confluent cells were subjected to trypsinisation in order to detach adherent cells from culture dishes. Prior to trypsin treatment cells were washed in PBS to remove medium with FCS, trypsin solution was applied and the plates were incubated for 5 min at 37°C. Trypsin activity was blocked by addition of DMEM with 10% (v/v) FCS. Cells were then diluted in fresh medium and were transferred to new plates.

2.2.5.2 Transfection of human colon cancer cells

The day before transfection cells were detached from the plates by trypsinisation and resuspended in growth medium. $1x10^6$ or $3x10^6$ cells were seeded in 10 ml of medium on 10 cm Petri dishes.

Prior to transfection cells were washed in PBS and were starved for 2 h at 37°C in 9 ml of DMEM medium without FCS and other supplements. Either Polyethylenimine (PEI) or Lipofectamin 2000 (Invitrogen) was used as transfection reagent. Per µg of plasmid DNA either 4 µl of PEI or 3 µl of Lipofectamin 2000 were added to 1 ml of DMEM, mixed and incubated at room temperature for 5 min. In the meantime plasmid DNA was placed into tubes. 1 ml of DMEM-transfection reagent mix was placed on the plasmid DNA and the tubes were inverted several times. This transfection-mix was incubated at room temperature to allow formation of micelles with plasmid DNA. After 20 min the transfection mix was added to the cells and dishes were shaken horizontally to distribute the mix all over the plate. Cells were kept over night in medium with transfection mix, which was replaced by DMEM with all supplements. Cells were left another 24 h to grow and were then harvested for the preparation of protein extracts. To assure transfection with equal amounts of plasmid DNA, empty plasmid was added to complement.

2.2.6 Statistics

Results are represented as the mean +/- standard deviation (SD).

Statistical significance between experimental groups was determined by an unpaired two-tailed Student's t-test.

3. Results

3.1 Constitutive IKK2/NF-κB activation in IECs results in focal inflammation of the colon and the small intestine

To investigate the effect of constitutive IKK2/NF-κB activity in intestinal epithelial cells in vivo, a transgenic mouse model was used, in which a FLAG-tagged constitutively active IKK2 construct (IKK2ca) together with the coding sequence for enhanced green fluorescent protein (eGFP) was introduced into the ubiquitously expressed Rosa26 locus (Fig. 5). The constitutively active IKK2ca molecule was generated by two serine to glutamate substitutions (S177 and S181) in the activation loop of IKK2, thereby mimicking the phosphorylations required for its full enzymatic activity (Sasaki et al., 2006). This expression cassette was preceded by a loxP flanked STOP-cassette, preventing uncontrolled expression of the IKK2ca transgene (R26IKK2ca$^{sFL/sFL}$). To express IKK2ca specifically in intestinal epithelial cells (IECs), R26IKK2ca$^{sFL/sFL}$ mice were crossed to mice expressing Cre recombinase under the control of the intestinal epithelial cell restricted villin promoter (Madison et al., 2002). (Fig. 5) The expression of IKK2ca was visualized by immunofluorescent stainings on colon cross sections of R26IKK2ca$^{sFL/sFL}$; villin Cre transgenic (IKK2ca^{IEChom}) mice, showing the presence of the FLAG-tagged IKK2ca only in colonic epithelial cells (Fig. 6a). Expression of IKK2 was highly increased in IKK2ca^{IEChom} mice both on mRNA expression level as assessed by quantitative real time PCR and in terms of protein abundance as shown by Western Blot analysis (Fig. 6b and 6c). Whereas mRNA levels of IKK2 were significantly higher in colon IECs of IKK2ca^{IEChom} mice, there was no difference in the expression levels of IKK1 in the colon of IKK2ca^{IEChom} versus control mice (Fig. 6b).

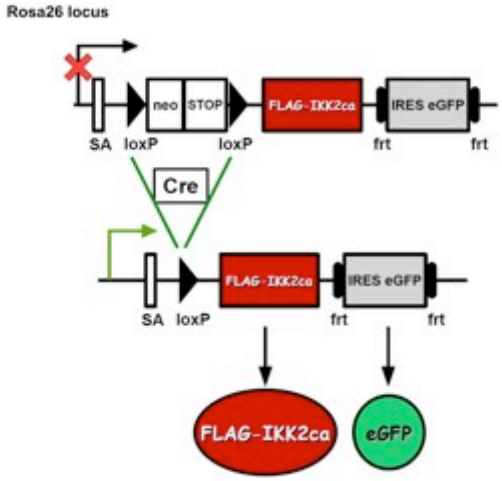

Figure 5
The coding sequence for FLAG-tagged constitutively active IKK2 (IKK2ca) followed by the DNA sequence for enhanced green fluorescent protein (eGFP) were inserted into the ubiquitously expressed Rosa26 locus under the control of the endogenous R26 promoter. A loxP-flanked stop cassette prevents uncontrolled expression of IKK2ca molecule. Upon Cre-mediated excision of the stop cassette IKK2ca-coding mRNA can be transcribed in the tissue of interest and FLAG-IKK2ca, as well as the eGFP are produced.
Figure was adapted from Sasaki et al., 2006.

Decreased steady state protein levels of IκBα, which upon phosphorylation by IKK2 is targeted for degradation, indicated an increased activation status of the NF-κB pathway in primary small intestinal IECs of IKK2ca^{IEChom} mice (Fig. 6c). An electrophoretic mobility shift assay (EMSA) with nuclear protein extracts from IECs from IKK2ca^{IEChom} mice showed increased NF-κB DNA binding activity (Fig. 6d). In contrast, no probe shift was observed when nuclear IEC extracts derived from IKK2ca^{sFL} or NEMO^{IEC-KO} mice, the latter ones completely lacking canonical NF-κB activity, were analysed. These results show that IECs from IKK2ca^{IEChom} mice produce high levels of IKK2ca and exhibit increased and persistent activation of NF-κB in the intestinal epithelium.

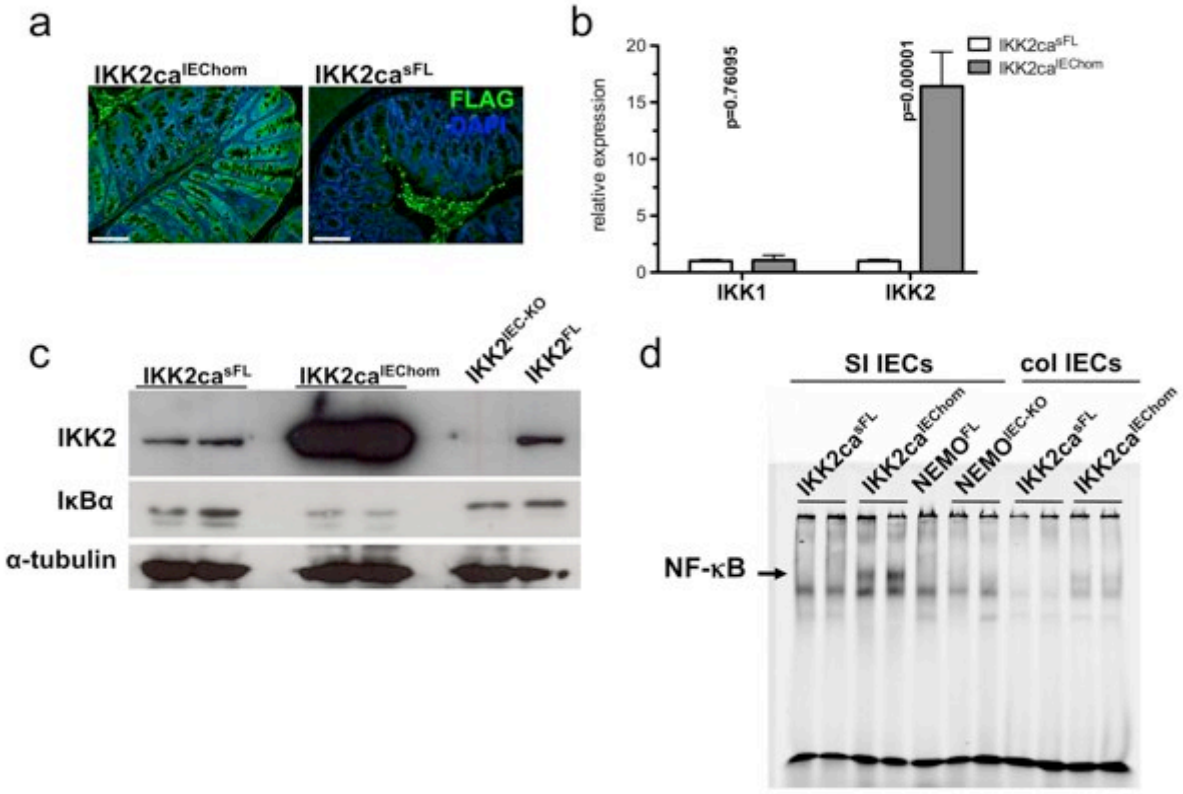

Figure 6 Expression of FLAG-IKK2ca in the intestinal epithelium of IKK2ca transgenic mice
a. Immunofluorescent staining for FLAG shows presence of FLAG-IKK2ca in epithelial cells of the colon in IKK2ca^{IEChom} and not IKK2ca^{sFL} mice.
b. Quantitative RT-PCR analysis revealed higher amounts of IKK2 mRNA in colon IECs from IKK2ca^{IEChom} mice compared to IKK2ca^{sFL} controls, whereas IKK1 was not expressed at different levels between genotypes. (n = 5)
c. WB analysis for IKK2 revealed increased levels of IKK2 protein in SI IECs of IKK2ca^{IEChom} animals. IKK2 was not detectable in IECs isolated from IKK2^{IEC-KO} mice, which lack IKK2 in the intestinal epithelium. IECs from IKK2ca^{IEChom} mice displayed a decrease in IκBα protein, indicative of IKK2 activity in IECs.
d. Increased NF-κB DNA binding as identified by a shift in NF-κB probe migration (marked by an arrow) in nuclear extracts from colon and small intestinal IECs of IKK2ca^{IEChom} mice versus IKK2ca^{sFL} controls. SI IECs from NEMO^{IEC-KO} mice did not exhibit DNA-binding of NF-κB members.
Scale bars represent 50 µm

IKK2ca^{IEChom} mice were born at the expected Mendelian ratio and exhibited healthy gross appearance. Endoscopic analysis of young adult mice at an age of six to eight

weeks did not reveal differences between IKK2ca^{sFL} control and IKK2ca^{IEChom} mice. The distal colon of IKK2ca^{IEChom} mice showed a normal vascularisation pattern and the mucosa was smooth and translucent resulting in a murine endoscopic index of colitis severity (MEICS) similar to control mice (Fig. 7a). Endoscopic images of the colon did not reveal differences between the two genotypes (Fig. 7b).

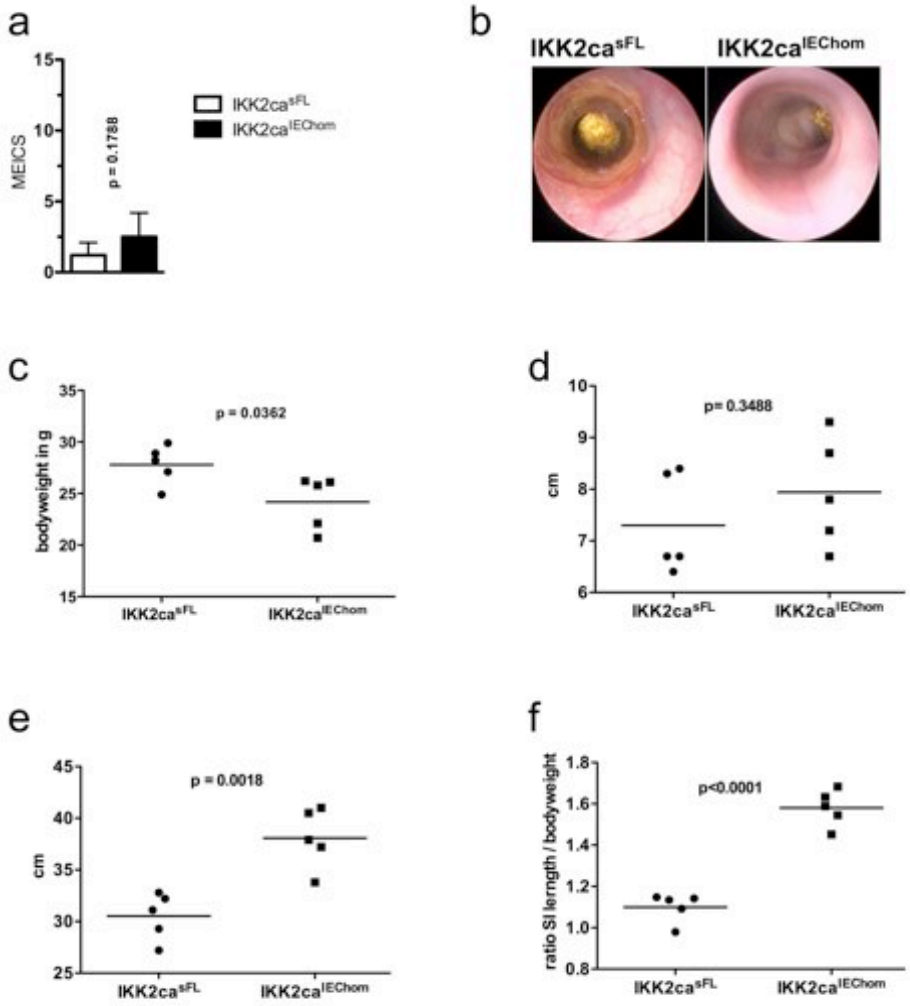

Figure 7 Reduced bodyweight and increased length of the small intestine in young IKK2ca^{IEChom} male mice

a. Endoscopic analysis of 7 to 9-week-old mice did not show signs of colonic inflammation as depicted by similar MEICS (murine endoscopic index for colitis severity) for IKK2ca^{sFL} (n = 5) and IKK2ca^{IEChom} (n = 10) animals.

b. Representative endoscopic colon images from 8-week-old IKK2ca^{sFL} and IKK2ca^{IEChom} mice.

c. Reduced bodyweight of IKK2ca^{IEChom} male mice at 10 weeks of age compared to age- and sex-matched IKK2ca^{sFL} controls. (n = 5)

d. No statistically significant difference in colon length was detectable between genotypes in 10-week-old male mice. (n = 5)

e. The same 10-week-old IKK2ca^{IEChom} male mice displayed a statistically significant increase in the length of the small intestine. (n = 5)

f. A significantly higher relative length of the small intestine compared to bodyweight of each mouse was observed in IKK2ca^{IEChom} male mice. (n = 5)

However at 10 weeks of age IKK2ca^{IEChom} mice showed a mild but statistically significant reduction in bodyweight that could point to intestinal disease (Fig. 7c). Furthermore, whereas there was no marked difference in the length of the colons, the small intestine of the same 10-week-old IKK2ca^{IEChom} mice was significantly longer than the small intestine of IKK2ca^{sFL} control mice (Fig. 7d and 7e). The relative length of the small intestine compared to the bodyweight of each individual animal was therefore significantly higher in IKK2ca^{IEChom} than in control mice (Fig. 7f).

On histological sections from the colon and the small intestine of 6-week-old mice signs of mild intestinal disease became overt in IKK2ca^{IEChom} mice. Whereas the distal colon did not show any obvious signs of pathology and only scattered areas with a slight increase in crypt length were found, the proximal colon of IKK2ca^{IEChom} mice displayed mucosal areas with infiltrating cells and inflammation-induced tissue alterations were detectable (Fig. 8a). For instance, some crypts located close to immune cell infiltrates exhibited alterations in the epithelial structure such as an increase in crypt length and densely packed epithelial cells. However, these changes appeared in a discontinuous pattern and never affected the whole tissue. In the small intestine histological tissue alterations were more obvious (Fig. 8b). Especially in the ileum, the distal part of the small intestine, crypts in IKK2ca^{IEChom} mice appeared to be much longer than in IKK2ca^{sFL} litter mates, leading to an overall thickening of the mucosa and concomitant shortening of villi. Furthermore, these elongated crypts in IKK2ca^{IEChom} animals were surrounded by inflammatory cells.

Whereas control mice harboured normal numbers of Paneth cells, identified by reddish granules on H&E stained sections at the bottom of ileal crypts, the amount of Paneth cells was markedly reduced in crypts from IKK2ca^{IEChom} mice (Fig. 8b compare higher magnifications at the bottom of the figure). Whereas some IKK2ca^{IEChom} crypts only contained few Paneth cells, some crypts indicated by white arrows in Fig. 8b did not have Paneth cells at all. Furthermore the ileum from IKK2ca^{IEChom} mice harboured elongated crypts with mislocalized Paneth cells, as shown in Fig. 8b and marked by a black arrow.

In the proximal small intestine differences between control and IKK2ca^{IEChom} animals were not as striking, but also in this region of the intestine an elongation of crypts and a mild increase in infiltrating cells was observed. Occasionally crypts were found to grow on top of each other and the mucosa was thickened.

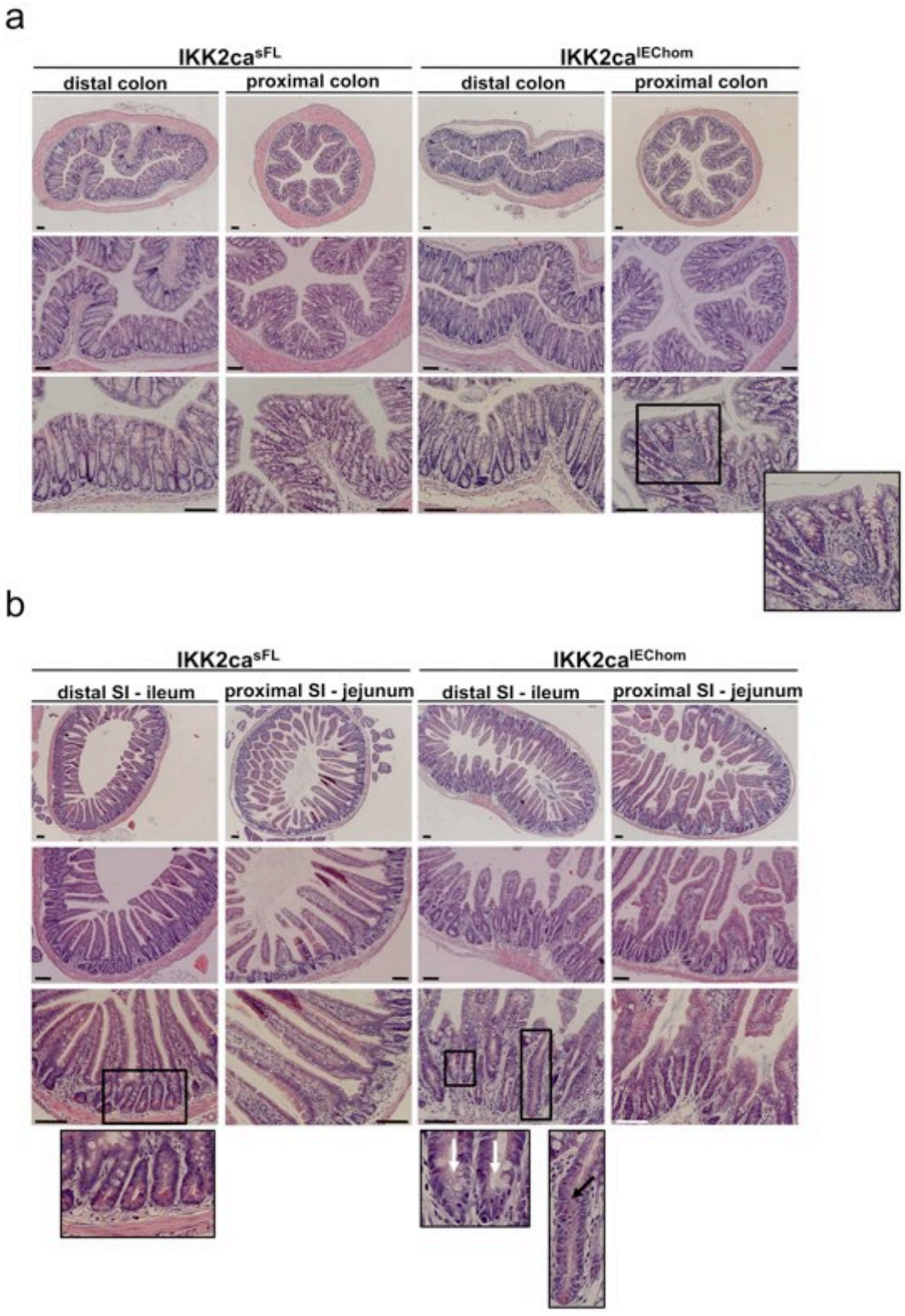

Figure 8 Inflammation in the intestine of young IKK2ca^{IEChom} mice
a. H&E stained histological sections from colons of 6-week-old IKK2ca^{IEChom} mice revealed mild crypt elongation in the distal part of the colon. In the proximal colon increased amounts of immune cells and defined infiltrates surrounding crypts were identified in IKK2ca^{IEChom} but not in IKK2ca^{sFL} mice.
b. Histological examination of small intestines of IKK2ca^{IEChom} mice revealed elongation of crypts especially in the ileum (distal small intestine). Ileal crypts of IKK2ca^{IEChom} mice frequently lacked Paneth cells, which can be identified by eosinophilic granules in crypt bases of wild-type mice (see inset with white arrows in IKK2ca^{IEChom} mouse). Black arrow in inset marks a mislocalized Paneth cell. Note the increase in SI diameter in IKK2ca^{IEChom} mice.
Scale bars represent 50 µm

To identify the nature of infiltrating cells in the mucosa of IKK2ca^{IEChom} mice immunohistochemical (IHC) stainings for Gr1, F4/80, CD3 and B220 were performed on colon and small intestinal cross sections from 6-week-old mice in order to visualize Gr1 positive granulocytes, macrophages, T-cells and B-cells respectively. Whereas control tissue was almost completely devoid of granulocytes, small numbers of Gr1 expressing cells were found in the colonic and small intestinal mucosa of IKK2ca^{IEChom} mice. In the ileum of IKK2ca^{IEChom} mice Gr1 positive granulocytes were located around the crypts and were also found in between epithelial cells (Fig. 9a).

F4/80 positive macrophages were more abundant in the proximal colon from IKK2ca^{IEChom} when compared to IKK2ca^{sFL} control mice, indicating that macrophage recruitment is increased in colonic mucosa of IKK2ca^{IEChom} mice (Fig. 9a). In control small intestines macrophages mostly localized to the lamina propria in the villi. In contrast, the small intestine of IKK2ca^{IEChom} mice showed a shift in F4/80 macrophage staining to the lamina propria surrounding the crypts, which is the area showing the highest inflammatory cell infiltration in this part of the intestine (Fig. 9a).
IHC for CD3 showed no marked difference in the amount of T-cells between IKK2ca^{IEChom} and control mice (Fig. 9a). Although areas showing inflammatory infiltrates contained higher numbers of CD3-positive T-cells, the overall difference was not as pronounced as for granulocytes and macrophages. The same result was obtained for B220-positive B-cells, for which only a slight increase in the presence of B-cells was observed in intestinal tissue of IKK2ca^{IEChom} mice (Fig. 9a). Together, these IHC data show that at young age mainly innate immune cells of the myeloid lineage contributed to inflammation in IKK2ca^{IEChom} mice, whereas cells of the adaptive immune system were less frequently involved.

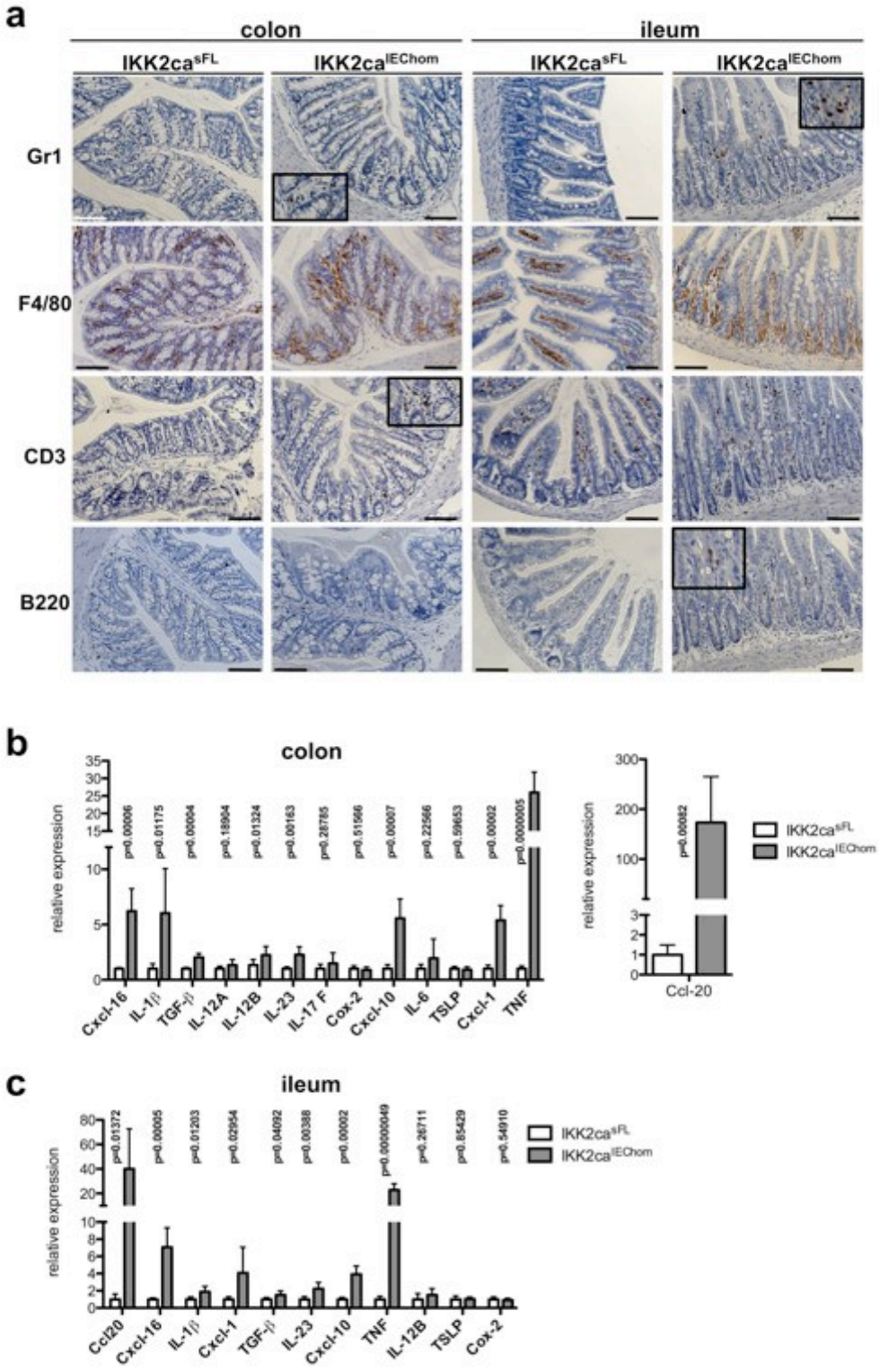

Figure 9 Increased recruitment of myeloid cells and elevated expression of inflammatory mediators in the intestine of young IKK2ca^{IEChom} mice

a. IHC for Gr1 and F4/80 revealed increased numbers of Gr1-positive granulocytes and F4/80-positive macrophages both in the colon and the small intestine of 6-week-old IKK2ca^{IEChom} mice. In the ileum macrophages accumulated around crypts in IKK2ca^{IEChom} mice, whereas in wild-type animals macrophages mainly localized to villi. The number of CD3 T-cells and B220-positive B-cells did not differ considerably between genotypes, neither in colon nor in small intestinal tissue.

b. Quantitative RT-PCR showed increased expression of a subset of inflammation-associated factors in colons of 7 to 8-week-old IKK2ca^{IEChom} mice compared to age matched IKK2ca^{sFL} controls. (n ≥ 6)

c. Increased amount of mRNA from inflammatory mediators detected by quantitative RT-PCR in the ileum of 7 to 8-week-old IKK2ca^{IEChom} mice. (n ≥ 6)

Scale bars represent 50 µm

Quantitative real time PCR (qRT-PCR) analysis on mRNA from proximal colon and ileum revealed increased expression of various inflammatory cytokines and chemokines in IKK2ca^{IEChom} mice (Fig. 9b and 9c). TNF mRNA was produced at much higher levels than in control tissue and Ccl20, a chemokine involved in the recruitment of Th17 and dendritic cells, showed massively increased expression in both proximal colon and ileum from IKK2ca-expressing mice. Other pro-inflammatory mediators such as Cxcl-16, Cxcl-10, IL-1β, and IL-23p19 were also produced at higher levels than in control tissue, indicating that IKK2ca^{IEChom} mice display clear signs of intestinal inflammation that affects both the colon and the small intestine. Interestingly, mRNA levels of inflammatory molecules such as IL-6 and cyclo-oxygenase 2 (Cox2), two NF-κB target genes that have a well-established role in intestinal inflammation, were not increased in IKK2ca^{IEChom} intestines. This indicates that intestinal epithelial restricted expression of IKK2ca results in the establishment of an inflammatory state in the colon and the small intestine that is characterized by the production of a very defined cytokine pattern.

Gene expression analysis on RNA isolated from IECs showed that these cytokines were produced mainly by the IKK2ca-expressing intestinal epithelium (Fig. 10). IKK2ca-expressing colon and small intestinal IECs produced higher mRNA levels of Ccl20, as observed also in mRNA derived from whole colon or small intestinal tissue from IKK2ca^{IEChom} mice (Brand, 2009; Schutyser et al., 2003). However, at the same time mRNA levels of other epithelial-derived chemokines such as Ccl25 and Ccl28 were not increased in IECs from IKK2ca^{IEChom} mice.

Furthermore, RegIIIγ was expressed at higher levels in colonic IECs from IKK2ca^{IEChom} mice (Fig. 10a). RegIIIγ is a C-type lectin with bactericidal functions that is secreted by Paneth cells of the small intestine and by epithelial cells of the colon (Ogawa et al., 2003). Its expression is induced by microbiota and is elevated under inflammatory conditions in IBD patients (Cash et al., 2006; Strober, 2006). The upregulation of RegIIIγ might indicate that the colonic epithelium of IKK2ca^{IEChom} mice is more responsive to the intestinal flora and induces the expression of a molecule involved in controlling bacterial outgrowth.

Therefore quantitative RT-PCR analysis showed that expression of IKK2ca in the intestinal epithelium of mice and concomitant persistent activation of NF-κB does not result in uncontrolled and unselective expression of NF-κB target genes. Instead, a specific cytokine and chemokine expression pattern is established, leading to

increased recruitment of myeloid cells in the colon and small intestine of young IKK2ca^{IEChom} mice.

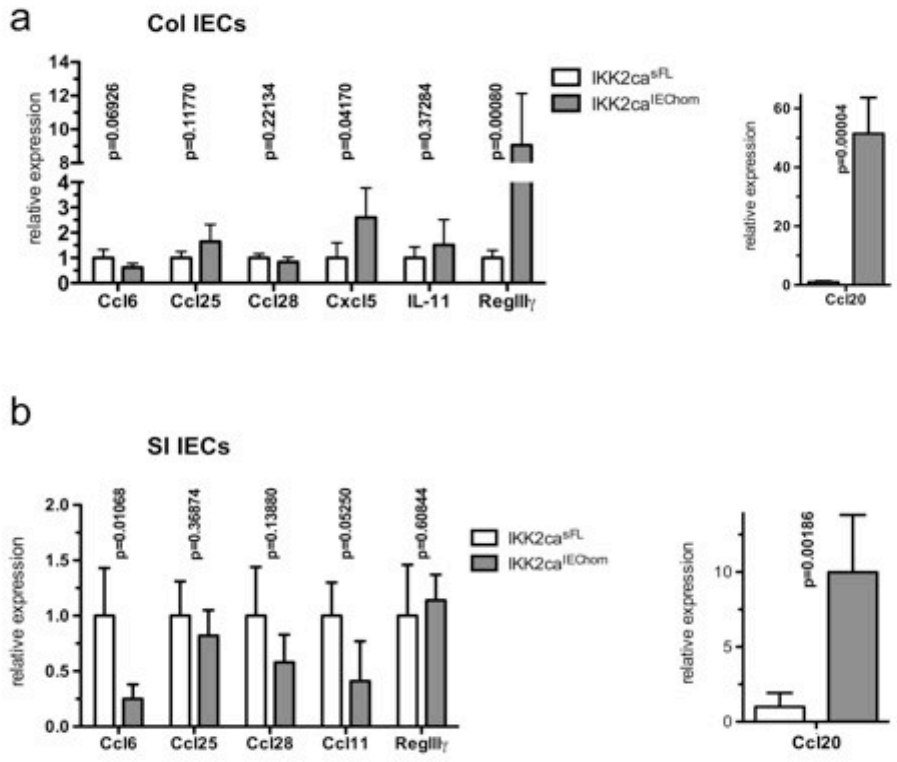

Figure 10 Elevated expression of inflammatory mediators in intestinal epithelial cells of IKK2ca^{IEChom} mice

a. A selective upregulation of epithelial cell derived inflammation-associated mediators was detectable by quantitative RT-PCR in colon IECs from IKK2ca^{IEChom} mice when compared to controls. (n = 5)

b. Differential expression of inflammatory molecules as assessed by RT-PCR analysis in small intestinal epithelial cells of IKK2ca^{IEChom} mice. (n = 5)

3.2 Expression of IKK2ca in the intestinal epithelium increases sensitivity to DSS-induced colitis and strongly enhances AOM-induced colon cancer development

It has been reported that deletion of either IKK2 or p65 in the intestinal epithelium renders mice more sensitive to DSS-induced colitis (Greten et al., 2004; Steinbrecher et al., 2008). Increased colitis severity in these mouse models is thought to result from the lack of anti-apoptotic functions exerted by NF-κB activation in the intestinal epithelium, since it was shown that DSS induced more extensive cell death of IECs in $IKK2^{IEC\text{-}KO}$ and $p65^{IEC\text{-}KO}$ mice (Greten et al., 2004; Steinbrecher et al., 2008). We therefore reasoned that persistent NF-κB activation as achieved by IKK2ca expression in IECs might prevent DSS-induced colitis. In order to investigate whether $IKK2ca^{IEChom}$ mice were indeed protected from DSS-mediated colonic inflammation, $IKK2ca^{IEChom}$ and $IKK2ca^{sFL}$ mice were given 2% DSS in the drinking water for six days and were provided with another two days of regular drinking water prior to sacrifice. Surprisingly, $IKK2ca^{IEChom}$ mice responded to the DSS treatment with a much more pronounced loss of bodyweight than control animals (Fig. 11a). DSS-elicited diarrhoea occurred much earlier in IKK2ca-expressing mice and was furthermore accompanied by the presence of blood in the stool, indicative of intestinal damage and bleeding, resulting in a heightened stool score compared to control animals (Fig. 11a).

Histological analysis of the colon from mice sacrificed at day 8 of the treatment protocol revealed more pronounced tissue damage in $IKK2ca^{IEChom}$ mice. Even though control mice exhibited mucosal ulceration and immune cell infiltration (Fig. 11b), epithelial ulceration was more severe in IKK2ca-expressing animals resulting in an almost complete lack of crypt structures (see Fig. 11b). In addition, $IKK2ca^{IEChom}$ mice harboured large immune cell infiltrates in the distal colon that could not be detected in control animals. Quantitative RT-PCR analysis of whole tissue mRNA from the distal colon revealed elevated expression levels of inflammatory cytokines and chemokines such as TNF, IL-1β, MCP-1 and Cxcl-1 (Fig. 11c). These results show that $IKK2ca^{IEChom}$ mice exhibit increased mucosal damage and enhanced intestinal inflammation upon DSS-induced colon injury than control mice. Therefore, persistent activation of the IKK2/NF-κB pathway in epithelial cells does not protect from DSS-mediated colitis development but rather sensitises mice to DSS-induced injury.

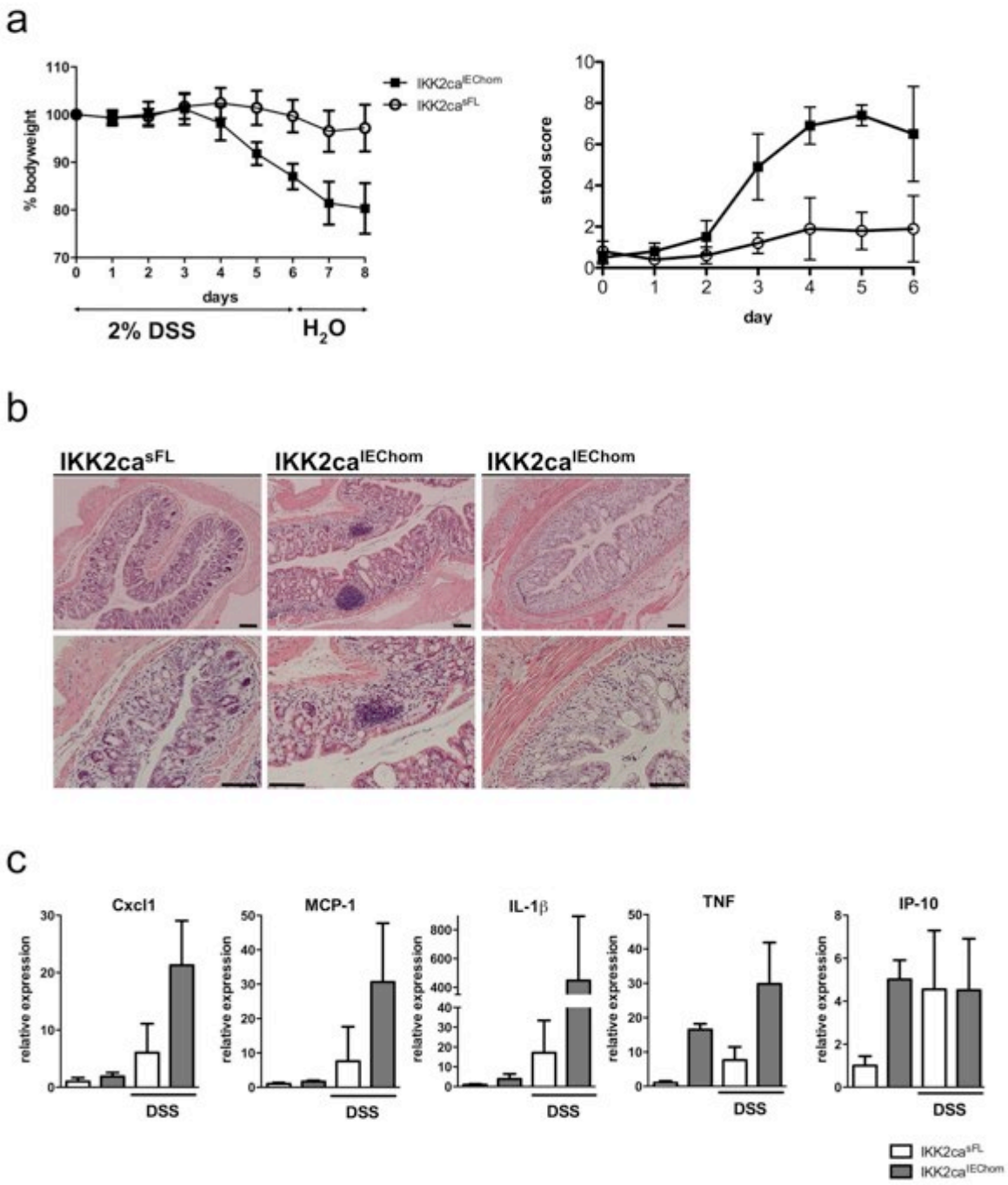

Figure 11 IKK2ca^{IEChom} mice exhibited increased sensitivity to DSS-induced colitis
a. DSS-feeding of IKK2ca^{IEChom} mice resulted in a more pronounced loss of bodyweight than in control IKK2ca^{sFL} animals, indicative of increased susceptibility to DSS-induced colitis. IKK2ca^{IEChom} mice developed a higher stool score (combined diarrhoea and intestinal bleeding score) than IKK2ca^{sFL} mice when treated with 2% DSS in the drinking water. (n = 10)
b. IKK2ca^{IEChom} mice showed more extended tissue damage in the colonic mucosa on day 8 of DSS treatment than IKK2ca^{sFL} controls. The colonic mucosa of IKK2ca^{IEChom} mice displayed more severe immune cell infiltration and increased epithelial erosion.
c. mRNA levels of pro-inflammatory molecules were increased in distal colon tissue of IKK2ca^{IEChom} mice upon DSS ingestion, when compared to IKK2ca^{sFL} control mice.
(n = 5 for naïve mice, n = 10 for DSS treated mice on day 8)
Scale bars represent 50 µm

To assess the *in vivo* role of epithelial IKK2/NF-κB activation in AOM/DSS induced colorectal cancer development, IKK2ca^{IEChom} and age-matched IKK2ca^{sFL} mice were subjected to an AOM/DSS treatment. Mice were injected intraperitoneally with 10 mg/kg bodyweight of the procarcinogen AOM and were immediately thereafter administered with DSS-containing drinking water. Since IKK2ca^{IEChom} mice showed an increased sensitivity to DSS-induced mucosal injury, all mice were fed 1,5% DSS through the drinking water for three days only. Whereas IKK2ca^{sFL} mice did not show considerable reduction of bodyweight, IKK2ca^{IEChom} mice exhibited a pronounced loss of bodyweight during these first days of the treatment (Fig. 12a). At the same time IKK2ca^{IEChom} mice showed severe intestinal bleeding and developed diarrhoea, which manifested in a heightened stool score (Fig. 12a). This elevated stool score of IKK2ca^{IEChom} mice persisted also after they were provided again with regular drinking water. Furthermore IKK2ca^{IEChom} mice experienced difficulties to recover from the DSS-induced mucosal insult, as shown by the slow rate of weight gain after removal of DSS. Although most AOM/DSS treatment protocols provide mice with several consecutive cycles of DSS feeding, the strong response of IKK2ca^{IEChom} mice to the first days of DSS-administration prompted us not to give any additional DSS to the mice until the end of the experiment (day 65). Since some IKK2ca^{IEChom} mice had lost more than 25% of their bodyweight and were moribund, they were sacrificed during the first 14 days of the treatment to avoid unnecessary suffering.

Endoscopic analysis performed on day 26 of the treatment (3 weeks after the removal of DSS) revealed that IKK2ca^{sFL} mice did not show signs of colitis and tissue damage and therefore had a low MEICS (Fig. 12b). In contrast, IKK2ca^{IEChom} mice exhibited a higher MEICS reflecting severe colonic inflammation, indicating that these animals were not able to recover from the initial DSS-induced inflammation. A final endoscopy performed prior to sacrifice on day 65 of the experiment showed that IKK2ca^{IEChom} animals had developed multiple tumours in the distal region of the colon, whereas control animals did not exhibit endoscopically detectable alterations in this area of the large intestine (Fig. 12c). The elevated MEICS assigned to IKK2ca^{IEChom} mice most probably also reflects the tumour-associated inflammation that is known to accompany tumour development.

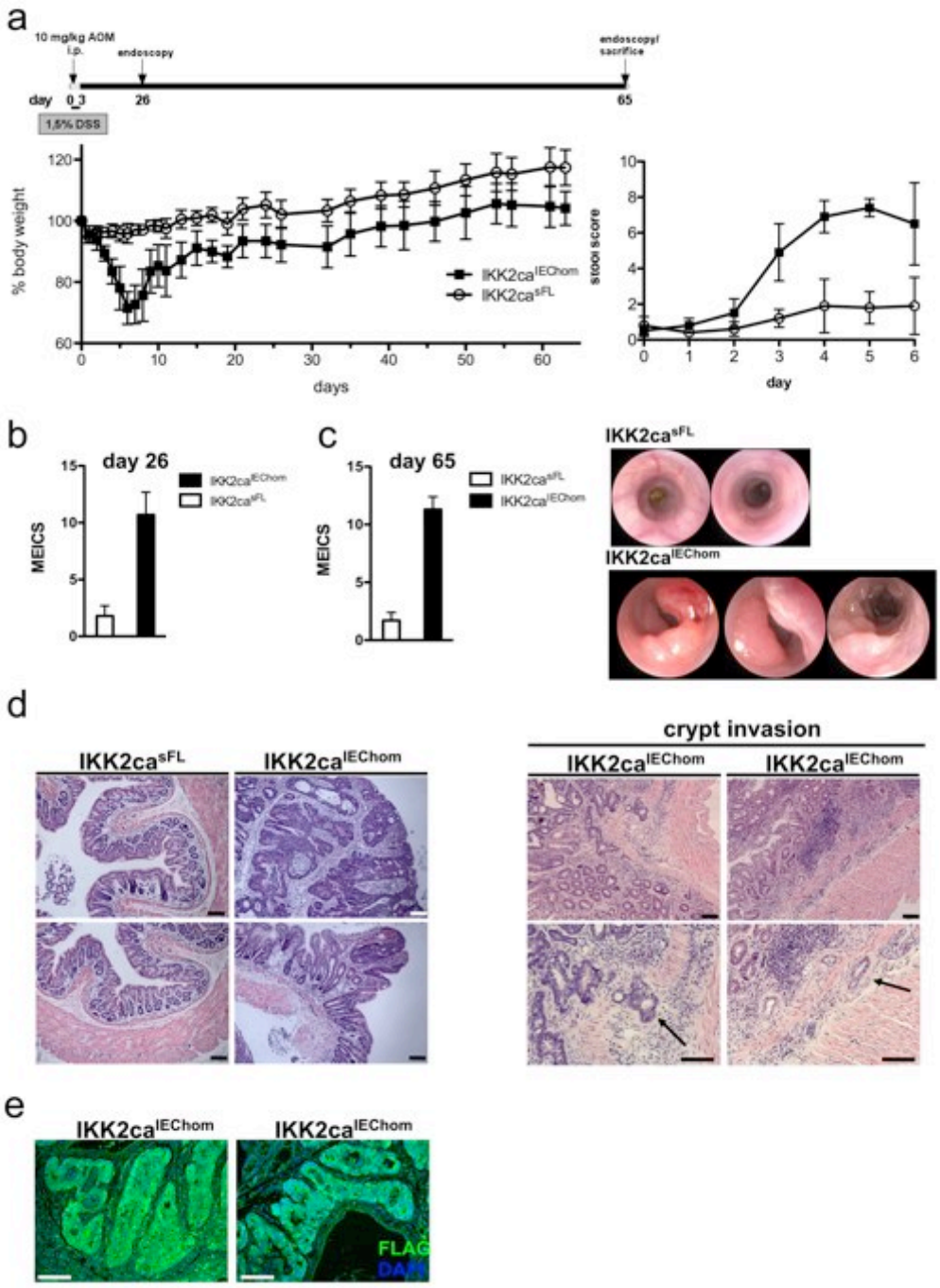

Figure 12 Pronounced AOM/DSS-induced tumour development in IKK2ca^{IEChom} mice
a. An AOM/DSS protocol including one intraperitoneal injection of 10 mg/kg bodyweight AOM and 3 days of 1,5% DSS fed ad libidum resulted in loss of bodyweight in IKK2ca^{IEChom} but not in IKK2ca^{sFL} animals. Diarrhoea and intestinal bleeding occurred in IKK2ca^{IEChom} but not in control mice at the beginning of the experiment. (n ≥ 9)
b. Endoscopy on day 26 of the treatment revealed inflammation in the distal colon of IKK2ca^{IEChom} mice, reflected in a heightened MEICS. (n ≥ 6)
c. Endoscopic examination on day 65 exhibited signs of inflammation and tumour growth in the distal colon area of IKK2ca^{IEChom} mice and a lack of lesions in IKK2ca^{sFL} animals. Representative endoscopic images of distal colons show tumours in IKK2ca-expressing animals and healthy appearance of distal colons in IKK2ca^{sFL} controls. (n ≥ 6)
d. Histological evaluation of colons after AOM/DSS treatment revealed the presence of broad based adenomatous lesions in IKK2ca^{IEChom} mice but not in controls. In more severely affected IKK2ca^{IEChom} animals invasive adenocarcinomas were identified by invasion of epithelial tissue into the submucosa, indicative of carcinoma development.
e. Immunofluorescent staining for FLAG shows that tumourous epithelial tissue in IKK2ca^{IEChom} mice produced FLAG-IKK2ca. Scale bars represent 50 µm

Histological evaluation of colon tissue did not reveal signs of lesion development in control mice, indicating that the applied protocol was to mild to induce tumourigenesis in these mice (Fig. 12d). In contrast, IKK2ca^{IEChom} mice had developed multiple broad based colonic lesions classified as advanced stage, mucus-producing adenomas. Interestingly, we also observed two IKK2ca^{IEChom} mice displaying events of crypt invasion into the submucosa (Fig. 12d right panel). Invasion of epithelial cells into the submucosa does not occur in adenomas, but happens in lesions that have advanced to the adenocarcinoma state. Therefore, AOM/DSS treatment also leads to adenocarcinoma development in the most severely affected IKK2ca^{IEChom} mice.

Importantly, immunofluorescent staining for FLAG on colon tissue of AOM/DSS-treated IKK2ca^{IEChom} mice indicated that also dysplastic tumour epithelium expressed FLAG-tagged IKK2ca and thus had not escaped Cre-mediated induction of IKK2ca expression (Fig. 12e).

These results therefore show that a mild AOM/DSS tumour protocol was sufficient to induce pronounced tumour growth (adenomatous lesions) and development of malignant adenocarcinomas in IKK2ca^{IEChom} mice, but was not strong enough to trigger a similar tumourigenic response in control mice. Therefore the expression of constitutively active IKK2 in the intestinal epithelium renders mice much more sensitive to AOM/DSS-induced tumour incidence and progression.

The above used AOM/DSS tumour induction protocol depends on inflammation-mediated promotion of tumour growth. Since IKK2ca^{IEChom} mice exhibited an increased susceptibility to DSS-induced intestinal inflammation, the enhanced tumourigenesis observed upon AOM/DSS treatment in these animals most probably, at least partially, resulted from increased and sustained colonic inflammation. In order to uncover potential cell intrinsic functions of IKK2ca in tumour development, we applied a chemically inducible tumour protocol that does not require inflammation for driving tumour growth. For this experiment mice were injected on a weekly basis with 10 mg/kg AOM for five consecutive weeks (Fig. 13). Using this protocol, wild-type C57Bl/6 mice normally show colonic tumour formation 30 weeks after the first AOM-injection (Neufert et al., 2007). Because 12 weeks after the first AOM injection most IKK2ca^{IEChom} mice appeared sick and displayed diarrhoea as well as loss of bodyweight, the animals were endoscopised already at week 13 and sacrificed thereafter. Endoscopic analysis revealed that all IKK2ca^{IEChom} mice had developed

multiple colonic tumours, whereas none of the IKK2ca^{sFL} mice displayed endoscopically detectable tumours. Histological sections revealed thickening of the colonic mucosa and confirmed the presence of big hyperplastic lesions with dysplastic crypts embedded in a reactive stroma in IKK2ca^{IEChom} mice (Fig. 13 left panel). Such lesions were found exclusively in IKK2ca^{IEChom} mice, as none of the control mice had developed tumours. Whereas the small intestine of AOM-injected control mice appeared normal, histological examination of the distal small intestine of IKK2ca^{IEChom} mice revealed the presence of hyperplastic lesions (Fig. 13 right panel). While ileal crypts were elongated, indicating hyperplasia, ileal villi of IKK2ca^{IEChom} mice were shortened and in some areas sparse. Furthermore, some crypts consisted of more than one epithelial cell layer, which is a sign for epithelial dysplasia. Overall the mucosal tissue was thickened and the lamina propria surrounding aberrantly formed crypt structures contained many inflammatory cells (see Fig. 13).

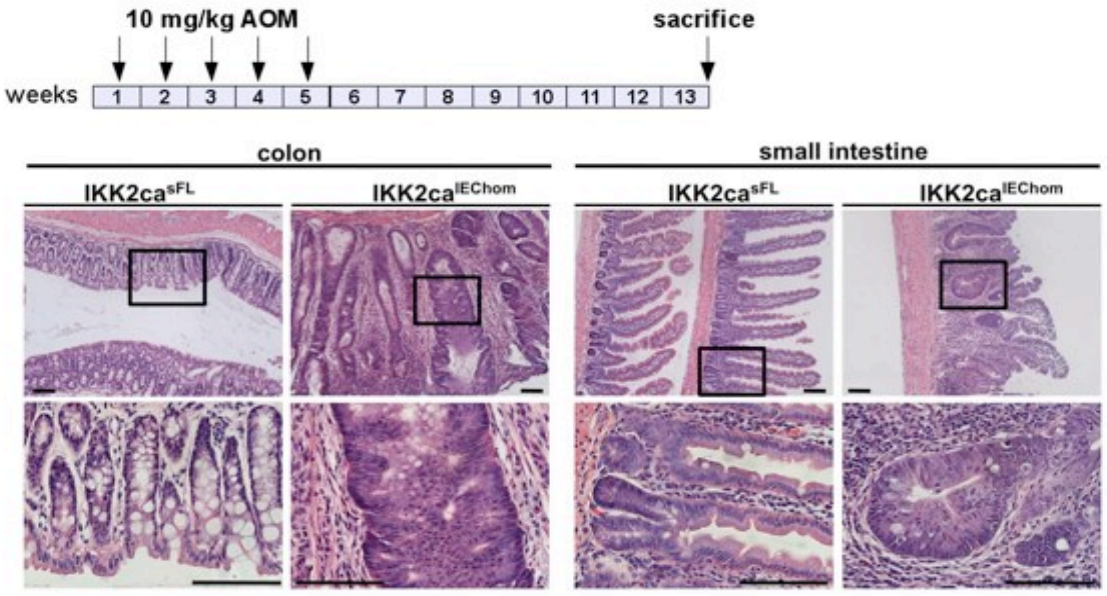

Figure 13 Repetitive AOM-administration triggered early tumour development in IKK2ca^{IEChom} mice

Five weekly injections with 10 mg/kg bodyweight AOM resulted in tumour growth in colons of IKK2ca^{IEChom} mice 13 weeks after the first injection. Wild-type mice did not display colon tumour growth under the same experimental conditions. The small intestine of IKK2ca^{IEChom} mice also showed histological alterations after this treatment. Whereas IKK2ca^{sFL} mice displayed a regular small intestinal tissue structure, in IKK2ca^{IEChom} mice villi were shortened, crypts were hyperplastic and the small intestinal mucosa was inflamed and thickened. ($n \geq 8$)
Scale bars represent 50 µm

These results thus show that IKK2ca^{IEChom} mice develop colon tumours upon repetitive AOM challenge at a time point when control animals had not developed any lesions yet. Furthermore, lesions occurred also in the small intestine of

IKK2ca^{IEChom} mice, a part of the intestinal tract that is normally not affected by AOM treatment.

3.3 Strong cooperativity between Wnt- and IKK2/NF-κB signalling in intestinal tumourigenesis

Mutations leading to activation of the Wnt-pathway are thought to be involved in intestinal cancer development in both humans and mice (Barker and Clevers, 2000). Accordingly, AOM-induced tumourigenesis in rodents was shown to be initiated by mutations mostly affecting β-catenin, the central player in the Wnt-signalling pathway, and thereby lead to its stabilisation (Greten et al., 2004; Takahashi and Wakabayashi, 2004; Tanaka et al., 2003).

Since IKK2ca^{IEChom} mice exhibited increased tumour formation in response to AOM-treatments, we sought to address the effect of IKK2ca in Wnt-induced intestinal tumour development. For this purpose, we used a genetic mouse model of intestinal tumourigenesis expressing a truncated version of the tumour suppressor Apc. The coding sequence of the Apc gene in these mice is interrupted by insertion of a Neo-cassette after amino acid 1638 and therefore these mice are referred to as Apc1638N. Mice that express the mutant Apc1638N allele in a heterozygous manner (Apc1638N homozygous mice are embryonically lethal) spontaneously develop intestinal lesions especially in the proximal part of the small intestine at an age of 5 to 6 months (Fodde et al., 1994). Lesions in the colon are rare and were reported to occur only in one-year-old Apc1638N animals (Fodde et al., 1994). For our studies we generated Apc1638N mice that expressed IKK2ca in IECs in a heterozygous manner (Apc1638N/IKK2ca^{IEChet}).

Whereas the colon of 16-week-old Apc1638N/IKK2ca^{sFL} mice on endoscopic examination did not show signs of tumour development, every monitored Apc1638N/IKK2ca^{IEChet} mouse harboured at least one clearly detectable distal colon tumour. Apc1638N/IKK2ca^{IEChet} mice had a higher MEICS when compared to Apc1638N/IKK2ca^{sFL}, IKK2ca^{sFL} and IKK2ca^{IEChet} mice, which could be caused by tumour associated inflammation (Fig. 14a). *Ex vivo* examination revealed tumour growth also in the proximal colon area in most Apc1638N/IKK2ca^{IEChet} animals (Fig. 14b). None of the control mice (Apc1638N/IKK2ca^{sFL}, IKK2ca^{sFL} and IKK2ca^{IEChet}mice) harboured macroscopically visible tumours in any part of the large intestine.

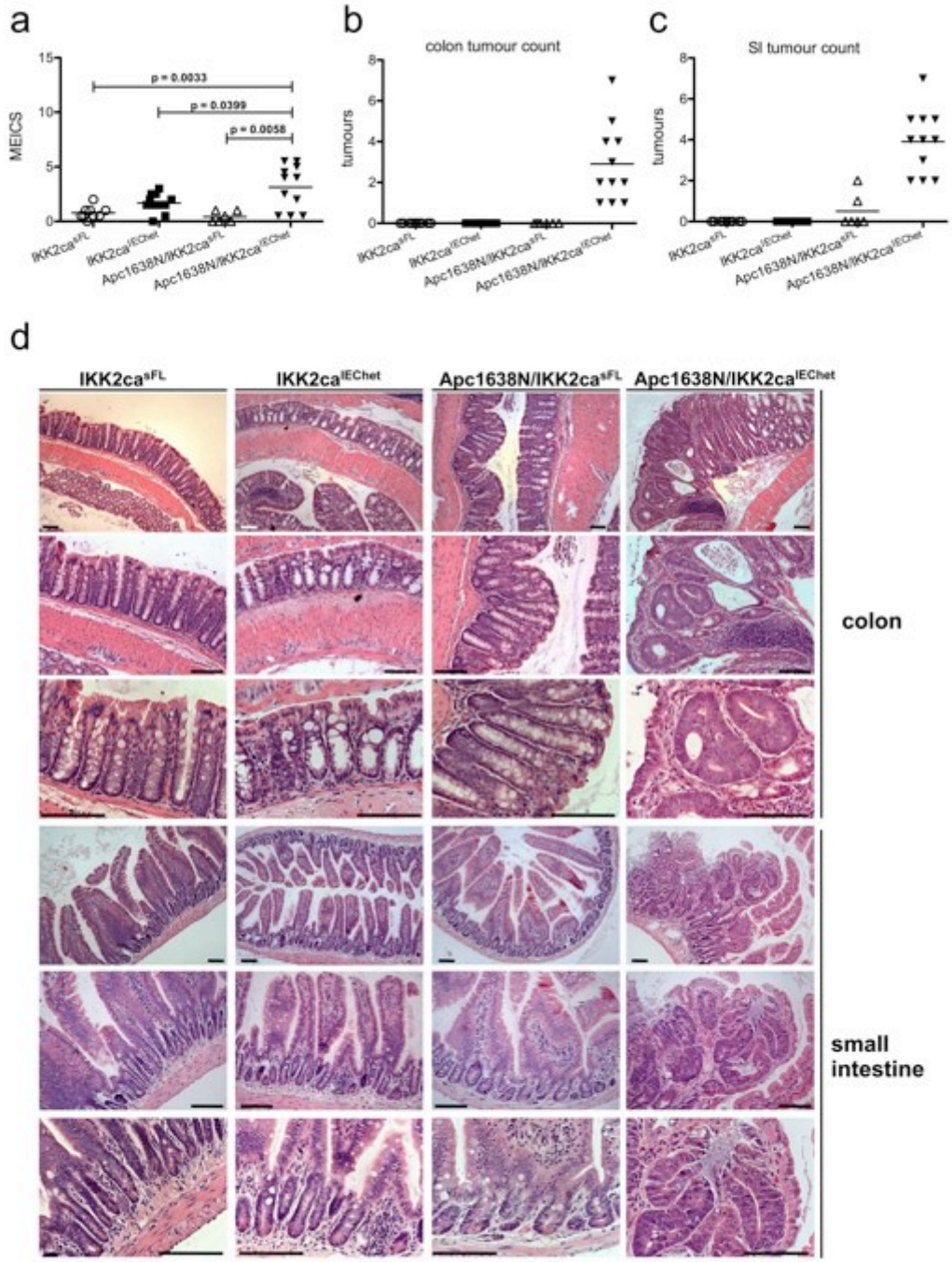

Figure 14 Accelerated tumour formation in Apc1638N/IKK2ca^{IEChet} mice

a. Endoscopy of distal colon did not demonstrate inflammation or presence of tumours in 4-month-old Apc1638N/IKK2ca^{sFL} mice (n = 6). Apc1638N/IKK2ca^{IEChet} mice (n = 11) exhibited a moderately increased MEICS due to tumour development and inflammation. IKK2ca^{sFL} (n = 9) and IKK2ca^{IEChet} (n = 11) mice appeared healthy.

b. Macroscopic examination of colons revealed tumour growth in all Apc1638N/IKK2ca^{IEChet} mice examined at 16 to 17 weeks of age (n = 11), whereas Apc1638N/IKK2ca^{sFL} (n = 6), IKK2ca^{IEChet} (n = 11) and IKK2ca^{sFL} mice (n = 9) did not have lesions.

c. The proximal halves of small intestines of all monitored four-month-old Apc1638N/IKK2ca^{IEChet} mice contained polypoid lesions (n = 11). Only 2 out of 6 Apc1638N/IKK2ca^{sFL} mice had developed one or two small polyps in the duodenal region of the small intestine. IKK2ca^{IEChet} (n = 11) and IKK2ca^{sFL} mice (n = 9) did not have small intestinal lesions.

d. Histological evaluation of colon and small intestinal sections from Apc1638N/IKK2ca^{IEChet} mice confirmed the presence of adenomatous tumours in both tissues. Lesions in the colon displayed hyperplastic, as well as dysplastic crypt growth characterized by a multilayered epithelium and loss of differentiated cells. Small intestinal polyps harboured hyperplastic and also dysplastic, aberrantly shaped crypts with epithelial stratification and loss of differentiation. No tumourous lesions were found in colon sections of any other genotype, and the small intestines appeared normal.

Scale bars represent 50 µm

The small intestine of 16 to 17-week-old mice was opened longitudinally and the whole tissue was screened for macroscopically visible polyps. As expected, none of the IKK2ca^{sFL} and IKK2ca^{IEChet} mice had lesions in the small intestine (Fig. 14c). While 2 out of 6 Apc1638N/IKK2ca^{sFL} mice contained 1 or 2 small polyps in the proximal duodenal part of the small intestine, all 11 Apc1638N/IKK2ca^{IEChet} mice had developed multiple clearly detectable polyps in the proximal half of the small intestine (Fig. 14c). This observation shows that heterozygous expression of IKK2ca in IECs strongly accelerates and amplifies tumour development in the small intestine of Apc1638N mice and furthermore leads to tumour growth also in the colon.

Histological examination of swiss-rolled colon tissue of Apc1638N/IKK2ca^{IEChet} mice confirmed the presence of lesions growing both in the distal and proximal part of the colon. Colonic tumours in these mice were characterized by hyperplastic elongated crypts and aberrantly shaped crypt structures growing on top of each other (Fig. 14d). Dysplastic crypts were identified by lack of differentiation and epithelial stratification, meaning that crypts were composed of multiple layers of epithelial cells. In addition, lesions were infiltrated with immune cells and occasionally developed submucosal oedema. The colonic mucosa of Apc1638N/IKK2ca^{sFL} mice appeared normal with no signs of altered crypt structures. No marked differences were observed in the histological appearance of colons from IKK2ca^{sFL} and IKK2ca^{IEChet} mice (Fig. 14d). In some cases though, IKK2ca^{IEChet} mice showed confined immune cell infiltrations in the mucosa (see Fig. 14d, colon). This occurred in a patchy, discontinuous fashion and did not lead to an alteration of the epithelial tissue architecture.

Polyps located in the proximal small intestine of 4-month-old Apc1638N/IKK2ca^{IEChet} animals displayed alteration of crypt villus organisation, with aberrantly formed crypts expanding to the villus area of the intestine (Fig. 14d). Enlarged crypts exhibiting epithelial stratification and loss of differentiation were growing on top of each other and made a major contribution to the polyp mass. Polyps additionally displayed immune cell infiltrates, which most probably reflected tumour associated inflammation. These kinds of lesions were not found in the small intestine of IKK2ca^{IEChet} or IKK2ca^{sFL} mice. These results provide experimental evidence that expression of IKK2ca in the intestinal epithelium of Apc1638N mice strongly synergized with Wnt-induced tumour formation, resulting in much earlier and more aggressive polyp formation in the intestine of Apc1638N/IKK2ca^{IEChet} mice.

Immunohistochemical staining for Ki67 revealed increased proliferation of IECs in hyperplastic and dysplastic crypts in Apc1638N/IKK2ca^{IEChet} mice (Fig. 15a). Colon tumours in Apc1638N/IKK2ca^{IEChet} mice exhinbited strongly enhanced proliferation, as most of the epithelial cells in the tumours were Ki67 positive. Also small intestinal polyps displayed increased proliferative activity, since Ki67 positive IECs were identified throughout the lesions including the mucosal area towards the lumen (Fig. 15a). The proliferation pattern of IECs in Apc1638N/IKK2ca^{sFL} mice in the colon and the small intestine was not altered when compared to control IKK2ca^{sFL} mice (Fig. 15a). Occasionally IKK2ca^{IEChet} mice showed scattered areas with increased IEC proliferation in colon and small intestinal tissue. This manifested in an extension of Ki67 positive cells towards the lumen. However overall the Ki67 staining pattern in both parts of the intestine did not differ considerably between IKK2ca^{IEChet} and IKK2ca^{sFL} mice at 4 months of age (Fig. 15a).

In order to address the level of β-catenin activation in intestinal lesions an immunostaining for Sox9, a transcription factor encoded by a β-catenin target gene, was performed. Sox9 normally is expressed at high levels in stem cells, in Paneth cells and in some subtypes of enteroendocrine cells, but is expressed to a lesser extent in non-differentiated TA cells. Almost all IECs in tumours growing in the colon of Apc1638N/IKK2ca^{IEChet} mice were positive for Sox9, suggesting that in these cells β-catenin was activated (Fig. 15b). Sox9 was also detected in IECs close to the apical part of dysplastic crypts, indicating that these cells had not undergone terminal differentiation and had maintained their proliferating capacities. This Sox9 expression pattern is in accordance with the Ki67 staining observed in these areas. Accordingly, small intestinal lesions of Apc1638N/IKK2ca^{IEChet} mice also exhibited an expansion of Sox9 expressing cells, suggesting that the β-catenin pathway was active in these cells as well. Overall the Sox9 and Ki67 staining patterns in tumourous tissues correlated, indicating an increase in β-catenin activity and concomitantly elevated proliferation capacity.

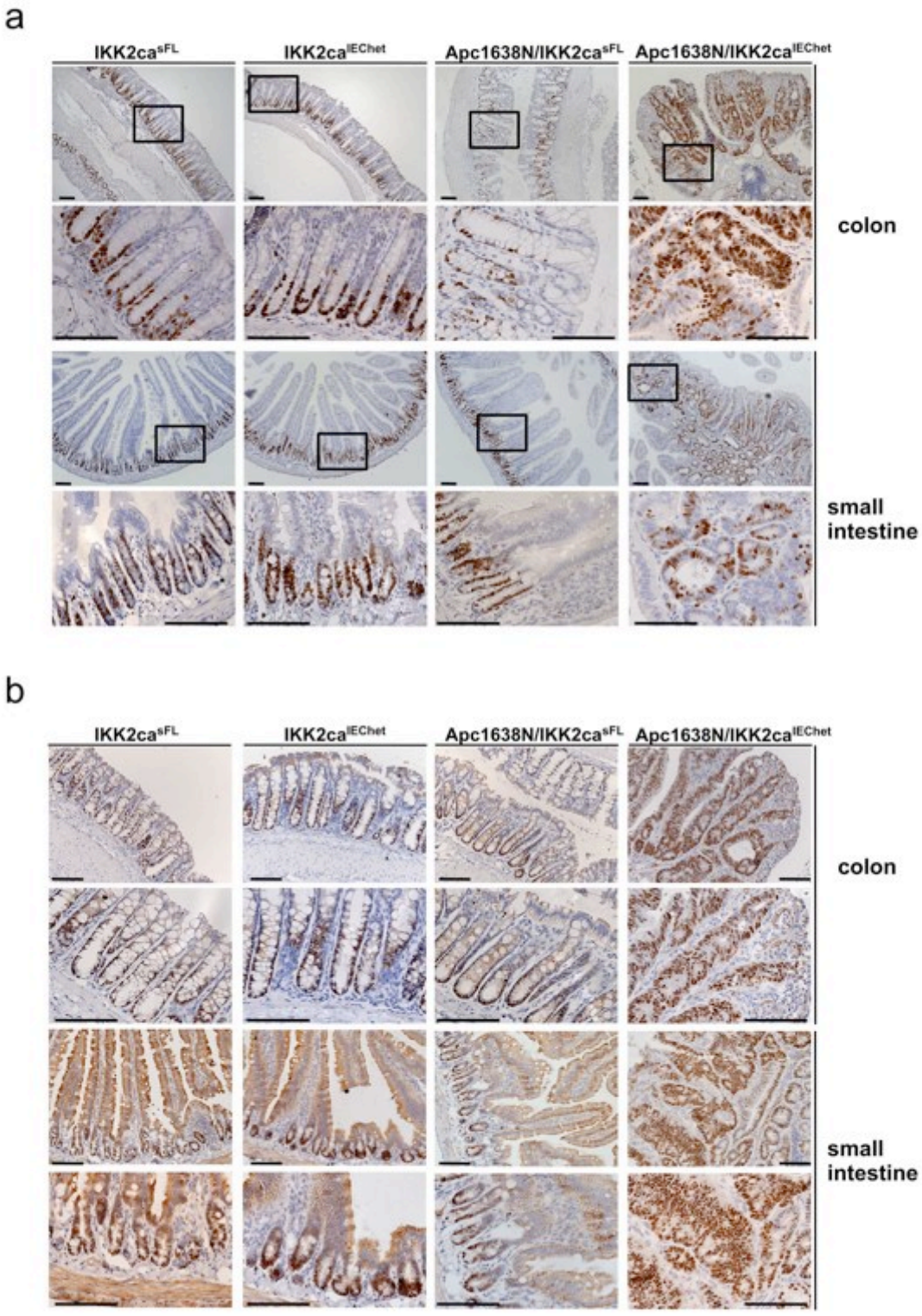

Figure 15 Increased proliferation and β-catenin activation in tumours of Apc1638N/IKK2ca^{IEChet} mice

a. Immunohistochemical staining for the proliferation marker Ki67 on colon and small intestinal sections revealed normal Ki67 staining patterns in both tissues of Apc1638N/IKK2ca^{sFL}, IKK2ca^{IEChet} and IKK2ca^{sFL} animals. However, Apc1638N/IKK2ca^{IEChet} mice showed increased epithelial proliferation in lesions of the colon and the small intestine.

b. Immunostaining for Sox9 revealed the presence of Sox9 expressing cells at the lower part of colonic crypts in both IKK2ca^{sFL} and IKK2ca^{IEChet} animals. The same staining pattern was also visible in Apc1638N/IKK2ca^{sFL} mice, whereas colon tumours in Apc1638N/IKK2ca^{IEChet} mice displayed strong Sox9 staining in all IECs. In the small intestine of IKK2ca^{sFL}, IKK2ca^{IEChet} and Apc1638N/IKK2ca^{sFL} mice Sox9 staining was restricted to the crypt area. Most epithelial cells of small intestinal polyps in Apc1638N/IKK2ca^{IEChet} mice were positive for Sox9. Scale bars represent 50 µm

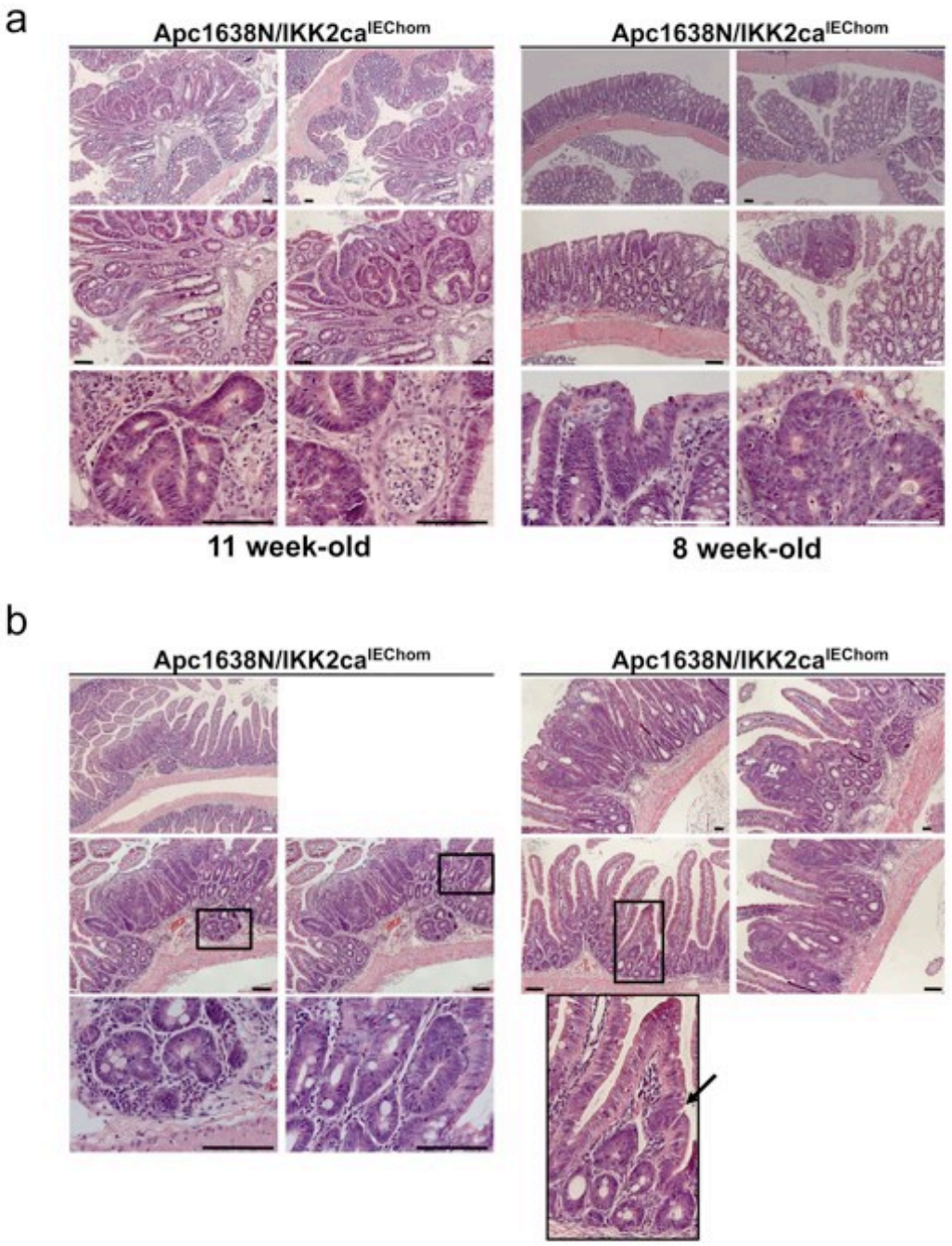

Figure 16 Early tumour development in Apc1638N/IKK2ca^{IEChom} mice
a. At 11 weeks of age Apc1638N/IKK2ca^{IEChom} mice exhibited advanced tumour growth in the colon. Also 8-week-old animals harboured dysplastic lesions in the proximal colon area.
b. Polyp formation in the small intestine was strongly accelerated in 8-week-old Apc1638N/IKK2ca^{IEChom} mice, resulting in severe crypt hyperplasia and ectopic crypt formation throughout the small intestine.
Scale bars represent 50 µm

When IKK2ca expression levels in IECs from Apc1638N mice were even more increased by generating Apc1638N/IKK2ca^{IEChom} mice, the development of tumourous lesions was further accelerated. Already at an age of 8 weeks the colon of Apc1638N/IKK2ca^{IEChom} animals contained hyperplastic crypts and also dysplastic tumourous tissue, whereas at 11 weeks of age tumour size and numbers in the colon

had further increased (Fig. 16a). The small intestine was more severely affected by polyp formation in these Apc1638N/IKK2ca^{IEChom} mice. Throughout the whole small intestine crypts were growing on top of each other, indicative for strongly enhanced proliferation and a lack of tissue organisation (Fig. 16b). Occasionally crypts crowded the basal part of the mucosa and formed clusters surrounded by few inflammatory cells and fibroblasts. Villi were short and sometimes contained crypt structures, indicating ectopic crypt formation (Fig. 16b). The latter culminated in crypt structures that grew in villi, generating so called crypt cysts, where IECs proliferate outside the regular crypt area.

3.4 Spontaneous intestinal tumour development accompanied by strong inflammation in aged IKK2ca^{IEChom} mice

The described in the previous section showed that epithelial specific expression of IKK2ca strongly enhanced tumourigenesis in different inflammation-dependent, carcinogen-induced and genetic models of intestinal cancer. These results suggest that constitutively increased IKK2 activity in IECs affects fundamental cellular processes important for intestinal carcinogenesis to promote tumour development. To address whether constitutively increased IKK2 activity was sufficient to induce spontaneous development of intestinal tumours, a cohort of IKK2ca^{IEChom} and littermate control mice ageing for 12 months was followed and tumour development was assessed by endoscopy and post-mortem macroscopic and histological examination.

At different time points during their lifetime a fraction of these animals became sick. Diseased mice suffered from diarrhoea and weight loss. More severely affected mice developed a rectal prolapse and intestinal bleeding as assessed on the presence of blood in loose stool. Rectal prolapse developed at random ages in IKK2ca^{IEChom} mice, with the youngest mouse displaying prolapse formation at 7 weeks of age. Mice with rectal prolapse were sacrificed and post-mortem analysis revealed, irrespective of their age, severe inflammation in the colonic mucosa. Cross sections of colon tissue revealed areas that were dramatically thickened and had a tumour-like appearance (Fig. 17a). These regions harboured aberrantly shaped hyperplastic and even dysplastic crypt structures (Fig. 17a and 17b), indicating that the early inflammatory phenotype of young mice had progressed into epithelial alterations in the colon.

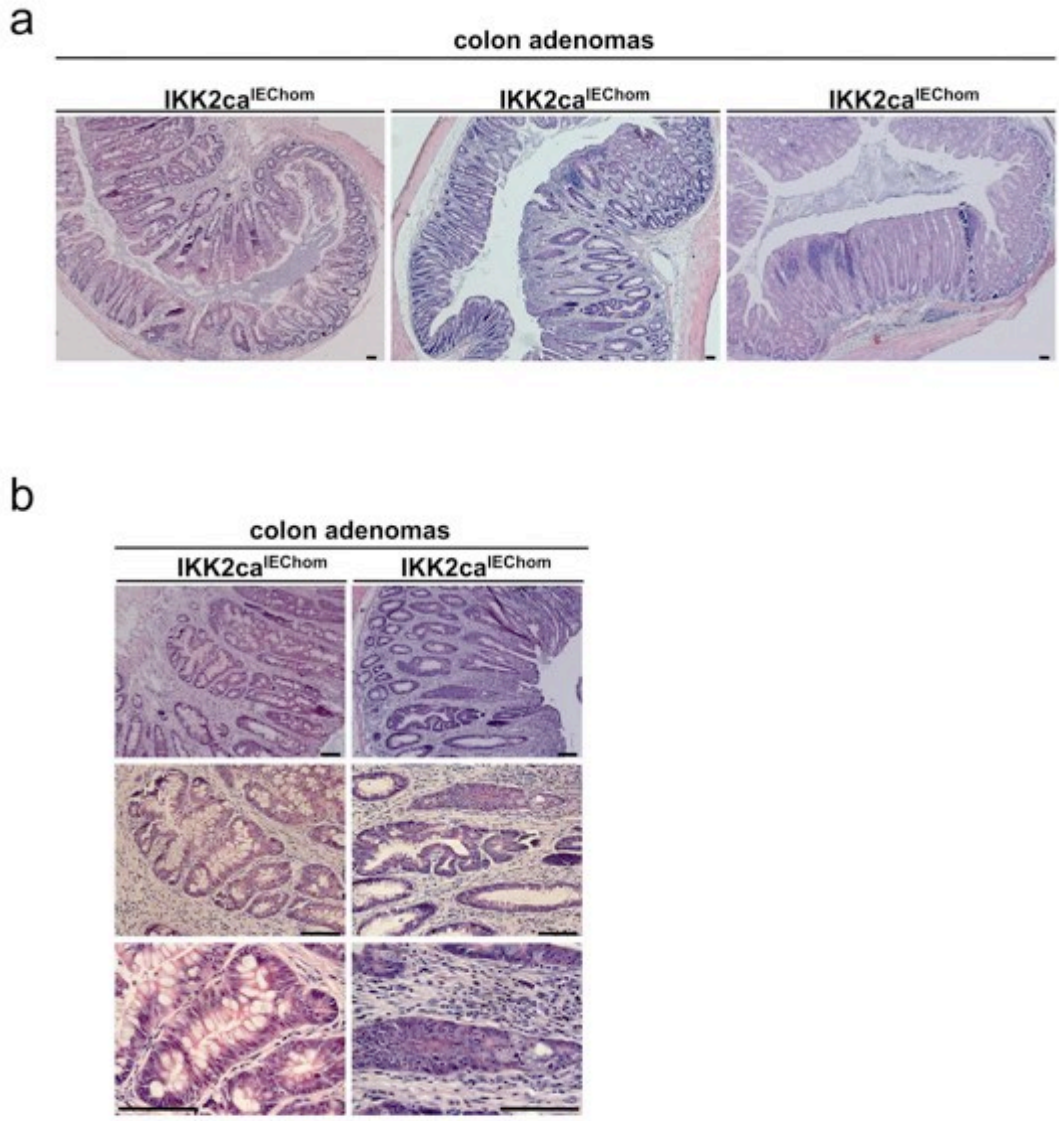

Figure 17 Epithelial dysplasia in the colon of IKK2ca^{IEChom} mice with rectal prolapse
a. Small power magnification of histological cross-sections from the colon depicting pronounced thickening of one part of the mucosa occurring in IKK2ca^{IEChom} mice that had developed a rectal prolapse.
b. High power magnification images reveal the presence of complex crypt structures (left panel) and epithelial dysplasia (right panel) in colon tissue from IKK2ca^{IEChom} animals with a rectal prolapse.
Scale bars represent 50 µm

IKK2ca^{IEChom} mice that had not developed a rectal prolapse and reached the age of at least 48 weeks were subjected to endoscopic examination. Endoscopy revealed inflammation of the distal colon in most monitored IKK2ca^{IEChom} mice, whereas age matched and cohoused control animals were healthy (Fig. 18a). Diseased animals showed bowel wall thickening, perturbations in the vessel structure and loose stool. Furthermore, the mucosal surface appeared granular. Endoscopy revealed the presence of tumour-like lesions in the distal part of the colon in about 50% of these old mice (Fig. 18b). Histological examination of colons from aged IKK2ca^{IEChom} mice demonstrated the presence of tumourous lesions not only in the distal area, but also

in the proximal part of the colon. The colon was inflamed, as reflected by infiltration of immune cells both in the mucosa and submucosa (Fig. 18c). Importantly, inflamed colons exhibited epithelial hyperplasia as identified by crypt elongation and the presence of aberrantly formed crypt shapes (denoted hyperplasia in colon histological sections of IKK2ca^{IEChom} mice in Fig. 18c). Hyperplastic colonic crypts had developed protrusions that grew out sideways from the crypt axis and resulted in complex crypt structures. Furthermore, about 30% of the aged IKK2ca^{IEChom} mice harboured colonic crypts that showed lack of differentiation and stratified epithelium (denoted as dysplasia in colon histological sections of IKK2ca^{IEChom} mice in Fig. 18c). These crypts were embedded in a so-called “reactive stroma”, which is a mucosa containing many inflammatory cells and myofibroblasts. Myofibroblasts are activated fibroblasts that produce various cytokines, chemokines and growth factors and that are thought to sustain inflammation and promote proliferation of adjacent cells (Franco et al., 2010). These myofibroblasts were identified by their elongated shape and reddish colour due to the strong eosin staining intensity of myofibres (indicated in the pop-up figure by a white arrow-head in Fig. 18c).

Also the small intestine of aged IKK2ca^{IEChom} mice exhibited signs of intestinal disease. The small intestine was enlarged, which is reflected in a larger diameter of the tissue visible on histological cross sections in Fig. 18d. Inflammatory cell infiltrates in the mucosa were located around the crypts and crypts arranged themselves on top of each other, indicative of enhanced proliferation (denoted as hyperplasia and adenoma in small intestine histological sections of IKK2ca^{IEChom} mice in Fig 18d). In 40% out of the analysed one-year-old IKK2ca^{IEChom} mice adenomatous lesions had developed either in the proximal or in the distal part of the small intestine. These adenomas harboured crypts that stacked on top of each other and had lost the regular pattern of crypt arrangement visible in control mice (see Fig. 18d). Such areas displayed loss of villus structures that were replaced by enlarged crypts growing in a disorganised way. Despite the pronounced hyperplasia of the small intestinal mucosa, differentiation of epithelial cells was not completely abrogated. Adenomatous crypts gave rise to goblet cells and epithelial stratification was rare. However, Paneth cells, which like goblet cells belong to the secretory cell lineage, were absent from adenomatous lesions (see adenoma in Fig. 18d). Therefore lesions identified in the small intestines of IKK2ca^{IEChom} mice were less advanced than colon tumours.

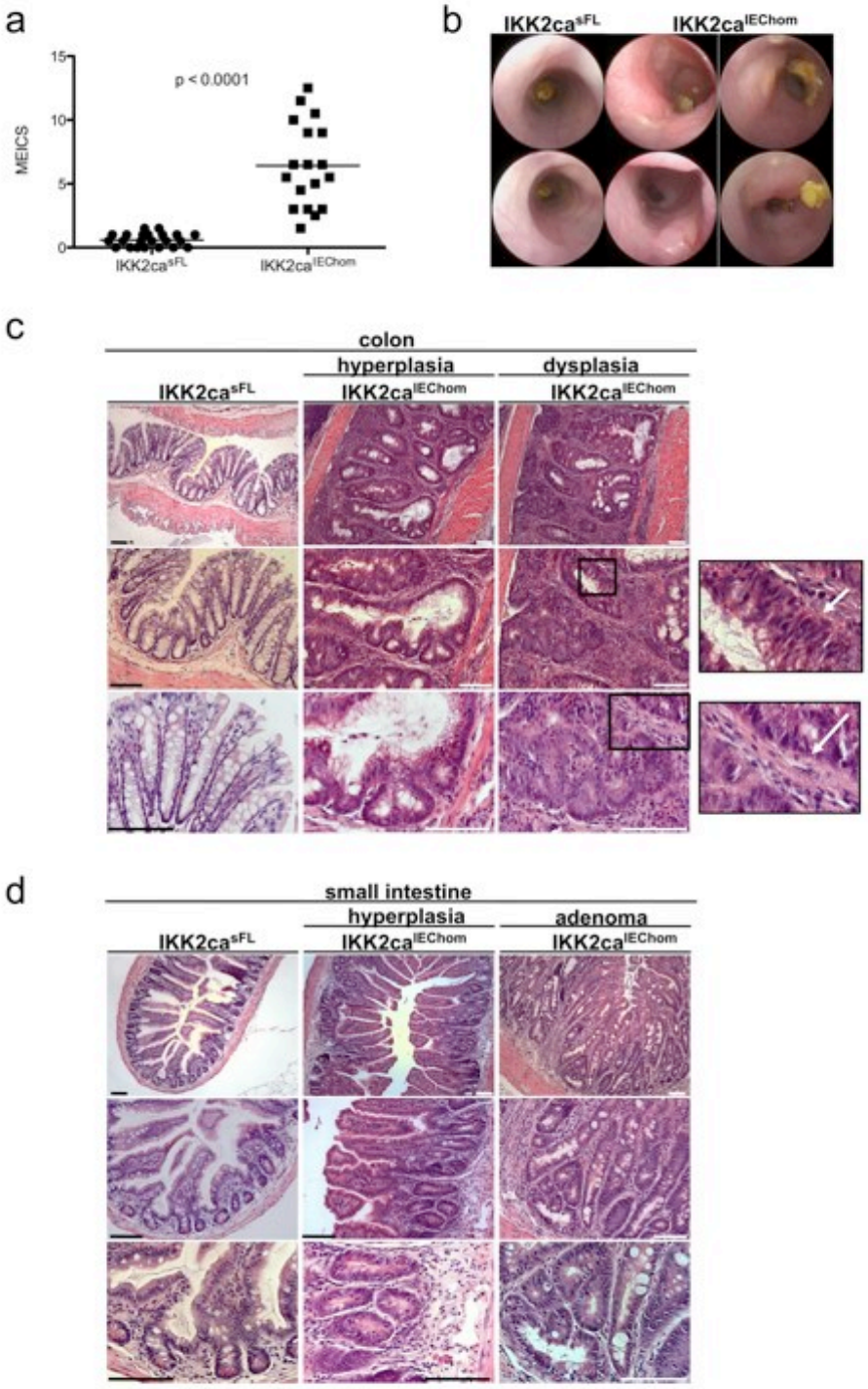

Figure 18 Spontaneous inflammation and intestinal tumourigenesis in old IKK2ca^{IEChom} mice
a. Endoscopy of aged mice (≥ 48 weeks) revealed heightened MEICS in IKK2ca^{IEChom} mice due to inflammation in the distal colon, as reflected in bowel wall thickening, altered vascularisation structure and granularity of the mucosa, indicating intestinal disease. (n≥18)
b. Representative endoscopic images depicting tumourous structures with distinctive vascularisation found in the distal colon of 50% of examined aged IKK2ca^{IEChom} mice. Age matched IKK2ca^{sFL} control animals did not show signs of inflammation or tumour growth.
c. Histological analysis of colon tissue from IKK2ca^{IEChom} mice revealed the presence of tumours characterized by a thickened mucosa, crypt hyperplasia and strong inflammation. More severely affected animals also harboured dysplastic crypt structures surrounded by inflammatory cells. White arrows indicate dysplastic IECs and myofibroblasts.
d. Histological examination of small intestines of IKK2ca^{IEChom} mice revealed inflammation also in this part of the gastrointestinal tract. Hyperplasia was identified by an increase in crypt numbers. Adenomas were present in more severely affected mice.
Scale bars represent 50 µm

Immunostaining for Ki67 revealed an increased number of proliferating epithelial cells in the tumourous colonic mucosa of IKK2ca^{IEChom} mice (Fig. 19a). All hyperplastic and dysplastic IECs in IKK2ca^{IEChom} mice were positive for Ki67. Furthermore, apical IECs lining the lumen also expressed Ki67, indicating that these cells had maintained their proliferating capacities and presumably had not undergone terminal differentiation. In age matched IKK2ca^{sFL} animals proliferating cells were restricted to the transit-amplifying region of colonic crypts (Fig. 19a).

Also small intestinal crypts of IKK2ca^{IEChom} mice exhibited an increased level of proliferation, as judged from the Ki67 staining pattern. The base of small intestinal crypts from control animals harbours the terminally differentiated Paneth cells that do not produce Ki67. Therefore, cells located at the crypt base are mostly negative for proliferation markers such as Ki67. The actively cycling Lgr5-positive stem cells, that do express Ki67, are thought to be responsible for some Ki67 positive nuclei present at crypt bases (Barker et al., 2007). This staining pattern is reflected in control small intestinal cross sections, as seen in Fig. 19a, where few Ki67 positive cells with elongated nuclei are located in between the Ki67 negative Paneth cells. In contrast, almost all crypt IECs from IKK2ca^{IEChom} mice were positive for Ki67, including the epithelial cells at the crypt base (Fig. 19a).

The staining pattern for Sox9 was perturbed in lesioned areas of IKK2ca^{IEChom} mice, both in the colon and the small intestine (Fig. 19b). Similar to the Ki67 immunohistochemistry, all IECs in hyperplastic colonic crypts strongly expressed Sox9. Also apical IECs at the very luminal part of the colonic mucosa were positive for this transcription factor that is indicative of β-catenin activity. In contrast, Sox9 expression in IECs of one-year-old IKK2ca^{sFL} mice was restricted to the lower two thirds of crypts. In the small intestine Sox9 producing IECs were visible throughout the adenomatous lesions of IKK2ca^{IEChom} mice, whereas in control tissue Sox9 positive cells were restricted to crypts (Fig. 19b).

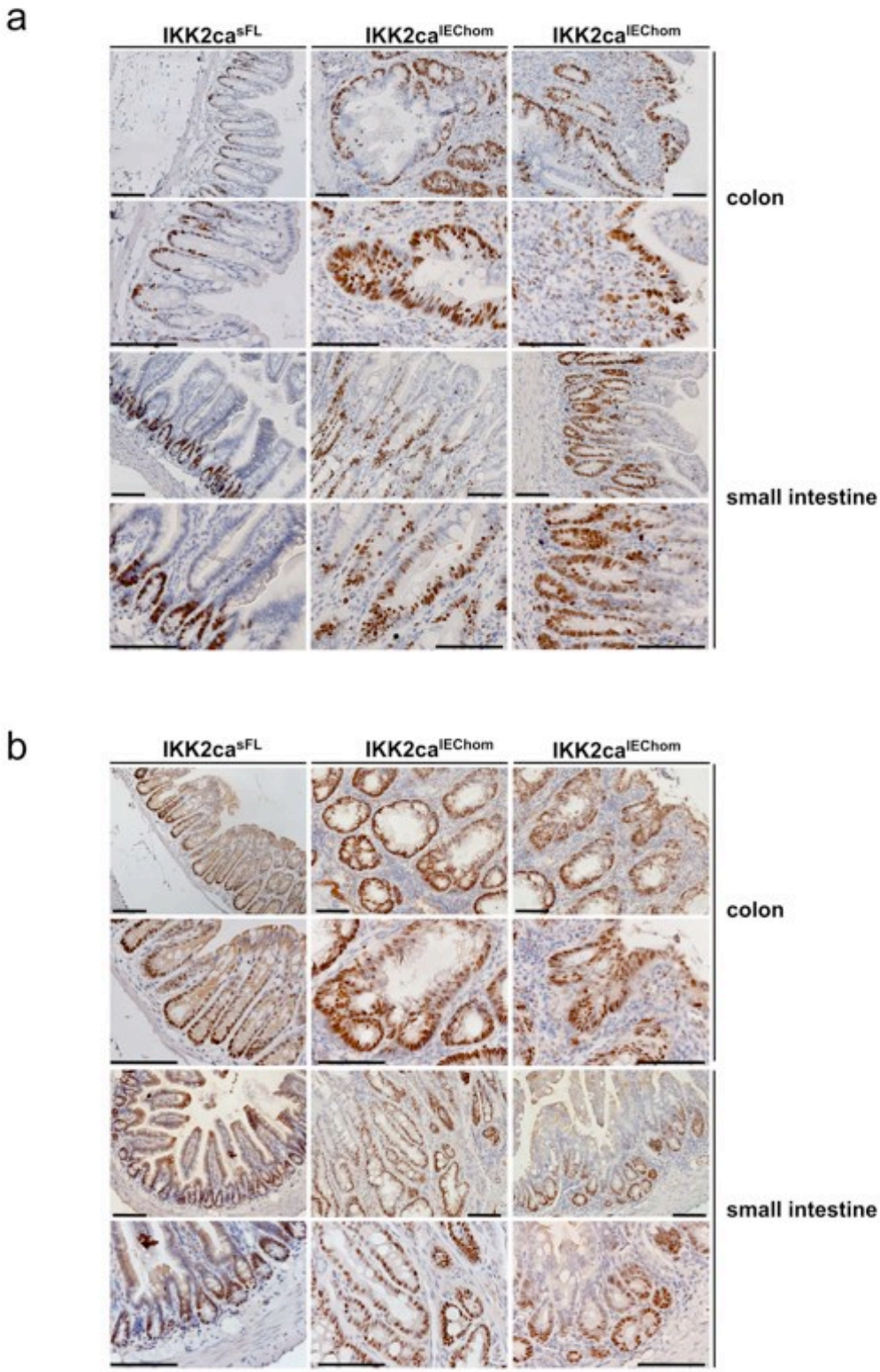

Figure 19 Increased proliferation and β-catenin activation in the intestinal epithelium of aged IKK2ca^{IEChom} mice

a. Immunohistochemical analysis for Ki67 expression revealed heightened proliferative activity in lesions of the colon and the small intestine of aged IKK2ca^{IEChom} mice, indicating an expansion of the proliferating epithelial compartment. Age matched IKK2ca^{sFL} mice displayed a normal staining pattern for Ki67 in both tissues.

b. Staining for Sox9 showed increased expression of this factor in IECs of tumours in IKK2ca^{IEChom} mice, indicating increased β-catenin activity in these areas. Staining for Sox9 was restricted to the proliferating crypt area both, in the colon and the small intestine of wild-type controls.

Scale bars represent 50 µm

These results show that epithelial restricted expression of constitutively active IKK2 is sufficient to induce tumour development in the colon and the small intestine of aged IKK2ca^{IEChom} mice. Tumourous lesions displayed enhanced activation of β-catenin as judged by increased levels of Sox9 expression and a concomitant increase in IEC proliferation.

3.5 Increased stabilisation and activation of β-catenin in the intestine of young IKK2ca^{IEChom} mice

To understand the mechanisms underlying spontaneous tumour development in IKK2ca^{IEChom} mice, young IKK2ca^{IEChom} mice that had not developed lesions yet were analysed in more detail. Since we observed a strong cooperativity between IKK2ca-expression and Wnt-signalling in tumour development, we assessed the status of b-catenin activity in young IKK2ca^{IEChom} animals. IHC for β-catenin showed increased abundance of the protein in colonic IECs from 8-week-old IKK2ca^{IEChom} mice compared to age matched controls (Fig. 20a). For this β-catenin IHC protocol, colon sections from IKK2ca^{IEChom} and IKK2ca^{sFL} mice were cut at the same thickness and placed on the same slide in order to make sure that control and transgenic tissue was treated the same way during the staining procedure and was exposed to 3,3'-Diaminobenzidine (DAB) for the same time during the enzymatic staining reaction. The observed difference in β-catenin levels on IHC was confirmed by Western Blot analzsis performed with protein extracts from colonic and small intestinal IECs (Fig. 20b and 20c). IKK2ca^{IEChom} mice showed higher protein levels of β-catenin in cytoplasmic and nuclear fractions of colon IECs when compared to IKK2ca^{sFL} controls. Importantly also protein levels of the active, N-terminally not phosphorylated and therefore degradation resistant form of β-catenin, were increased in both cell fractions from IKK2ca-expressing colonic IECs (Fig. 20b). The level of total b-catenin protein was also elevated in primary small intestinal IECs as seen in Fig. 20c, where crude protein extracts were probed for β-catenin expression. Higher amounts of nuclear as well as active β-catenin imply that IECs from young IKK2ca^{IEChom} mice have higher β-catenin transcriptional activity than control mice.

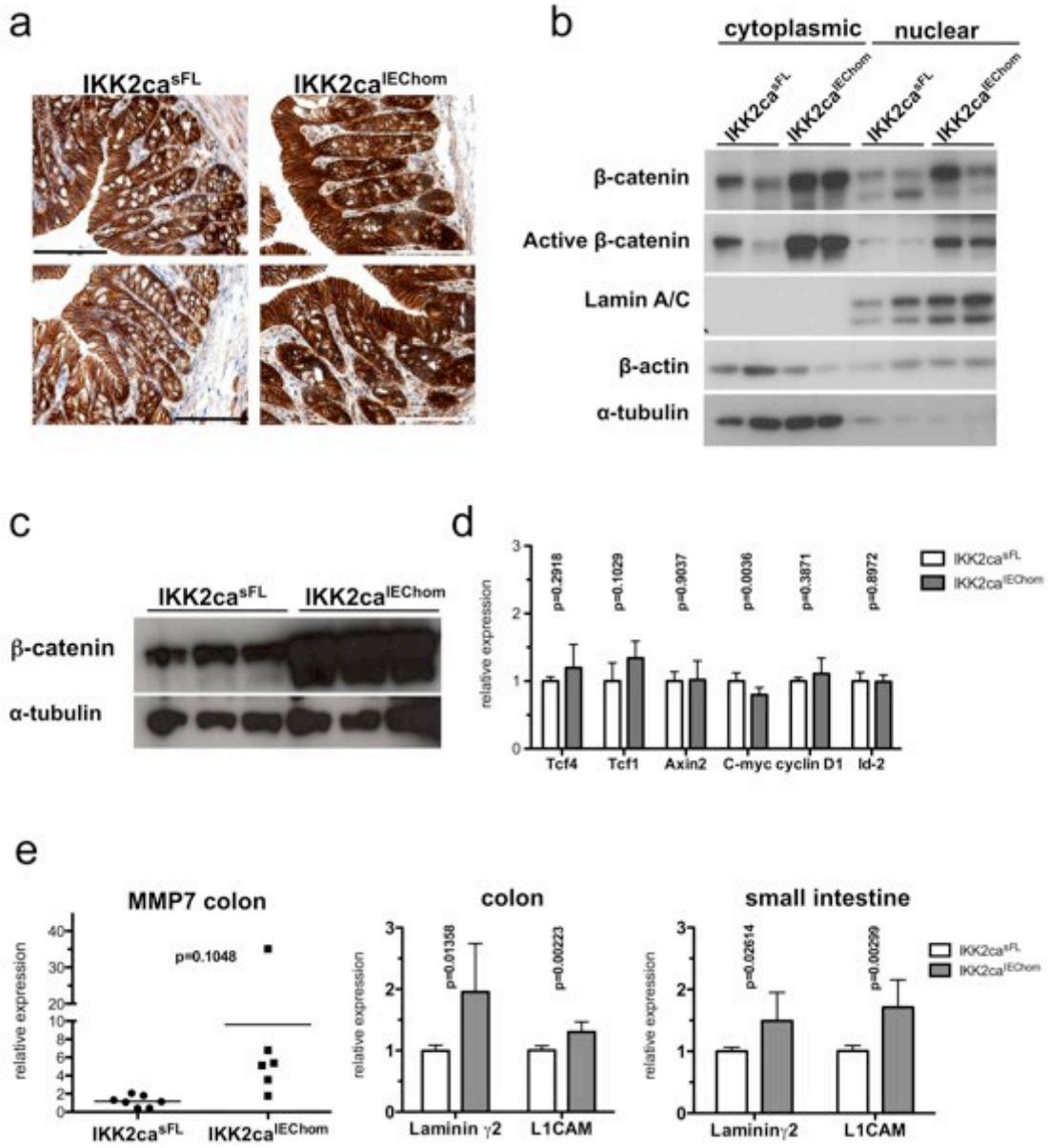

Figure 20 Increased levels of β-catenin and selective induction of β-catenin target genes in the intestine of young IKK2ca^{IEChom} mice

a. Immunohistochemical staining for β-catenin revealed an increased abundance of β-catenin in colon IECs of 9-week-old IKK2ca^{IEChom} mice when compared to age matched IKK2ca^{sFL} littermates.

b. Western Blot analysis of nuclear and cytoplasmic extracts prepared from colon epithelial cells from 8-week-old animals revealed increased amounts of β-catenin in cytoplasmic and nuclear fractions from IKK2ca-expressing IECs compared to protein extracts prepared from wild-type mice. Importantly, active N-terminally non-phosphorylated and therefore degradation resistant β-catenin accumulated at higher levels in cytoplasmic and nuclear extracts from colon IECs of IKK2ca^{IEChom} mice.

c. Lysates of small intestinal IECs derived from IKK2ca^{IEChom} mice contained higher amounts of β-catenin when compared to protein extracts from IKK2ca^{sFL} control mice.

d. Quantitative RT-PCR analysis did not reveal differential mRNA expression of various β-catenin target genes and Wnt-signalling components in colon IECs from 8-week-old IKK2ca^{IEChom} and IKK2ca^{sFL} mice. (n = 5)

e. Increased mRNA levels of a subset of β-catenin target genes were identified in colon and small intestinal tissue of IKK2ca^{IEChom} mice at 7 to 8 weeks of age when compared to age matched controls. MRNAs coding MMP7, Laminin γ2 and L1CAM, that are known to be under the control of β-catenin, were produced at higher levels in IKK2ca^{IEChom} mice when compared to IKK2ca^{sFL} controls. (n ≥ 6)

Scale bars represent 50 µm

Despite these observations suggesting higher β-catenin transcriptional activity, quantitative RT-PCR did not reveal increased expression levels of a number of β-catenin target genes such as c-myc, Cyclin D1 and Axin2 in colon IECs from IKK2ca^{IEChom} mice at eight weeks of age (Fig. 20d). However, some β-catenin regulated genes were expressed at higher levels in the intestine of IKK2ca^{IEChom} mice. Indeed, mRNA levels of MMP7 were increased in proximal colon tissue of IKK2ca^{IEChom} mice. Laminin γ2 and L1CAM were higher in both the colon and the small intestine of IKK2ca^{IEChom} mice when compared to IKK2ca^{sFL} controls (Fig. 20e). These results show that a subset of β-catenin regulated genes is expressed at higher levels in IKK2ca^{IEChom} animals, suggesting that in IKK2ca-expressing IECs the transcriptional activity of β-catenin is increased in a target gene specific manner.

Since the Wnt-β-catenin signalling pathway is essential for maintaining IEC proliferation and since increased levels of β-catenin activity are indicative of enhanced proliferation, we stained intestinal tissue from 10-week-old mice for Ki67. In the colon of IKK2ca^{IEChom} mice Ki67 positive cells were expanded towards the lumen, indicating that the proliferating TA compartment was extended (Fig. 21a). In the small intestine differences between controls and IKK2ca^{IEChom} animals were even more obvious (Fig. 21a). As mentioned above, terminally differentiated Paneth cells that do not express Ki67 reside in ileal crypt bases, resulting in a lack of Ki67 staining in this area. Few Ki67 positive cells found in this region originate from stem cells, which do express nuclear Ki67. Whereas this staining pattern was seen in IKK2ca^{sFL} mice, in IKK2ca^{IEChom} animals nearly all crypt cells were positive for Ki67. This increase in proliferating crypt cells is indicative for heightened β-catenin activation in IECs, correlating with the data shown in Fig. 20.

Immunohistochemical staining for Sox9 was performed to evaluate β-catenin activity. Sox9 was produced in higher amounts in IECs of young IKK2ca^{IEChom} mice, as seen by increased Sox9 staining intensity in 10-week-old IKK2ca^{IEChom} mice on the one hand and by an extension of Sox9 producing cells in colonic crypts towards the apical part of the mucosa on the other hand (Fig. 21b). In the small intestine Sox9 is highly expressed in stem cells and in Paneth cells, whereas the expression level decreases in the TA compartment and disappears at the crypt-villus-junction, where IECs undergo terminal differentiation (Bastide et al., 2007; Blache et al., 2004). Some subtypes of enteroendocrine cells in the colon and the small intestine maintain nuclear Sox9 expression also upon differentiation (Bastide et al., 2007). At the crypt

base high levels of Sox9 mark stem cells with elongated and triangular shaped nuclei surrounded by a slim cytoplasmic margin. Paneth cells, which also show strong Sox9 staining, are big cells that have a small roundish nucleus and a big amount of cytoplasm. In 10-week-old IKK2ca^{sFL} mice these distinct cell type characteristics can be distinguished at the ileal crypt bases as depicted in Fig. 21b. In IKK2ca^{IEChom} mice though such discrimination between cell types is not possible. All IKK2ca^{IEChom} crypt bottom cells show strong Sox9 staining intensity and the morphological differences between the nuclei and the cell shapes cannot be appreciated. Therefore it seems that in young IKK2ca^{IEChom} animals either the stem cells are expanded and have displaced the Paneth cells, or Paneth cell precursors do not undergo differentiation and continue to proliferate. Alternatively, it is possible that TA cells that have extended towards the crypt bottom replaced Paneth cells and therefore in IKK2ca^{IEChom} mice occupy the crypt bases.

In line with reduced Paneth cell numbers, MMP7 mRNA was expressed in lower amounts in the ileum of young IKK2ca^{IEChom} animals, as shown by quantitative RT-PCR analysis (Fig. 21c). MMP7 is responsible for the activation of defensins, small anti-microbial factors that are also produced by Paneth cells (Keshav, 2006; Wehkamp and Stange, 2006; Wilson et al., 1995). Lower levels of MMP7 in the ileum of IKK2ca^{IEChom} mice point towards a Paneth cell defect that might lead to an impaired regulation of the intestinal microflora.

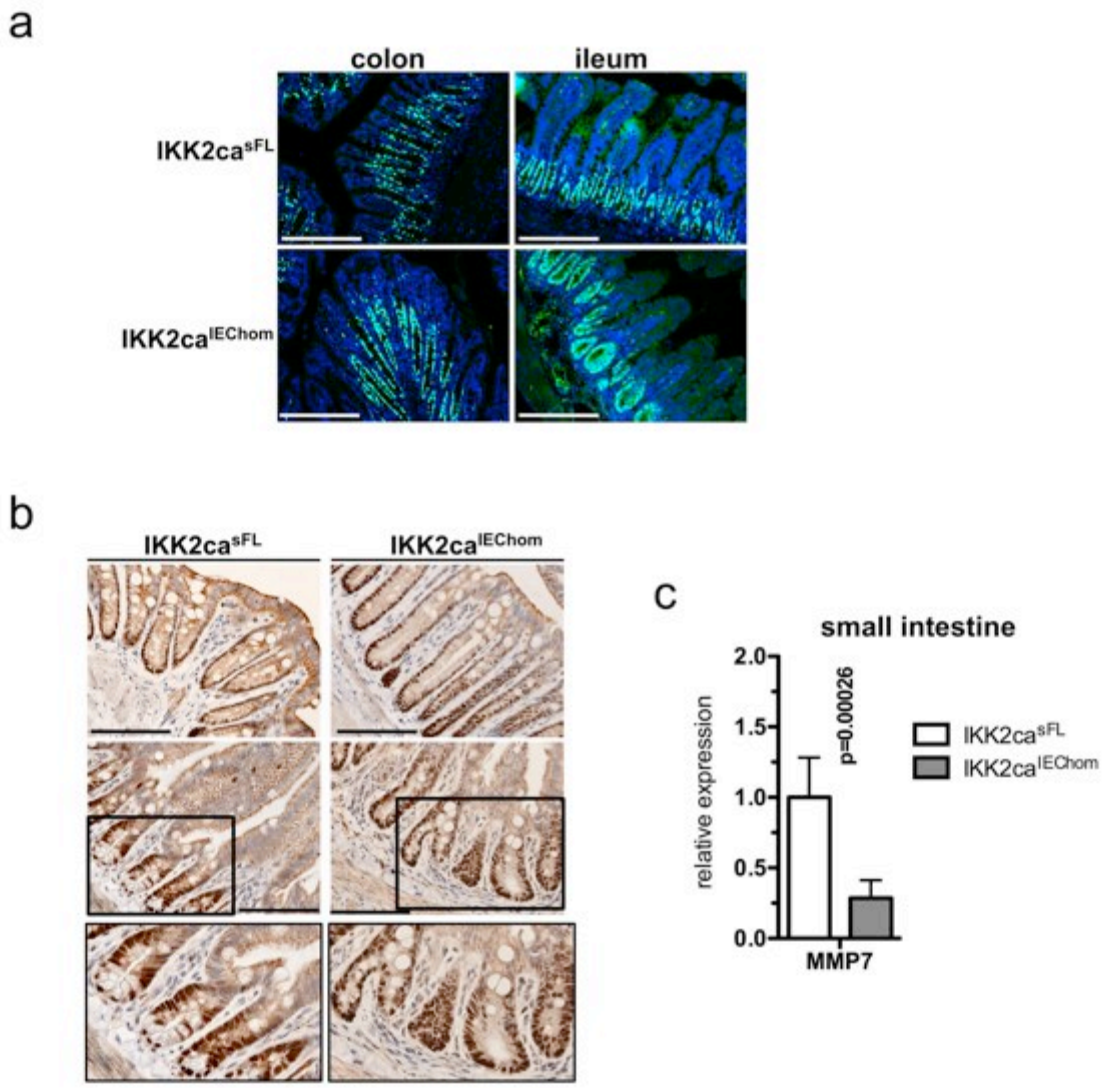

Figure 21 Enhanced proliferation and Sox9 expression in the intestine of young IKK2ca^{IEChom} mice

a. Immunofluorescent staining for Ki67 indicated increased proliferation of IECs in the colon and the small intestine of IKK2ca^{IEChom} mice at 10 weeks of age. In IKK2ca^{IEChom} animals Ki67 positive epithelial cells were extended towards the colonic lumen when compared to IKK2ca^{sFL} controls. In small intestinal crypts of IKK2ca^{sFL} mice Ki67 marks the transit amplifying cells, whereas the crypt bases, which harbour terminally differentiated Paneth cells, are mostly negative for Ki67. All IECs in small intestinal crypts of IKK2ca^{IEChom} mice were positive for Ki67.

b. Immunostaining for Sox9 revealed elevated Sox9 expression in the colon of 10-week-old IKK2ca^{IEChom} mice. In the small intestine Sox9 IHC allowed identification of Paneth cells and stem cells in IKK2ca^{sFL} but not in IKK2ca^{IEChom} mice.

c. Quantitative RT-PCR for MMP7 on distal small intestinal tissue revealed a reduction of MMP7 mRNA in IKK2ca^{IEChom} mice compared to IKK2ca^{sFL} controls, indicating reduced numbers of Paneth cells, which are the main producers of MMP7 in the small intestine of mice. ($n \geq 6$)

Scale bars represent 50 µm

3.6 Perturbation of stem cells in the intestine of young IKK2ca^{IEChom} mice

Since the patterns of Sox9 and Ki67 expression observed in young IKK2ca^{IEChom} mice pointed towards a potential alteration of stem cell status, quantitative RT-PCR analysis was performed to assess the expression levels of stem cell associated factors in the colon and the small intestine of 7 to 8 week old mice. Quantitative RT-PCRs revealed increased expression of Ascl2, Olfm4 and TnfRsF19 in the proximal colon of IKK2ca^{IEChom} mice compared to IKK2ca^{sFL} controls (Fig. 22a). These factors have been shown to be exclusively produced by epithelial stem cells in the intestine (van der Flier et al., 2009) and therefore might point towards an altered state of this cell type in IKK2ca^{IEChom} mice. CD44, a receptor for hyaluronan acid (Goodison et al., 1999), was reported to be expressed at high levels in crypt-base cells that still undergo cell divisions while its expression is down-regulated when these IECs differentiate (Wielenga et al., 1999). More recently CD44 has been shown to be a marker of human colon cancer stem cells (Dalerba et al., 2007). In colons of young IKK2ca^{IEChom} mice mRNA levels of CD44 were mildly elevated when compared to littermate controls, indicating that IKK2ca^{IEChom} mice harbour more undifferentiated, proliferating epithelial cells than control mice. Also the ileum of IKK2ca^{IEChom} mice produced higher amounts of mRNA's encoding stem cell associated factors. Indeed, Ascl2, Bmi-1, and CD44 mRNA levels were significantly upregulated in the ileum of IKK2ca^{IEChom} mice (Fig. 22b). In contrast to the observed higher levels of Olfm4 in the colon, mRNA for this stem cell associated factor was not upregulated in the small intestine of IKK2ca^{IEChom} mice, indicating differential regulation of Olfm4 between colon and small intestine (compare Fig. 22a and 22b).

Surprisingly, leucine-rich repeat-containing G protein-coupled receptor 5 (Lgr5 or G-protein coupled receptor 49, Gpr49), which currently is the most widely accepted marker for intestinal epithelial stem cells, was not upregulated on mRNA level in the colon or in the small intestine of IKK2ca^{IEChom} mice (see Fig. 22A and 22b). Instead, in the colon of IKK2ca^{IEChom} mice Lgr5 was even expressed at significantly lower levels than in the colon of control mice (Fig. 22a). Furthermore, mRNA levels of CD133 (also known as prominin-1), which encodes a cell surface molecule in stem cells and their immediate descendants (Snippert et al., 2009), were also not altered in the intestine of IKK2ca^{IEChom} mice (compare Fig. 22a and 22b).

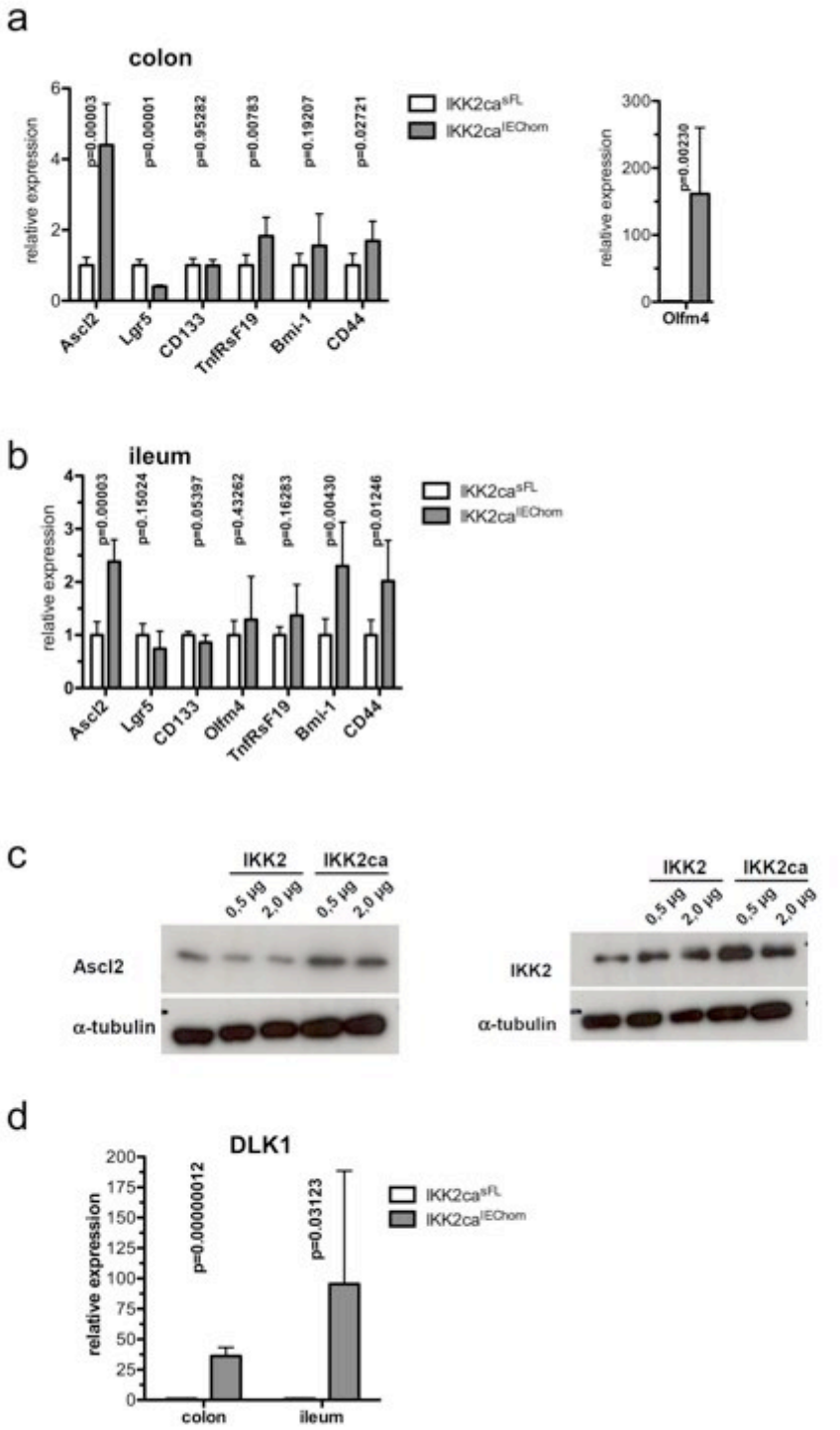

Figure 22 Increased expression of a subset of stem cell associated factors in the intestine of IKK2ca^{IEChom} mice

a. and **b.** Quantitative RT-PCR analysis exhibited elevated expression of intestinal epithelial stem cell associated factors in the colon (**a.**) and the small intestine (**b.**) of IKK2ca^{IEChom} compared to IKK2ca^{sFL} control mice. (n ≥ 6)

c. Western Blot analysis of protein extracts from human colon cancer HCT116 cells transfected with plasmids coding for IKK2, IKK2ca or empty vector revealed an upregulation of Ascl2 protein in cells expressing IKK2ca.

d. Quantitative RT-PCR showed that DLK1 mRNA was present in higher amounts in the colon and the small intestine of IKK2ca^{IEChom} mice when compared to IKK2ca^{sFL} littermates. (n ≥ 6)

These data obtained by quantitative RT-PCR show that the mRNA levels of a number of stem cell associated factors are differentially expressed in IKK2ca^{IEChom} mice when compared to controls, suggesting that IKK2ca expression in IECs might directly affect crypt stem cells.

In order to investigate whether IKK2ca-mediated NF-kB activation has a direct effect on expression of stem cell associated factors, HCT116 cells were transfected with plasmids coding for IKK2, IKK2ca, or vector controls. As revealed by Western Blot analysis, HCT116 cells transfected with IKK2ca coding plasmid showed increased Ascl2 protein levels (Fig. 22c). As expression of wild-type IKK2 did not result in elevation of Ascl2 protein amounts, expression levels of Ascl2 might correlate directly with IKK2 kinase activity and subsequent NF-kB activation. These experiments thus point towards a direct role for IKK2/NF-kB activation in inducing the production of Ascl2.

In addition to these findings, quantitative RT-PCR for DLK1 (Drosophila homologue of Delta-like 1, also known as pre-adipocyte factor 1, Pref-1) revealed increased mRNA levels in both the colon and the small intestine of 7 to 8-week-old IKK2ca^{IEChom} mice (Fig. 22d). DLK1 is transcriptionally upregulated upon deletion of Apc and it prevents the differentiation of pre-adipocytes via upregulation of Sox9 (Dong et al., 2004; Sansom et al., 2004; Wang and Sul, 2009)

3.7 Activation of non-immune cells and DNA damage in the intestine of IKK2ca^{IEChom} mice

It has been shown that cells of the tumour microenvironment play an important role in sustaining tumour growth by producing cytokines, chemokines and growth factors (Coussens and Werb, 2002). Recent reports underscored the importance of fibroblasts in promoting tumour growth and expansion (Erez et al., 2010; Vermeulen et al., 2010).

To check for the presence of activated fibroblasts we stained colon sections from IKK2ca^{IEChom} animals for αSMA (alpha smooth muscle actin), which is a marker specifically expressed by activated fibroblasts (also termed myofibroblasts) (Eyden et al., 2009). Control mice showed considerably fewer αSMA positive cells in the colonic mucosa than IKK2ca^{IEChom} mice (Fig. 23c). In an inflammatory and tumourous environment activation of fibroblasts and their subsequent differentiation into myofibroblasts occurs due to the presence of inflammatory cytokines such as TNF,

IL-1β and TGF-β, all of which were produced at higher levels already in young IKK2ca^{IEChom} animals (see Fig. 9B and 9c). Therefore, immunohistochemical staining for αSMA was also performed on colon tissue from young IKK2ca^{IEChom} and IKK2ca^{sFL} animals. As shown in Figure 23c the mucosa of IKK2ca-expressing mice harboured more αSMA positive myofibroblasts than colon tissue from controls. This finding indicates that increased IKK2/NF-kB activity in the intestinal epithelium of mice leads to activation not only of immune cells but also of fibroblasts in the surrounding stroma.

For tumourigenesis it is crucial that tumour-initiating cells develop, which are largely independent from environmental cues and divide in a deregulated manner, a process also known as transformation. Transformation of cells occurs when mutations in oncogenes or tumour suppressor genes have taken place. DNA damage that occurs in inflammatory conditions due to increased ROS production can increase the probability of mutation incidence. In the course of a DNA damage response histone 2A.X is phosphorylated, giving rise to the so-called γH2A.X epitope that is used as a marker for DNA damage (Kinner et al., 2008). To investigate the amount of DNA damage in IECs of IKK2ca^{IEChom} mice, an IHC staining for γH2A.X was performed. Whereas differences between control animals and IKK2ca^{IEChom} mice in the colon at 6 weeks of age were minor, obvious differences in γH2A.X staining frequency and intensity of crypt epithelial cells were found in the ileum of IKK2ca^{IEChom} mice (Fig. 23a and 23b). Nuclei of IKK2ca-expressing IECs exhibited a speckled staining pattern for γH2A.X that is characteristic upon focal DNA damage. Since mice at this age also display some signs of ileal inflammation, increased levels of γH2A.X in the ileum of IKK2ca^{IEChom} mice could be indicative for more DNA damage due to ROS that are produced under inflammatory conditions.

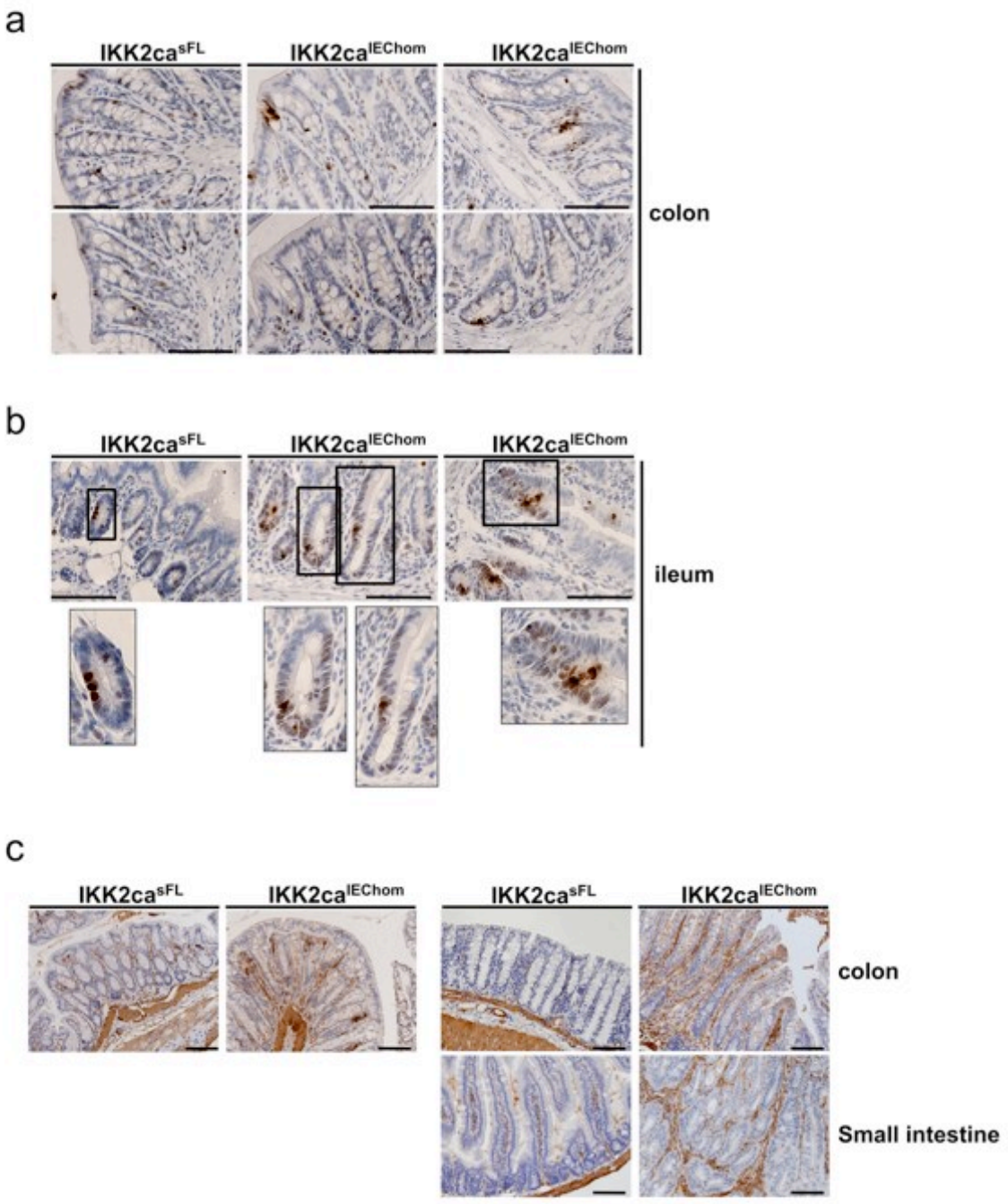

Figure 23 Higher levels of γH2A.X positive nuclei and increased number of αSMA expressing myofibroblasts in the intestine of IKK2ca^{IEChom} mice
a. Slightly increased levels of γH2A.X positive nuclei in the proximal colon of 6-week-old IKK2ca^{IEChom} mice.
b. Higher numbers of γH2A.X positive nuclei in the small intestine of 6-week-old IKK2ca^{IEChom} mice compared to age matched control animals.
c. Increased amount of αSMA-expressing activated stromal fibroblasts in the intestine of young and aged IKK2ca^{IEChom} mice.
Scale bars represent 50 µm

The spontaneous intestinal tumour occurrence in aged IKK2ca^{IEChom} mice therefore most probably results from DNA-damage associated mutations in onco- and tumour suppressor genes in IECs, increased activation β-catenin and a concomitant increase in proliferation and maybe an alteration in the status of stem cells. Finally the

generation of a tumour promoting microenvironment composed of activated immune cells and stromal fibroblasts sustain and support epithelial tumour development.

4. Discussion

4.1 What is the role of constitutive IKK2/NF-κB activity in the intestinal epithelium?

The NF-κB signalling pathway is believed to play a major role in tumour development, since it regulates expression of genes involved in cell survival, proliferation and inflammatory responses (Karin, 2006). NF-κB has been proposed to act in tumour cells themselves, where it confers resistance to apoptosis and enhances proliferation. Indeed, many primary cancers as well as cancer cell lines display not only increased but also constitutive activation of NF-κB (Prasad et al., 2010). In cells of the tumour microenvironment NF-κB acts to promote inflammation through transcriptional upregulation of inflammatory mediators that act like growth factors on tumour cells and thereby sustain tumour growth (Coussens and Werb, 2002; Greten et al., 2004). Due to these diverse functions exerted by NF-κB transcription factors, the NF-κB pathway has been proposed to link inflammation and cancer (Karin, 2006).

Indeed, multiple studies illustrated that activation of NF-κB is important for tumour development and controls basic processes required for carcinogenesis. For instance, IKK2 deletion in myeloid cells reduced the expression of tumour growth supporting cytokines and growth factors and thereby reduced tumour development in the AOM/DSS mouse model of carcinogen-initiated inflammation-driven colon cancer (Greten et al., 2004). Furthermore the activation of NF-κB in cancer-associated fibroblasts was shown to be important for skin carcinogenesis by coordinating the expression of fibroblast-derived proinflammatory factors promoting macrophage recruitment, neovascularisation and tumour growth (Erez et al., 2010). These reports underscore the importance of NF-κB in the promotion of carcinogenesis by acting in cells of the tumour micronevironment to induce the production of factors supporting tumour growth.

The role of NF-κB activation in tumour cells is less clear. IKK2 deletion in epithelial cells reduced the incidence of AOM/DSS-induced colon cancer (Greten et al., 2004) and N-methyl-N-nitrosourea (MNU) induced gastric cancer (Sakamoto et al., 2010), which is in line with the pro-survival functions of NF-κB. Moreover, inhibition of NF-κB by expression of an IκBα supper-repressor (IκBα-SR) or by ablation of p65/RelA in lung epithelial cells reduced the incidence of oncogene-induced lung cancer

(Basseres et al., 2010; Meylan et al., 2009). The aforementioned reports therefore imply that NF-κB activity in tumour cells contributes to tumour development.

However, inhibition of NF-κB in cells of the skin or the liver had opposite effects in different models of carcinogenesis. Expression of IκBα-SR in epidermal keratinocytes synergized with oncogenic Ras to induce epidermal cancer (Dajee et al., 2003), or even led to spontaneous tumour development (van Hogerlinden et al., 1999). On the other hand ablation of IKK2 in melanocytes was protective from oncogenic Ras induced melanoma development (Yang et al., 2010).

Similarly, NF-κB blockade in hepatocytes through the expression of IκBα-SR in the Mdr2-deficient mouse model inhibited inflammation-associated liver cancer development (Pikarsky et al., 2004). In contrast, deletion of IKK2 in hepatocytes sensitized mice to chemical diethylnitrosamine (DEN) induced hepatocarcinogenesis (Maeda et al., 2005), and deletion of NEMO/IKKγ specifically in liver parenchymal cells even resulted in spontaneous development of hepatocellular carcinomas in mice (Luedde et al., 2007).

These findings show that NF-κB signalling exerts a very complex role during carcinogenesis in pre-malignant cells and that the outcome of NF-κB signalling depends on the tissue and the cancer model applied. These results also indicate that NF-κB activation in pre-malignant or tumour cells in addition to its very well-known anti-apoptotic functions is likely to affect different processes fundamental for carcinogenesis. Thus, it is not clear at which stage during tumour development NF-κB activation is crucial and whether the activation of NF-κB per se is sufficient to drive cancer development.

Experimental evidence presented in this thesis supports the idea that – at least in the intestine – NF-κB activation contributes to tumourigenesis already in pre-malignant cells and that NF-κB activation in tumour cells is sufficient to initiate all the necessary processes needed for tumour maintenance. Indeed, intestinal epithelial cell restricted expression of constitutively active IKK2 strongly enhances tumourigenesis in chemical and genetic intestinal cancer models in mice. Moreover, IKK2ca expression in IECs is sufficient to alter intestinal homoeostasis through IEC intrinsic and paracrine functions exerted by the microenvironment, which triggered inflammation and tumour development both in the colon and the small intestine.

By inducing the expression of various inflammatory cytokines and chemokines, epithelial IKK2/NF-κB activation caused the recruitment and activation of

inflammatory cells, contributing to a mucosal microenvironment that supports and sustains intestinal carcinogenesis. However, it is remarkable that although IKK2ca expression induced strong activation of NF-κB signalling in IECs, only a subset of the known NF-κB-regulated cytokines and chemokines were induced. IL-6 for instance, which is a well-known NF-κB-inducible cytokine and has been implicated in colorectal carcinogenesis (Becker et al., 2004; Bollrath et al., 2009; Grivennikov et al., 2009), was not expressed at higher levels in IKK2ca^{IEChom} mice. Yet, TNF and to a lesser extent IL-1β were upregulated in both the SI and colon of IKK2ca^{IEChom} mice. These factors were most probably implicated in IKK2ca-mediated intestinal tumour development since they have been attributed important roles in regulating intestinal inflammation and carcinogenesis (Dinarello, 2010; Popivanova et al., 2008). The most highly upregulated gene in IKK2ca-expressing IECs in the colon and the small intestine was Ccl20, a chemokine that has been reported to induce tumour cell growth and migration in human colorectal cancer (Ghadjar et al., 2009). Cxcl-16, which has been suggested to promote inflammation-associated tumour development together with its receptor Cxcr6 was also highly induced in the intestine of IKK2ca^{IEChom} mice (Darash-Yahana et al., 2009). Therefore, the expression of IKK2ca in IECs induces the production of specific cytokines and chemokines with important pro-tumourigenic activities.

Already at young age, these inflammatory mediators caused an increased abundance of inflammatory cells in the colonic and small intestinal mucosa of IKK2ca^{IEChom} mice. Constant activation of the IKK2/NF-κB pathway in IECs mainly resulted in recruitment of innate immune cells, such as F4/80-postitive macrophages and Gr1-positive granulocytes. In the small intestine macrophages and also granulocytes tended to accumulate around the crypt base, which is the region where the stem cells and the TA cells are located. Since it has been reported that intestinal tumours originate from crypt stem cells (Barker et al., 2009), increased myeloid cell infiltration in this area is likely to contribute to the spontaneous intestinal tumour development in IKK2ca^{IEChom} mice by creating a tumour-supportive microenvironment. In addition to increased myeloid cell numbers, IKK2ca^{IEChom} mice exhibited an accumulation of myofibroblasts in the colon. Through the secretion of growth factors, activated αSMA-positive fibroblasts play an important role in tumour growth (Franco et al., 2010). Activation of fibroblasts is mediated by inflammatory cytokines, such as IL-1β and TGF-β (Erez et al., 2010), both of which were expressed in intestinal tissue from IKK2ca^{IEChom} mice, indicating that IKK2ca-

expression in IECs not only increases the number of mucosal innate immune cells but also activates stromal fibroblasts.

These IKK2ca-mediated alterations together constituted a state of intestinal inflammation, which eventually resulted in tumour growth in the colon and the small intestine. Epidemiological studies have revealed that chronic inflammation is a major risk factor for cancer (Karin, 2006), and this notion was confirmed in mouse models of intestinal tumourigenesis. For instance, in the AOM/DSS-induced intestinal cancer protocol DSS-elicited colitis promotes tumour development initiated by AOM-induced DNA mutations, whereas AOM applied alone induces cancer at lower incidence (Neufert et al., 2007; Tanaka et al., 2003). Persistent inflammation can lead to cancer development also in the absence of prior carcinogen exposure. IL-10 deficient mice, for instance, suffer from spontaneous chronic colitis (Berg et al., 1996; Kuhn et al., 1993) that led to colorectal cancer formation in 60% of 6-month-old IL-10$^{-/-}$ animals housed under SPF-conditions (Berg et al., 1996). Furthermore, Mucin2$^{-/-}$ animals, that displayed subclinical intestinal inflammation, develop spontaneous lesions throughout the intestinal tract (Velcich et al., 2002; Yang et al., 2008). These studies show that inflammatory processes can be a sufficient driving force for intestinal tumourigenesis, suggesting that altered intestinal immune homoeostasis in IKK2ca^{IEChom} mice could lead to the development of tumours in the intestine.

Interestingly, the observed difference in tumourigenesis incidence between the small and the large intestine with a prevailing occurrence of adenomas in the colon of IKK2ca^{IEChom} animals is reminiscent of a similar situation in human patients, where tumourigenesis occurs more frequently in the colon (Vallabhapurapu and Karin, 2009). Apart from inflammation, which appeared to be more severe in the colon, the difference in bacterial load could provide an explanation for this phenomenon. The amount of commensal bacteria is higher in the colon when compared to the small intestine (Wells et al., 2010). Indeed, bacteria can have a tumour promoting effect in inflammation mediated colon cancer models. For instance, AOM-induced tumour incidence decreased dramatically in germ-free IL-10 deficient mice, providing experimental evidence that bacteria are essential for inflammation and carcinogenesis. Furthermore, deletion of MyD88 in IL-10$^{-/-}$ mice prevented AOM-mediated tumourigenesis, underscoring the importance of bacterial signalling for cancer development (Uronis et al., 2009). Also human commensal bacteria were shown to induce tumour formation in mice through activation of Stat3 and Th17

signalling (Wu et al., 2009). These studies show that in the absence of commensal bacteria tumour incidence is greatly diminished, suggesting that increased tumourigenesis in the colon could indeed result from a higher bacterial load. However, whether commensal bacteria are an important driving force for adenoma fromation in IKK2ca^{IEChom} mice could only be addressed if IKK2ca^{IEChom} animals were housed under germ-fee conditions, in which intestinal bacteria are absent. Also treatment of IKK2ca^{IEChom} mice with antibiotics could help to understand the impact of commensal bacteria in tumour development in these mice.

Though the above-mentioned data point towards a crucial role of inflammation for tumourigenesis in IKK2ca^{IEChom} mice, there are studies suggesting that inflammation alone is unlikely to be sufficient for initiating intestinal tumourigenesis. For instance, a mouse model suffering from severe Crohn's disease like chronic ileal inflammation caused by increased TNF expression was not sufficient to induce intestinal tumours (Kontoyiannis et al., 1999). This indicates that high levels of TNF and the inflammatory mediators induced by TNF do not suffice to induce tumour growth.

More direct indications that IKK2ca-induced inflammation by itself might not be sufficient to explain tumour development in IKK2ca^{IEChom} mice comes from studies overexpressing IKK2 in other organs. For instance, high levels of IKK2 expression in the skin led to the spontaneous development of an inflammatory skin disease with similarities to interface dermatitis (Page et al., 2010). Though disease was chronic and progressed in severity, IKK2-transgenic mice did not develop skin tumours, indicating that increased levels of IKK2 and concomitant inflammatory disease are not sufficient to trigger cancer development in the skin.

Furthermore, temporarily induced expression of constitutively active IKK2 in pancreatic acinar cells resulted in spontaneous development of acute pancreatitis (Baumann et al., 2007) associated with increased production of inflammatory mediators and immune cells infiltration. However, this temporal increase in activation of NF-κB signalling in pancreatic acini did not lead to tumour development. Therefore, persistent activation of IKK2 in the pancreas disrupts tissue homeostasis and induces an inflammatory condition that is not sufficient for driving tumourigenesis.

These observations might suggest that inflammation per se is not enough to induce tumour development in the intestine of IKK2ca^{IEChom} mice. However, it might also point to an intestine-specific pro-tumourigenic cell-intrinsic effect of IKK2 activation.

In this respect, intestinal tumourigenesis is mostly associated with mutations leading to activation of the Wnt-signalling pathway (Pinto and Clevers, 2005). Wnt-signalling controls normal epithelial homoeostasis and mutations activating this pathway cause intestinal tumours in humans and mice (Barker and Clevers, 2000; Clevers, 2006; Fodde and Brabletz, 2007). Various mouse models of intestinal tumourigenesis that heterozygously express truncated versions of the tumour suppressor Apc have been established. Upon loss of the heterozygous wild-type Apc allele, β-catenin accumulates and activates transcription of Wnt target genes. This results in aberrant IEC proliferation and intestinal tumour growth in these mice. However, also carcinogenesis driven by AOM depends on mutations in components of this pathway, since mutations causing stabilisation of β-catenin, the central player of Wnt-signalling, are frequently found in AOM-induced tumours (Greten et al., 2004; Takahashi and Wakabayashi, 2004).

4.2 Cooperation between Wnt- and NF-κB signalling in intestinal tumour development

IKK2ca^{IEChom} mice developed many tumourous lesions in the colon after a mild AOM/DSS regimen that did not induce any tumours in control mice. Considering the high sensitivity of IKK2ca^{IEChom} mice to DSS-induced colonic inflammation, an increase in tumour load upon AOM/DSS treatment in these mice most probably results from increased colitis and associated tissue damage. However, IKK2ca^{IEChom} mice also exhibited increased tumourigenesis in an AOM-induced colon cancer model that does not depend on inflammation mediated tumour promotion (Neufert et al., 2007). Therefore, DSS-induced mucosal injury is not necessary to drive AOM-induced tumourigenesis in IKK2ca^{IEChom} mice. Nevertheless we showed that young IKK2ca^{IEChom} mice already suffer from inflammatory intestinal disease and produce higher amounts of proinflammatory mediators than control animals. Therefore, also AOM-induced tumour development in the intestine of IKK2ca^{IEChom} mice could partially result from ongoing inflammation that is absent in IKK2ca^{sFL} mice.

Since activating mutations in β-catenin are a common outcome of AOM treatment, enhanced AOM-induced tumour development observed in IKK2ca^{IEChom} mice could also be caused by cooperation between Wnt- and IKK2-mediated signalling in intestinal tumourigenesis.

A strong tumour promotive effect exerted by IKK2ca in Wnt-induced intestinal tumour development in Apc1638N/IKK2ca^{IEChet} mice provided more direct evidence for cooperation between these pathways. Not only did polyp formation in the small intestine occur much earlier in Apc1638N/IKK2ca^{IEChet} than in Apc1638N/IKK2ca^{sFL} mice, there was also a shift in tumour localisation towards the colon. While in Apc1638N mice colon lesions are very rare and only occur in aged mice (Fodde et al., 1994), all Apc1638N/IKK2ca^{IEChet} mice analysed at 4 months of age had at least one colon tumour. Tumourigenesis in Apc mutant mice depends on loss of the wild-type Apc allele. The increased tumour incidence in Apc1638N/IKK2ca^{IEChet} mice could be explained by a more frequent loss of wild-type Apc in Apc1638N/IKK2ca^{IEChet} versus Apc1638N/IKK2ca^{sFL} mice.

Taken together the data presented herein point towards a synergistic effect between Wnt- and IKK2/NF-κB-signalling in intestinal epithelial cells that contributes to tumour development in chemical as well as genetic models of intestinal cancer in mice.

4.3 Impact of IKK2ca-expression on β-catenin stability and activity in IECs

In support of an effect of IKK2ca on Wnt signalling, IKK2ca^{IEChom} mice expressed higher amounts of nuclear as well as active β-catenin protein in IECs. Higher levels of the β-catenin target gene Sox9 were identified by immunohistochemical staining in IECs from IKK2ca^{IEChom} than IKK2ca^{sFL} mice, indicating that the transcriptional activity of β-catenin in these IECs was enhanced. Interestingly, Sox9 acts as a negative feedback regulator of β-catenin/Tcf4 and thereby prevents the expression of a subset of β-catenin target genes (Mori-Akiyama et al., 2007). Increased production of Sox9 in IKK2ca-expressing IECs therefore could provide an explanation for the fact that some β-catenin/Tcf4 target genes, such as c-myc and cyclin D1, were not increased in IECs from IKK2ca^{IEChom} mice (see Fig. 20). These observations suggest that expression of IKK2ca in IECs initiates a complex regulatory transcriptional network. In fact, the picture becomes even more complicated when one considers that NF-κB activation in chondrocytes represses Sox9 (Murakami et al., 2000). This might indicate either that increased β-catenin activity in IECs overrules the inhibitory function of NF-κB on Sox9 expression, or that inhibition of Sox9 transcription by NF-κB could be cell type specific and might not occur in the intestinal epithelium.

Nevertheless, since *in vitro* experiments suggested IKK2 rather to exert a negative regulatory effect on β-catenin activity, it is surprising that IKK2ca expression in IECs enhanced the activation of β-catenin and resulted in increased expression of at least

some of its target genes. IKK2 expression in murine embryonic fibroblasts (MEFs) and COS cells repressed β-catenin mediated transcription (Jensen et al., 1964; Lamberti et al., 2001). Furthermore, NF-κB activity in colon, liver and breast cancer was proposed to inhibit β-catenin activation by inducing the expression of Izts2 (leucine zipper tumour suppressor 2), a molecule interacting with β-catenin and regulating its nuclear export (Cho et al., 2008). Therefore, our results point towards alternative mechanisms leading to the accumulation of this protein. It has been reported that robust activation of β-catenin in colon cancer cells requires additional cues apart from Wnt-ligand stimulation or Wnt-activating mutations (Rasola et al., 2007; Vermeulen et al., 2010). For instance, growth factors such as HGF and PDGF have been proposed to induce transcriptional activity of β-catenin through initiating PI3K/Akt signalling. Indeed, Akt-mediated phosphorylation of GSK3β was shown to decrease degradation of cytoplasmic β-catenin (Fukumoto et al., 2001; Kaler et al., 2009b; Korkaya et al., 2009). In addition, through phosphorylation of Serine552 of β-catenin, Akt induces its nuclear translocation and transcriptional activation in intestinal epithelial cells (Fang et al., 2007). Although growth factors are expressed in high amounts by stromal myofibroblasts (Pietras and Ostman, 2010), which are present in the intestine of IKK2ca^{IEChom} mice already at young age, the possible link between increased epithelial β-catenin activity and growth factor induced Akt activation in these mice remains to be investigated.

Furthermore, it has been reported that cytokines secreted by infiltrating immune cells can regulate activation of β-catenin in epithelial cells. Macrophages were shown to activate β-catenin in colon and gastric tumour cells by producing IL-1β and TNF (Kaler et al., 2009a; Kaler et al., 2009b; Oguma et al., 2008). Whereas macrophage derived TNF activated Wnt-signaling by inducing GSK3β phosphorylation in an NF-κB independent manner, IL-1β activated β-catenin via NF-κB-dependent induction of PDK1/Akt-mediated GSK3β phosphorylation. In addition, also activation of β-catenin by progastrin-induced GSK3β phosporylation relied on IKK activation (Oguma et al., 2008; Umar et al., 2009). Therefore constitutive activation of IKK2/NF-κB in the intestinal epithelium might mediate stabilisation of β-catenin by inducing inhibitory phosphorylation of GSK3β by Akt. These studies suggest that IKK2ca might achieve accumulation of β-catenin either in a paracrine way, by acting on cells of the microenvironment, or in a cell intrinsic way acting directly on PDK1/Akt signalling.

Another possible cell intrinsic mechanism by which IKK2ca expression could lead to stabilisation of β-catenin in IECs is by limiting the capacity of the β-TrCP E3 ubiquitin ligase. Since β-TrCP is required for degradation of both β-catenin and IκB proteins, high expression levels of IKK2ca in IECs might induce continuous degradation of IκB proteins and thereby reduce availability of β-TrCP for β-catenin degradation.

In line with the knowledge that the Wnt-signalling cascade is responsible for maintaining the proliferative capacities of the intestinal epithelium, we observed an increased amount of proliferating (Ki67 positive) IECs in the intestine of young IKK2ca^{IEChom} mice. In IKK2ca^{IEChom} mice Sox9-expressing, proliferating and therefore not terminally differentiated colonic IECs were extended towards the apical region of crypts. Also in small intestinal crypts the number of Sox9 positive cells was increased when compared to controls. This enhanced proliferative activity likely contributed to the tumour prone phenotype of IKK2ca^{IEChom} animals.

4.4 Effect of IKK2ca-expression in IECs on intestinal epithelial stem cells

In addition to epithelial proliferation, the Wnt-signaling pathway also regulates the fate of intestinal crypt stem cells, which are the cells of origin of intestinal cancers (Barker et al., 2009). We observed that all cells in the base of SI crypts, which in wild-type mice harbour few Ki67 positive stem cells and terminally differentiated Ki67 negative Paneth cells, stained strongly with Ki67 antibodies in IKK2ca^{IEChom} mice. Furthermore, immunohistochemical staining for Sox9 in crypt bases of the small intestine from IKK2ca^{IEChom} mice did not allow the clear identification of Paneth cells or stem cells as in control crypts. These observations suggested that the stem cell compartment in IKK2ca^{IEChom} mice either exhibits an increased proliferative activity or cells from the TA compartment are extended towards the crypt base.

An alteration in stem cell status was indicated by increased transcription of stem cell associated factors in the intestine of IKK2ca^{IEChom} mice. Some of the stem cell associated factors transcribed at higher levels in IKK2ca^{IEChom} mice contained NF-κB binding sites in their promoters, such as CD44, Olfm4, and Bmi-1 (Chin et al., 2008; Dutton et al., 2007; Hinz et al., 2002). Furthermore we identified a conserved NF-κB binding site in the proximal promoter region of Ascl2, suggesting that expression of this transcription factor could be under the control of NF-κB. However, since CD44 and Ascl2 are β-catenin/Tcf4 target genes (Sansom et al., 2004; van der Flier et al., 2009), increased β-catenin activity in IKK2ca-expressing IECs could contribute to the

elevated expression of these factors. Since IKK2ca upregulated Ascl2 expression in HCT116 cells, human colon carcinoma cells that contain a point mutation in β-catenin leading to its constitutive activation (Gayet et al., 2001), elevated IKK2/NF-κB activity might synergize with β-catenin to increase Ascl2 expression. Similarly, the hyaluronic acid receptor CD44 that is produced by not terminally differentiated epithelial crypt cells is a target gene of both NF-κB and β-catenin/Tcf4 (Hinz et al., 2002; van de Wetering et al., 2002; van der Flier et al., 2009).

In contrast to CD44 and Ascl2, Olfm4 expression is regulated in a β-catenin-independent manner (van der Flier et al., 2009) and is induced by NF-κB in gastric cancer cells (Chin et al., 2008; Kim et al., 2010). Therefore high amounts of Olfm4 in the colon of IKK2ca^{IEChom} mice most probably result from increased NF-κB activity. Since expression of Olfm4 is elevated in the intestinal epithelium of IBD patients (Shinozaki et al., 2001), high levels of Olfm4 mRNA could result from inflammation in the colon of IKK2ca^{IEChom} mice. Also Bmi-1 is an NF-κB target gene that so far was not shown to be under the transcriptional control of β-catenin/Tcf4 (Dutton et al., 2007; van der Flier et al., 2009), suggesting that its upregulation in small intestine from IKK2ca^{IEChom} mice might be solely due to enhanced NF-κB activation.

Lgr5 (Gpr49), the currently most widely accepted marker for crypt base columnar stem cells, is a Wnt target gene and its expression was furthermore shown to depend on Ascl2 (Barker et al., 2007; van der Flier et al., 2009). Although both Ascl2 mRNA and β-catenin protein were present at higher levels in the intestinal epithelium of IKK2ca^{IEChom} mice, Lgr5 mRNA was not increased in the intestine of these mice. The forecited inhibition of β-catenin activity by Sox9 (Mori-Akiyama et al., 2007) could provide a possible explanation for this observation. Alternatively, high levels of IKK2/NF-κB activity might impair Lgr5 expression by a so far unknown mechanism.
Intestinal tissue from IKK2ca^{IEChom} mice also displayed higher mRNA levels of DLK1, a factor that prevents differentiation of cultured IECs and has been assigned a role in tumour development (Dong et al., 2004; Guda et al., 2007). Increased expression of DLK1 in IKK2ca^{IEChom} mice might contribute to their sensitivity for intestinal tumourigenesis.

The altered expression of stem cell associated factors in IKK2ca^{IEChom} compared to IKK2ca^{sFL} mice indicates that constitutive activation of IKK2/NF-κB in the intestinal epithelium either directly, through cell intrinsic mechanisms, or indirectly, through paracrine functions, affects the stem cell compartment.

5. Concluding Remarks

The data presented in this thesis show that epithelial restricted expression of constitutively active IKK2 in the intestine is sufficient to induce and sustain chronic intestinal inflammation and subsequent tumour development in mice. Expression of IKK2ca rendered pre-malignant IECs capable to induce all the cell-intrinsic and microenvironmental changes that are necessary for tumourigenesis, suggesting that persistent activation of IKK2/NF-κB, at least in the intestinal epithelium, can play a causative role in tumourigenesis. A recent report identified an amplification of the IKK2 locus in different human cancers by large-scale unbiased genomic analysis of somatic copy number alterations, suggesting that also in human cancers activation of NF-κB in tumour cells could play a direct role in tumour development (Beroukhim et al., 2010).

Bibliography

Adhikari, A., Xu, M., and Chen, Z.J. (2007). Ubiquitin-mediated activation of TAK1 and IKK. Oncogene *26*, 3214-3226.

Barker, N., and Clevers, H. (2000). Catenins, Wnt signaling and cancer. Bioessays *22*, 961-965.

Barker, N., Ridgway, R.A., van Es, J.H., van de Wetering, M., Begthel, H., van den Born, M., Danenberg, E., Clarke, A.R., Sansom, O.J., and Clevers, H. (2009). Crypt stem cells as the cells-of-origin of intestinal cancer. Nature *457*, 608-611.

Barker, N., van Es, J.H., Kuipers, J., Kujala, P., van den Born, M., Cozijnsen, M., Haegebarth, A., Korving, J., Begthel, H., Peters, P.J.*, et al.* (2007). Identification of stem cells in small intestine and colon by marker gene Lgr5. Nature *449*, 1003-1007.

Basseres, D.S., Ebbs, A., Levantini, E., and Baldwin, A.S. (2010). Requirement of the NF-kappaB subunit p65/RelA for K-Ras-induced lung tumorigenesis. Cancer Res *70*, 3537-3546.

Bastide, P., Darido, C., Pannequin, J., Kist, R., Robine, S., Marty-Double, C., Bibeau, F., Scherer, G., Joubert, D., Hollande, F.*, et al.* (2007). Sox9 regulates cell proliferation and is required for Paneth cell differentiation in the intestinal epithelium. J Cell Biol *178*, 635-648.

Batlle, E., Henderson, J.T., Beghtel, H., van den Born, M.M., Sancho, E., Huls, G., Meeldijk, J., Robertson, J., van de Wetering, M., Pawson, T.*, et al.* (2002). Beta-catenin and TCF mediate cell positioning in the intestinal epithelium by controlling the expression of EphB/ephrinB. Cell *111*, 251-263.

Baumann, B., Wagner, M., Aleksic, T., von Wichert, G., Weber, C.K., Adler, G., and Wirth, T. (2007). Constitutive IKK2 activation in acinar cells is sufficient to induce pancreatitis in vivo. J Clin Invest *117*, 1502-1513.

Becker, C., Fantini, M.C., Schramm, C., Lehr, H.A., Wirtz, S., Nikolaev, A., Burg, J., Strand, S., Kiesslich, R., Huber, S.*, et al.* (2004). TGF-beta suppresses tumor progression in colon cancer by inhibition of IL-6 trans-signaling. Immunity *21*, 491-501.

Becker, C., Fantini, M.C., Wirtz, S., Nikolaev, A., Kiesslich, R., Lehr, H.A., Galle, P.R., and Neurath, M.F. (2005). In vivo imaging of colitis and colon cancer development in mice using high resolution chromoendoscopy. Gut *54*, 950-954.

Berg, D.J., Davidson, N., Kuhn, R., Muller, W., Menon, S., Holland, G., Thompson-Snipes, L., Leach, M.W., and Rennick, D. (1996). Enterocolitis and colon cancer in interleukin-10-deficient mice are associated with aberrant cytokine production and CD4(+) TH1-like responses. J Clin Invest *98*, 1010-1020.

Beroukhim, R., Mermel, C.H., Porter, D., Wei, G., Raychaudhuri, S., Donovan, J., Barretina, J., Boehm, J.S., Dobson, J., Urashima, M.*, et al.* (2010). The landscape of somatic copy-number alteration across human cancers. Nature *463*, 899-905.

Bjerknes, M., and Cheng, H. (1981). The stem-cell zone of the small intestinal epithelium. I. Evidence from Paneth cells in the adult mouse. Am J Anat *160*, 51-63.

Blache, P., van de Wetering, M., Duluc, I., Domon, C., Berta, P., Freund, J.N., Clevers, H., and Jay, P. (2004). SOX9 is an intestine crypt transcription factor, is regulated by the Wnt pathway, and represses the CDX2 and MUC2 genes. J Cell Biol *166*, 37-47.

Bollrath, J., Phesse, T.J., von Burstin, V.A., Putoczki, T., Bennecke, M., Bateman, T., Nebelsiek, T., Lundgren-May, T., Canli, O., Schwitalla, S.*, et al.* (2009). gp130-mediated Stat3 activation in enterocytes regulates cell survival and cell-cycle progression during colitis-associated tumorigenesis. Cancer Cell *15*, 91-102.

Brabletz, T., Jung, A., Dag, S., Hlubek, F., and Kirchner, T. (1999). beta-catenin regulates the expression of the matrix metalloproteinase-7 in human colorectal cancer. Am J Pathol *155*, 1033-1038.

Brand, S. (2009). Crohn's disease: Th1, Th17 or both? The change of a paradigm: new immunological and genetic insights implicate Th17 cells in the pathogenesis of Crohn's disease. Gut *58*, 1152-1167.

Brittan, M., and Wright, N.A. (2004). Stem cell in gastrointestinal structure and neoplastic development. Gut *53*, 899-910.

Cash, H.L., Whitham, C.V., Behrendt, C.L., and Hooper, L.V. (2006). Symbiotic bacteria direct expression of an intestinal bactericidal lectin. Science *313*, 1126-1130.

Chin, K.L., Aerbajinai, W., Zhu, J., Drew, L., Chen, L., Liu, W., and Rodgers, G.P. (2008). The regulation of OLFM4 expression in myeloid precursor cells relies on NF-kappaB transcription factor. Br J Haematol *143*, 421-432.

Cho, H.H., Song, J.S., Yu, J.M., Yu, S.S., Choi, S.J., Kim, D.H., and Jung, J.S. (2008). Differential effect of NF-kappaB activity on beta-catenin/Tcf pathway in various cancer cells. FEBS Lett *582*, 616-622.

Clevers, H. (2006). Wnt/beta-catenin signaling in development and disease. Cell *127*, 469-480.

Cooper, H.S., Murthy, S.N., Shah, R.S., and Sedergran, D.J. (1993). Clinicopathologic study of dextran sulfate sodium experimental murine colitis. Lab Invest *69*, 238-249.

Coussens, L.M., and Werb, Z. (2002). Inflammation and cancer. Nature *420*, 860-867.

Crawford, H.C., Fingleton, B.M., Rudolph-Owen, L.A., Goss, K.J., Rubinfeld, B., Polakis, P., and Matrisian, L.M. (1999). The metalloproteinase matrilysin is a target of beta-catenin transactivation in intestinal tumors. Oncogene *18*, 2883-2891.

Dajee, M., Lazarov, M., Zhang, J.Y., Cai, T., Green, C.L., Russell, A.J., Marinkovich, M.P., Tao, S., Lin, Q., Kubo, Y.*, et al.* (2003). NF-kappaB blockade and oncogenic Ras trigger invasive human epidermal neoplasia. Nature *421*, 639-643.

Dalerba, P., Dylla, S.J., Park, I.K., Liu, R., Wang, X., Cho, R.W., Hoey, T., Gurney, A., Huang, E.H., Simeone, D.M.*, et al.* (2007). Phenotypic characterization of human colorectal cancer stem cells. Proc Natl Acad Sci U S A *104*, 10158-10163.

Darash-Yahana, M., Gillespie, J.W., Hewitt, S.M., Chen, Y.Y., Maeda, S., Stein, I., Singh, S.P., Bedolla, R.B., Peled, A., Troyer, D.A.*, et al.* (2009). The chemokine CXCL16 and its receptor, CXCR6, as markers and promoters of inflammation-associated cancers. PLoS One *4*, e6695.

Dinarello, C.A. (2010). Why not treat human cancer with interleukin-1 blockade? Cancer Metastasis Rev *29*, 317-329.

Dong, M., Guda, K., Nambiar, P.R., Nakanishi, M., Lichtler, A.C., Nishikawa, M., Giardina, C., and Rosenberg, D.W. (2004). Azoxymethane-induced pre-adipocyte factor 1 (Pref-1) functions as a differentiation inhibitor in colonic epithelial cells. Carcinogenesis *25*, 2239-2246.

Dutton, A., Woodman, C.B., Chukwuma, M.B., Last, J.I., Wei, W., Vockerodt, M., Baumforth, K.R., Flavell, J.R., Rowe, M., Taylor, A.M.*, et al.* (2007). Bmi-1 is induced by the Epstein-Barr virus oncogene LMP1 and regulates the expression of viral target genes in Hodgkin lymphoma cells. Blood *109*, 2597-2603.

Ea, C.K., Deng, L., Xia, Z.P., Pineda, G., and Chen, Z.J. (2006). Activation of IKK by TNFalpha requires site-specific ubiquitination of RIP1 and polyubiquitin binding by NEMO. Mol Cell *22*, 245-257.

Erez, N., Truitt, M., Olson, P., Arron, S.T., and Hanahan, D. (2010). Cancer-Associated Fibroblasts Are Activated in Incipient Neoplasia to Orchestrate Tumor-Promoting Inflammation in an NF-kappaB-Dependent Manner. Cancer Cell *17*, 135-147.

Ermolaeva, M.A., Michallet, M.C., Papadopoulou, N., Utermohlen, O., Kranidioti, K., Kollias, G., Tschopp, J., and Pasparakis, M. (2008). Function of TRADD in tumor necrosis factor receptor 1 signaling and in TRIF-dependent inflammatory responses. Nat Immunol *9*, 1037-1046.

Eyden, B., Banerjee, S.S., Shenjere, P., and Fisher, C. (2009). The myofibroblast and its tumours. J Clin Pathol *62*, 236-249.

Fang, D., Hawke, D., Zheng, Y., Xia, Y., Meisenhelder, J., Nika, H., Mills, G.B., Kobayashi, R., Hunter, T., and Lu, Z. (2007). Phosphorylation of beta-catenin by AKT promotes beta-catenin transcriptional activity. J Biol Chem *282*, 11221-11229.

Fevr, T., Robine, S., Louvard, D., and Huelsken, J. (2007). Wnt/beta-catenin is essential for intestinal homeostasis and maintenance of intestinal stem cells. Mol Cell Biol *27*, 7551-7559.

Fodde, R., and Brabletz, T. (2007). Wnt/beta-catenin signaling in cancer stemness and malignant behavior. Curr Opin Cell Biol *19*, 150-158.

Fodde, R., Edelmann, W., Yang, K., van Leeuwen, C., Carlson, C., Renault, B., Breukel, C., Alt, E., Lipkin, M., Khan, P.M.*, et al.* (1994). A targeted chain-termination mutation in the mouse Apc gene results in multiple intestinal tumors. Proc Natl Acad Sci U S A *91*, 8969-8973.

Fodde, R., Smits, R., and Clevers, H. (2001). APC, signal transduction and genetic instability in colorectal cancer. Nat Rev Cancer *1*, 55-67.

Franco, O.E., Shaw, A.K., Strand, D.W., and Hayward, S.W. (2010). Cancer associated fibroblasts in cancer pathogenesis. Semin Cell Dev Biol *21*, 33-39.

Fukumoto, S., Hsieh, C.M., Maemura, K., Layne, M.D., Yet, S.F., Lee, K.H., Matsui, T., Rosenzweig, A., Taylor, W.G., Rubin, J.S.*, et al.* (2001). Akt participation in the Wnt signaling pathway through Dishevelled. J Biol Chem *276*, 17479-17483.

Gayet, J., Zhou, X.P., Duval, A., Rolland, S., Hoang, J.M., Cottu, P., and Hamelin, R. (2001). Extensive characterization of genetic alterations in a series of human colorectal cancer cell lines. Oncogene *20*, 5025-5032.

Ghadjar, P., Rubie, C., Aebersold, D.M., and Keilholz, U. (2009). The chemokine CCL20 and its receptor CCR6 in human malignancy with focus on colorectal cancer. Int J Cancer *125*, 741-745.

Gilmore, A.P. (2005). Anoikis. Cell Death Differ *12 Suppl 2*, 1473-1477.

Goodison, S., Urquidi, V., and Tarin, D. (1999). CD44 cell adhesion molecules. Mol Pathol *52*, 189-196.

Greten, F.R., Eckmann, L., Greten, T.F., Park, J.M., Li, Z.W., Egan, L.J., Kagnoff, M.F., and Karin, M. (2004). IKKbeta links inflammation and tumorigenesis in a mouse model of colitis-associated cancer. Cell *118*, 285-296.

Grivennikov, S., Karin, E., Terzic, J., Mucida, D., Yu, G.Y., Vallabhapurapu, S., Scheller, J., Rose-John, S., Cheroutre, H., Eckmann, L.*, et al.* (2009). IL-6 and Stat3 are required for survival of intestinal epithelial cells and development of colitis-associated cancer. Cancer Cell *15*, 103-113.

Guda, K., Marino, J.N., Jung, Y., Crary, K., Dong, M., and Rosenberg, D.W. (2007). Strain-specific homeostatic responses during early stages of Azoxymethane-induced colon tumorigenesis in mice. Int J Oncol *31*, 837-842.

Hayden, M.S., and Ghosh, S. (2008). Shared principles in NF-kappaB signaling. Cell *132*, 344-362.

He, T.C., Sparks, A.B., Rago, C., Hermeking, H., Zawel, L., da Costa, L.T., Morin, P.J., Vogelstein, B., and Kinzler, K.W. (1998). Identification of c-MYC as a target of the APC pathway. Science *281*, 1509-1512.

Hinz, M., Lemke, P., Anagnostopoulos, I., Hacker, C., Krappmann, D., Mathas, S., Dorken, B., Zenke, M., Stein, H., and Scheidereit, C. (2002). Nuclear factor kappaB-dependent gene expression profiling of Hodgkin's disease tumor cells, pathogenetic significance, and link to constitutive signal transducer and activator of transcription 5a activity. J Exp Med *196*, 605-617.

Jensen, F.C., Girardi, A.J., Gilden, R.V., and Koprowski, H. (1964). Infection of Human and Simian Tissue Cultures with Rous Sarcoma Virus. Proc Natl Acad Sci U S A *52*, 53-59.

Kajino-Sakamoto, R., Inagaki, M., Lippert, E., Akira, S., Robine, S., Matsumoto, K., Jobin, C., and Ninomiya-Tsuji, J. (2008). Enterocyte-derived TAK1 signaling prevents epithelium apoptosis and the development of ileitis and colitis. J Immunol *181*, 1143-1152.

Kaler, P., Augenlicht, L., and Klampfer, L. (2009a). Macrophage-derived IL-1beta stimulates Wnt signaling and growth of colon cancer cells: a crosstalk interrupted by vitamin D3. Oncogene *28*, 3892-3902.

Kaler, P., Godasi, B.N., Augenlicht, L., and Klampfer, L. (2009b). The NF-kappaB/AKT-dependent Induction of Wnt Signaling in Colon Cancer Cells by Macrophages and IL-1beta. Cancer Microenviron.

Karin, M. (2006). Nuclear factor-kappaB in cancer development and progression. Nature *441*, 431-436.

Keshav, S. (2006). Paneth cells: leukocyte-like mediators of innate immunity in the intestine. J Leukoc Biol *80*, 500-508.

Kim, K.K., Park, K.S., Song, S.B., and Kim, K.E. (2010). Up regulation of GW112 Gene by NF kappaB promotes an antiapoptotic property in gastric cancer cells. Mol Carcinog *49*, 259-270.

Kinner, A., Wu, W., Staudt, C., and Iliakis, G. (2008). Gamma-H2AX in recognition and signaling of DNA double-strand breaks in the context of chromatin. Nucleic Acids Res *36*, 5678-5694.

Kitajima, S., Morimoto, M., Sagara, E., Shimizu, C., and Ikeda, Y. (2001). Dextran sodium sulfate-induced colitis in germ-free IQI/Jic mice. Exp Anim *50*, 387-395.

Klaus, A., and Birchmeier, W. (2008). Wnt signalling and its impact on development and cancer. Nat Rev Cancer *8*, 387-398.

Kontoyiannis, D., Pasparakis, M., Pizarro, T.T., Cominelli, F., and Kollias, G. (1999). Impaired on/off regulation of TNF biosynthesis in mice lacking TNF AU-rich elements: implications for joint and gut-associated immunopathologies. Immunity *10*, 387-398.

Korinek, V., Barker, N., Moerer, P., van Donselaar, E., Huls, G., Peters, P.J., and Clevers, H. (1998). Depletion of epithelial stem-cell compartments in the small intestine of mice lacking Tcf-4. Nat Genet *19*, 379-383.

Korkaya, H., Paulson, A., Charafe-Jauffret, E., Ginestier, C., Brown, M., Dutcher, J., Clouthier, S.G., and Wicha, M.S. (2009). Regulation of mammary stem/progenitor cells by PTEN/Akt/beta-catenin signaling. PLoS Biol *7*, e1000121.

Kuhn, R., Lohler, J., Rennick, D., Rajewsky, K., and Muller, W. (1993). Interleukin-10-deficient mice develop chronic enterocolitis. Cell *75*, 263-274.

Laken, S.J., Papadopoulos, N., Petersen, G.M., Gruber, S.B., Hamilton, S.R., Giardiello, F.M., Brensinger, J.D., Vogelstein, B., and Kinzler, K.W. (1999). Analysis of masked mutations in familial adenomatous polyposis. Proc Natl Acad Sci U S A *96*, 2322-2326.

Lamberti, C., Lin, K.M., Yamamoto, Y., Verma, U., Verma, I.M., Byers, S., and Gaynor, R.B. (2001). Regulation of beta-catenin function by the IkappaB kinases. J Biol Chem *276*, 42276-42286.

Li, L., and Clevers, H. (2010). Coexistence of quiescent and active adult stem cells in mammals. Science *327*, 542-545.

Luedde, T., Beraza, N., Kotsikoris, V., van Loo, G., Nenci, A., De Vos, R., Roskams, T., Trautwein, C., and Pasparakis, M. (2007). Deletion of NEMO/IKKgamma in liver parenchymal cells causes steatohepatitis and hepatocellular carcinoma. Cancer Cell *11*, 119-132.

Madison, B.B., Dunbar, L., Qiao, X.T., Braunstein, K., Braunstein, E., and Gumucio, D.L. (2002). Cis elements of the villin gene control expression in restricted domains of the vertical (crypt) and horizontal (duodenum, cecum) axes of the intestine. J Biol Chem *277*, 33275-33283.

Maeda, S., Kamata, H., Luo, J.L., Leffert, H., and Karin, M. (2005). IKKbeta couples hepatocyte death to cytokine-driven compensatory proliferation that promotes chemical hepatocarcinogenesis. Cell *121*, 977-990.

Marshman, E., Booth, C., and Potten, C.S. (2002). The intestinal epithelial stem cell. Bioessays *24*, 91-98.

McGuckin, M.A., Eri, R., Simms, L.A., Florin, T.H., and Radford-Smith, G. (2009). Intestinal barrier dysfunction in inflammatory bowel diseases. Inflamm Bowel Dis *15*, 100-113.

Meylan, E., Dooley, A.L., Feldser, D.M., Shen, L., Turk, E., Ouyang, C., and Jacks, T. (2009). Requirement for NF-kappaB signalling in a mouse model of lung adenocarcinoma. Nature *462*, 104-107.

Mori-Akiyama, Y., van den Born, M., van Es, J.H., Hamilton, S.R., Adams, H.P., Zhang, J., Clevers, H., and de Crombrugghe, B. (2007). SOX9 is required for the differentiation of paneth cells in the intestinal epithelium. Gastroenterology *133*, 539-546.

Moser, A.R., Pitot, H.C., and Dove, W.F. (1990). A dominant mutation that predisposes to multiple intestinal neoplasia in the mouse. Science *247*, 322-324.

Murakami, S., Lefebvre, V., and de Crombrugghe, B. (2000). Potent inhibition of the master chondrogenic factor Sox9 gene by interleukin-1 and tumor necrosis factor-alpha. J Biol Chem *275*, 3687-3692.

Nenci, A., Becker, C., Wullaert, A., Gareus, R., van Loo, G., Danese, S., Huth, M., Nikolaev, A., Neufert, C., Madison, B.*, et al.* (2007). Epithelial NEMO links innate immunity to chronic intestinal inflammation. Nature *446*, 557-561.

Neufert, C., Becker, C., and Neurath, M.F. (2007). An inducible mouse model of colon carcinogenesis for the analysis of sporadic and inflammation-driven tumor progression. Nat Protoc *2*, 1998-2004.

Ogawa, H., Fukushima, K., Naito, H., Funayama, Y., Unno, M., Takahashi, K., Kitayama, T., Matsuno, S., Ohtani, H., Takasawa, S.*, et al.* (2003). Increased expression of HIP/PAP and regenerating gene III in human inflammatory bowel disease and a murine bacterial reconstitution model. Inflamm Bowel Dis *9*, 162-170.

Oguma, K., Oshima, H., Aoki, M., Uchio, R., Naka, K., Nakamura, S., Hirao, A., Saya, H., Taketo, M.M., and Oshima, M. (2008). Activated macrophages promote Wnt signalling through tumour necrosis factor-alpha in gastric tumour cells. EMBO J *27*, 1671-1681.

Okayasu, I., Hatakeyama, S., Yamada, M., Ohkusa, T., Inagaki, Y., and Nakaya, R. (1990). A novel method in the induction of reliable experimental acute and chronic ulcerative colitis in mice. Gastroenterology *98*, 694-702.

Page, A., Navarro, M., Garin, M., Perez, P., Casanova, M.L., Moreno, R., Jorcano, J.L., Cascallana, J.L., Bravo, A., and Ramirez, A. (2010). IKKbeta leads to an inflammatory skin disease resembling interface dermatitis. J Invest Dermatol *130*, 1598-1610.

Pasparakis, M., Luedde, T., and Schmidt-Supprian, M. (2006). Dissection of the NF-kappaB signalling cascade in transgenic and knockout mice. Cell Death Differ *13*, 861-872.

Pietras, K., and Ostman, A. (2010). Hallmarks of cancer: interactions with the tumor stroma. Exp Cell Res *316*, 1324-1331.

Pikarsky, E., Porat, R.M., Stein, I., Abramovitch, R., Amit, S., Kasem, S., Gutkovich-Pyest, E., Urieli-Shoval, S., Galun, E., and Ben-Neriah, Y. (2004). NF-kappaB functions as a tumour promoter in inflammation-associated cancer. Nature *431*, 461-466.

Pinto, D., and Clevers, H. (2005). Wnt, stem cells and cancer in the intestine. Biol Cell *97*, 185-196.

Popivanova, B.K., Kitamura, K., Wu, Y., Kondo, T., Kagaya, T., Kaneko, S., Oshima, M., Fujii, C., and Mukaida, N. (2008). Blocking TNF-alpha in mice reduces colorectal carcinogenesis associated with chronic colitis. J Clin Invest *118*, 560-570.

Prasad, S., Ravindran, J., and Aggarwal, B.B. (2010). NF-kappaB and cancer: how intimate is this relationship. Mol Cell Biochem *336*, 25-37.

Radtke, F., and Clevers, H. (2005). Self-renewal and cancer of the gut: two sides of a coin. Science *307*, 1904-1909.

Rajewsky, K., Gu, H., Kuhn, R., Betz, U.A., Muller, W., Roes, J., and Schwenk, F. (1996). Conditional gene targeting. J Clin Invest *98*, 600-603.

Rasola, A., Fassetta, M., De Bacco, F., D'Alessandro, L., Gramaglia, D., Di Renzo, M.F., and Comoglio, P.M. (2007). A positive feedback loop between hepatocyte growth factor receptor and beta-catenin sustains colorectal cancer cell invasive growth. Oncogene *26*, 1078-1087.

Rennick, D., Davidson, N., and Berg, D. (1995). Interleukin-10 gene knock-out mice: a model of chronic inflammation. Clin Immunol Immunopathol *76*, S174-178.

Reya, T., and Clevers, H. (2005). Wnt signalling in stem cells and cancer. Nature *434*, 843-850.

Roda, G., Sartini, A., Zambon, E., Calafiore, A., Marocchi, M., Caponi, A., Belluzzi, A., and Roda, E. (2010). Intestinal epithelial cells in inflammatory bowel diseases. World J Gastroenterol *16*, 4264-4271.

Sakamoto, K., Hikiba, Y., Nakagawa, H., Hayakawa, Y., Yanai, A., Akanuma, M., Ogura, K., Hirata, Y., Kaestner, K.H., Omata, M.*, et al.* (2010). Inhibitor of kappaB kinase beta regulates gastric carcinogenesis via interleukin-1alpha expression. Gastroenterology *139*, 226-238 e226.

Sansom, O.J., Reed, K.R., Hayes, A.J., Ireland, H., Brinkmann, H., Newton, I.P., Batlle, E., Simon-Assmann, P., Clevers, H., Nathke, I.S.*, et al.* (2004). Loss of Apc in vivo immediately perturbs Wnt signaling, differentiation, and migration. Genes Dev *18*, 1385-1390.

Sasaki, Y., Derudder, E., Hobeika, E., Pelanda, R., Reth, M., Rajewsky, K., and Schmidt-Supprian, M. (2006). Canonical NF-kappaB activity, dispensable for B cell development, replaces BAFF-receptor signals and promotes B cell proliferation upon activation. Immunity *24*, 729-739.

Sauer, B., and Henderson, N. (1988). Site-specific DNA recombination in mammalian cells by the Cre recombinase of bacteriophage P1. Proc Natl Acad Sci U S A *85*, 5166-5170.

Schutyser, E., Struyf, S., and Van Damme, J. (2003). The CC chemokine CCL20 and its receptor CCR6. Cytokine Growth Factor Rev *14*, 409-426.

Scoville, D.H., Sato, T., He, X.C., and Li, L. (2008). Current view: intestinal stem cells and signaling. Gastroenterology *134*, 849-864.

Shinozaki, S., Nakamura, T., Iimura, M., Kato, Y., Iizuka, B., Kobayashi, M., and Hayashi, N. (2001). Upregulation of Reg 1alpha and GW112 in the epithelium of inflamed colonic mucosa. Gut *48*, 623-629.

Shtutman, M., Zhurinsky, J., Simcha, I., Albanese, C., D'Amico, M., Pestell, R., and Ben-Ze'ev, A. (1999). The cyclin D1 gene is a target of the beta-catenin/LEF-1 pathway. Proc Natl Acad Sci U S A *96*, 5522-5527.

Snippert, H.J., van Es, J.H., van den Born, M., Begthel, H., Stange, D.E., Barker, N., and Clevers, H. (2009). Prominin-1/CD133 marks stem cells and early progenitors in mouse small intestine. Gastroenterology *136*, 2187-2194 e2181.

Steinbrecher, K.A., Harmel-Laws, E., Sitcheran, R., and Baldwin, A.S. (2008). Loss of epithelial RelA results in deregulated intestinal proliferative/apoptotic homeostasis and susceptibility to inflammation. J Immunol *180*, 2588-2599.

Strober, W. (2006). Immunology. Unraveling gut inflammation. Science *313*, 1052-1054.

Su, L.K., Kinzler, K.W., Vogelstein, B., Preisinger, A.C., Moser, A.R., Luongo, C., Gould, K.A., and Dove, W.F. (1992). Multiple intestinal neoplasia caused by a mutation in the murine homolog of the APC gene. Science *256*, 668-670.

Suzuki, R., Kohno, H., Sugie, S., Nakagama, H., and Tanaka, T. (2006). Strain differences in the susceptibility to azoxymethane and dextran sodium sulfate-induced colon carcinogenesis in mice. Carcinogenesis *27*, 162-169.

Tada, K., Okazaki, T., Sakon, S., Kobarai, T., Kurosawa, K., Yamaoka, S., Hashimoto, H., Mak, T.W., Yagita, H., Okumura, K.*, et al.* (2001). Critical roles of TRAF2 and TRAF5 in tumor necrosis factor-induced NF-kappa B activation and protection from cell death. J Biol Chem *276*, 36530-36534.

Takahashi, M., Nakatsugi, S., Sugimura, T., and Wakabayashi, K. (2000). Frequent mutations of the beta-catenin gene in mouse colon tumors induced by azoxymethane. Carcinogenesis *21*, 1117-1120.

Takahashi, M., and Wakabayashi, K. (2004). Gene mutations and altered gene expression in azoxymethane-induced colon carcinogenesis in rodents. Cancer Sci *95*, 475-480.

Tanaka, T., Kohno, H., Suzuki, R., Yamada, Y., Sugie, S., and Mori, H. (2003). A novel inflammation-related mouse colon carcinogenesis model induced by azoxymethane and dextran sodium sulfate. Cancer Sci *94*, 965-973.

Tetsu, O., and McCormick, F. (1999). Beta-catenin regulates expression of cyclin D1 in colon carcinoma cells. Nature *398*, 422-426.

Ukena, S.N., Singh, A., Dringenberg, U., Engelhardt, R., Seidler, U., Hansen, W., Bleich, A., Bruder, D., Franzke, A., Rogler, G.*, et al.* (2007). Probiotic Escherichia coli Nissle 1917 inhibits leaky gut by enhancing mucosal integrity. PLoS One *2*, e1308.

Umar, S., Sarkar, S., Wang, Y., and Singh, P. (2009). Functional cross-talk between beta-catenin and NFkappaB signaling pathways in colonic crypts of mice in response to progastrin. J Biol Chem *284*, 22274-22284.

Uronis, J.M., Muhlbauer, M., Herfarth, H.H., Rubinas, T.C., Jones, G.S., and Jobin, C. (2009). Modulation of the intestinal microbiota alters colitis-associated colorectal cancer susceptibility. PLoS One *4*, e6026.

Vallabhapurapu, S., and Karin, M. (2009). Regulation and function of NF-kappaB transcription factors in the immune system. Annual review of immunology *27*, 693-733.

van de Wetering, M., Sancho, E., Verweij, C., de Lau, W., Oving, I., Hurlstone, A., van der Horn, K., Batlle, E., Coudreuse, D., Haramis, A.P.*, et al.* (2002). The beta-catenin/TCF-4 complex imposes a crypt progenitor phenotype on colorectal cancer cells. Cell *111*, 241-250.

van der Flier, L.G., and Clevers, H. (2009). Stem cells, self-renewal, and differentiation in the intestinal epithelium. Annu Rev Physiol *71*, 241-260.

van der Flier, L.G., van Gijn, M.E., Hatzis, P., Kujala, P., Haegebarth, A., Stange, D.E., Begthel, H., van den Born, M., Guryev, V., Oving, I.*, et al.* (2009). Transcription factor achaete scute-like 2 controls intestinal stem cell fate. Cell *136*, 903-912.

van Hogerlinden, M., Rozell, B.L., Ahrlund-Richter, L., and Toftgard, R. (1999). Squamous cell carcinomas and increased apoptosis in skin with inhibited Rel/nuclear factor-kappaB signaling. Cancer Res *59*, 3299-3303.

Varfolomeev, E., Goncharov, T., Fedorova, A.V., Dynek, J.N., Zobel, K., Deshayes, K., Fairbrother, W.J., and Vucic, D. (2008). c-IAP1 and c-IAP2 are critical mediators of tumor necrosis factor alpha (TNFalpha)-induced NF-kappaB activation. J Biol Chem *283*, 24295-24299.

Varfolomeev, E., and Vucic, D. (2008). (Un)expected roles of c-IAPs in apoptotic and NFkappaB signaling pathways. Cell Cycle *7*, 1511-1521.

Velcich, A., Yang, W., Heyer, J., Fragale, A., Nicholas, C., Viani, S., Kucherlapati, R., Lipkin, M., Yang, K., and Augenlicht, L. (2002). Colorectal cancer in mice genetically deficient in the mucin Muc2. Science *295*, 1726-1729.

Vermeulen, L., De Sousa, E.M.F., van der Heijden, M., Cameron, K., de Jong, J.H., Borovski, T., Tuynman, J.B., Todaro, M., Merz, C., Rodermond, H.*, et al.* (2010). Wnt activity defines colon cancer stem cells and is regulated by the microenvironment. Nat Cell Biol *12*, 468-476.

Vlantis, K., and Pasparakis, M. (2010). Role of TNF in pathologies induced by nuclear factor kappaB deficiency. Curr Dir Autoimmun *11*, 80-93.

Wang, C., Deng, L., Hong, M., Akkaraju, G.R., Inoue, J., and Chen, Z.J. (2001). TAK1 is a ubiquitin-dependent kinase of MKK and IKK. Nature *412*, 346-351.

Wang, Y., and Sul, H.S. (2009). Pref-1 regulates mesenchymal cell commitment and differentiation through Sox9. Cell Metab *9*, 287-302.

Wehkamp, J., and Stange, E.F. (2006). Paneth cells and the innate immune response. Curr Opin Gastroenterol *22*, 644-650.

Wells, J.M., Loonen, L.M., and Karczewski, J.M. (2010). The role of innate signaling in the homeostasis of tolerance and immunity in the intestine. Int J Med Microbiol *300*, 41-48.

Wielenga, V.J., Smits, R., Korinek, V., Smit, L., Kielman, M., Fodde, R., Clevers, H., and Pals, S.T. (1999). Expression of CD44 in Apc and Tcf mutant mice implies regulation by the WNT pathway. Am J Pathol *154*, 515-523.

Wilson, C.L., Heppner, K.J., Rudolph, L.A., and Matrisian, L.M. (1995). The metalloproteinase matrilysin is preferentially expressed by epithelial cells in a tissue-restricted pattern in the mouse. Mol Biol Cell *6*, 851-869.

Wong, W.W., Gentle, I.E., Nachbur, U., Anderton, H., Vaux, D.L., and Silke, J. (2010). RIPK1 is not essential for TNFR1-induced activation of NF-kappaB. Cell Death Differ *17*, 482-487.

Wu, S., Rhee, K.J., Albesiano, E., Rabizadeh, S., Wu, X., Yen, H.R., Huso, D.L., Brancati, F.L., Wick, E., McAllister, F.*, et al.* (2009). A human colonic commensal promotes colon tumorigenesis via activation of T helper type 17 T cell responses. Nat Med *15*, 1016-1022.

Xiao, G., Harhaj, E.W., and Sun, S.C. (2001). NF-kappaB-inducing kinase regulates the processing of NF-kappaB2 p100. Mol Cell *7*, 401-409.

Yang, J., Splittgerber, R., Yull, F.E., Kantrow, S., Ayers, G.D., Karin, M., and Richmond, A. (2010). Conditional ablation of Ikkb inhibits melanoma tumor development in mice. J Clin Invest *120*, 2563-2574.

Yang, K., Popova, N.V., Yang, W.C., Lozonschi, I., Tadesse, S., Kent, S., Bancroft, L., Matise, I., Cormier, R.T., Scherer, S.J.*, et al.* (2008). Interaction of Muc2 and Apc on Wnt signaling and in intestinal tumorigenesis: potential role of chronic inflammation. Cancer Res *68*, 7313-7322.

Acknowledgements

First of all I would like to express my gratitude to Prof. Manolis Pasparakis, who gave me the opportunity to do my PhD work in his laboratory. I would like to thank him for showing constant interest in the progress of my work, for the scientific guidance and encouragement during the last 4 years.

I am deeply indebted to Andy Wullaert, my supervisor in the lab, for showing a lot of patience in teaching me all the techniques and for investing time in reading and suggesting corrections for this manuscript. Furthermore I would like to thank him for always being supportive in case of need. I wish to acknowledge the members of the "gut group": Andy Wullaert, Vanessa Majada-Fernandez and Patrick Welz for the invaluable support and the remarkable teamwork that created a unique atmosphere in the lab.

Moreover, I would like to thank all the members of the Pasparakis Laboratory for making time there so much worth it and for the support I experienced during the last years. Particularly I wish to acknowledge Apostolis Polykratis, Nikoletta Papadopoulou, Teresa Corona and Ulrike Resch for scientific discussion and personal support. Laurens Wachsmuth I wish to thank for always being helpful when hard- and software were disobliging.

I would like to express my thankfulness to our brilliant team of technical assistants for the tremendous helpfulness in case of need and for making life in the lab so much more comfortable and joyful. I am very grateful for the countless sections that were patiently prepared by Daniela Beier, Elza Mahlberg and Julia von Rhein and I owe many thanks to Daniela Beier for the excellent assistance in IHC. Jennifer Buchholz and Bianca Wolff I would like to thank for taking care of mice and Claudia Uthoff-Hachenberg and Brigitte Hülser for all the genotyping and help in all kinds of situations.

My thanks also go to Dr. Martin Hafner, who was always very helpful and invested a lot of time in bureaucratic issues of all sorts and to Silke Röpke for her help in various occasions.

Dr. Anna Bigas I would like to acknowledge for providing us with transfection plasmids and intestinal cancer cell lines. I wish to thank Prof. Tania Roskams for teaching us how to evaluate histological tissue sections of the intestine.

Last, but not least, I would like to thank my family for their loving support during all this time and for constantly being there for me. I would like to sincerely thank Cristian Dan Neacsu for his long-lasting support in every situation that came along, for his unflagging patience and for always believing in me.

Erklärung

Ich versichere, dass ich die von mir vorgelegte Dissertation selbständig angefertigt, die benutzten Quellen und Hilfsmittel vollständig angegeben und die Stellen der Arbeit − einschließlich Tabellen, Karten und Abbildungen −, die anderen Werken im Wortlaut oder dem Sinn nach entnommen sind, in jedem Einzelfall als Entlehnung kenntlich gemacht habe; dass diese Dissertation noch keiner anderen Fakultät oder Universität zur Prüfung vorgelegen hat; dass sie noch nicht veröffentlicht worden ist sowie, dass ich eine solche Veröffentlichung vor Abschluss des Promotionsverfahrens nicht vornehmen werde. Die Bestimmungen der Promotionsordnung sind mir bekannt. Die von mir vorgelegte Dissertation ist von Prof. Dr. Manolis Pasparakis betreut worden.

Datum Katerina Vlantis

Teile dieser Arbeit wurden veröffentlicht in

Vlantis, K., Wullaert, A., Sasaki, Y., Schmidt-Supprian, M., Rajewsky, K., Roskams, T., Pasparakis, M.
Constitutive IKK2 activation in intestinal epithelial cells induces intestinal tumors in mice.
Journal of Clinical Investigation, Vol. 121 (7): 2781-93, 2011

Curriculum Vitae

Personal Data

Name:	Katerina
Surname:	Vlantis
Date of Birth:	09 July 1982
Place of Birth:	Mönchengladbach (Germany)
Nationality:	German
Home address:	Zülpicher Str. 44 50674 Cologne Germany
Business address:	University of Cologne Institute for Genetics AG Pasparakis Zülpicher Str. 47a 50674 Cologne Germany
Phone:	+49-221-470-1649
Email:	vlantisk@uni-koeln.de

Education

2001	Graduation from German School of Athens, Dörpfeld Gymnasium, Athens, Greece (Abitur)
2001-2005	Studies in Biology at the University of Cologne, Cologne, Germany
12/2005	Oral Diploma examination at the University of Cologne
2006-2007	Diploma thesis in Genetics, Institute for Genetics, University of Cologne
01/2007	Graduation from the University of Cologne, Diploma Biology

Research career

2006-2007	Diploma Thesis: „Untersuchung zur G1-Stabilität und Funktionalität von Rca1 in *Drosophila* Schneiderzellen" Institute for Genetics, Department of Developmental Genetics, AG Sprenger, Cell Cycle Regulation, University of Cologne

	Supervisor: PD Dr. rer. nat Frank Sprenger
Since 02/2007	Graduate Student at the University of Cologne (Dr. rer. nat), AG Pasparakis, Mouse Genetics and Inflammation

Work experience

10/2003-02/2004	Student Assistant in Zoology practical, Institute for Zoology, University of Cologne
10/2003-02/2004	Applied Biotechnology/Microbiology training; AG Krämer, Supervisor Dr. A. Burkovsky, Institute for Biochemistry, University of Cologne
02 – 03/2004	Practical training in biological techniques (Microscopy, HPLC, Histology; in situ Hybridisation; Molecular Biology techniques) Institute for Zoology, University of Cologne
06 – 07/2004	Practical training in Neurology, AG Göpfert, Supervisors PD Dr. M. Göpfert and Dr. J. Alberts Institute for Zoology, University of Cologne
02 – 04/2005	Practical training in Genetics, Molecular Biology, AG Sprenger, Institute for Genetics, University of Cologne

Congresses/Workshops

Retreat SFB 635 Posttranslational control of protein function
January 30-31, 2006, Germany

2nd ENII-MUGEN Summer School in advanced Immunology
April 14-21, 2007 in Sardinia, Italy

II Falk Gastro Conference: Mechanisms of Intestinal Inflammation
October 09-10, 2007 in Dresden, Germany
Poster Presentation: The role of TNF signalling and apoptosis in spontaneous colitis development in $NEMO^{IEC-KO}$ mice

International Symposium „Frontiers in Allergy and Autoimmunity“
May 30-31, 2008 in Mainz, Germany

12th International TNF Conference
April 26-29, 2009 in San Lorenzo de El Escorial, Madrid, Spain
Talk: The role of TNF-signalling in colitis development in $NEMO^{IEC-KO}$ mice

Basic Real-Time PCR Training, System 7900, Applied Biosystems
May 19-20, 2009 in Darmstadt, Germany

Ingenuity Pathway Analysis Training, Ingenuity Systems
February 24, 2010 in Cologne, Germany

Core competences

Methods and techniques

- Standard molecular biology techniques, e.g. DNA and RNA extraction, PCR, quantitative RealTime PCR, protein extraction, Western Blots, EMSA etc.
- Histology, tissue sectioning, Immunofluorescence and Immunohistochemistry stainings
- Microscopy
- Handling of mice, *in vivo* High Resolution Mini Colon Endoscopy of mice, intraperitoneal injections
- Dissection of mouse tissues, isolation of intestinal epithelial cells from colon and small intestine
- Cloning, transformation, transfection, cell culture of mammalian and insect cells
- Basic neurobiology techniques

Languages

German, Greek	mother tongue
English	fluent both oral and written
French	basic knowledge

IT skills

Standard Microsoft Office Software (Word, Excel, Powerpoint); GraphPad Prism; Ingenuity Systems Pathway analysis;

November, 2010

Related Commentary, page 2551 Research article

Constitutive IKK2 activation in intestinal epithelial cells induces intestinal tumors in mice

Katerina Vlantis,[1] Andy Wullaert,[1] Yoshiteru Sasaki,[2,3] Marc Schmidt-Supprian,[2,4] Klaus Rajewsky,[2] Tania Roskams,[5] and Manolis Pasparakis[1]

[1]Institute for Genetics, Center for Molecular Medicine (CMMC), and Cologne Excellence Cluster on Cellular Stress Responses in Aging-Associated Diseases (CECAD), University of Cologne, Cologne, Germany. [2]Immune Disease Institute, Boston, Massachusetts, USA. [3]RIKEN Center for Developmental Biology, Laboratory for Stem Cell Biology, Kobe, Japan. [4]Max Planck Institute of Biochemistry, Martinsried, Germany. [5]Department of Pathology, University Hospitals, University of Leuven, Leuven, Belgium.

Many cancers display increased NF-κB activity, and NF-κB inhibition is known to diminish tumor development in multiple mouse models, supporting an important role of NF-κB in carcinogenesis. NF-κB activation in premalignant or cancer cells is believed to promote tumor development mainly by protecting these cells from apoptosis. However, it remains unclear to what extent NF-κB activation exhibits additional protumorigenic functions in premalignant cells that could be sufficient to induce spontaneous tumor development. Here we show that expression of constitutively active IκB kinase 2 (IKK2ca) in mouse intestinal epithelial cells (IECs) induced spontaneous tumors in aged mice and also strongly enhanced chemical- and Apc mutation–mediated carcinogenesis. IECs expressing IKK2ca displayed altered Wnt signaling and increased proliferation and elevated expression of genes encoding intestinal stem cell–associated factors including Ascl2, Olfm4, DLK1, and Bmi-1, indicating that increased IKK2/NF-κB activation synergized with Wnt signaling to drive intestinal tumorigenesis. Moreover, IECs expressing IKK2ca produced cytokines and chemokines that induced the recruitment of myeloid cells and activated stromal fibroblasts to become myofibroblasts, thus creating a tumor-promoting microenvironment. Taken together, our results show that constitutively increased activation of IKK2/NF-κB signaling in the intestinal epithelium is sufficient to induce the full spectrum of cell-intrinsic and stromal alterations required for intestinal tumorigenesis.

Introduction

The IκB kinase (IKK)/NF-κB signaling pathway controls the expression of many genes regulating immune and inflammatory responses, cell survival, and proliferation and is believed to be centrally involved in carcinogenesis. Many cancer cell lines, but also primary tumors, display constitutively increased NF-κB activity, and inhibition of NF-κB compromises the survival and growth of cultured cancer cells, suggesting that NF-κB is important for the survival of at least some types of tumors (1). Furthermore, NF-κB inhibition diminished tumor development in mouse models, supporting an important role for NF-κB in carcinogenesis (2–6).

IKK2/IKKβ-mediated NF-κB activation was proposed to provide a link between inflammation and carcinogenesis by acting both in cancer cells and in cells of the microenvironment to promote tumor development (7, 8). IKK2 ablation in myeloid cells reduced the expression of cytokines and growth factors supporting tumor growth and diminished tumor development in the azoxymethane/dextran sulfate sodium (AOM/DSS) mouse model of carcinogen-initiated inflammation-associated colon cancer (5). In addition, NF-κB activation in cancer-associated fibroblasts was recently shown to be important for skin carcinogenesis by coordinating the expression of fibroblast-derived proinflammatory factors promoting macrophage recruitment, neovascularization, and tumor growth (9). These studies demonstrated that NF-κB promotes carcinogenesis by acting in cells of the tumor microenvironment to induce the expression of factors supporting tumor growth. In line with its well-established prosurvival functions, IKK2 ablation in colonic or gastric epithelial cells reduced the incidence of AOM/DSS-induced colon cancer (5) and carcinogen N-methyl-N-nitrosourea–induced (MNU-induced) gastric cancer (6). In addition, NF-κB inhibition by expression of an IκBα superrepressor (IκBα-SR) or by ablation of p65/RelA in lung epithelial cells reduced the incidence of oncogenic Ras–induced lung cancer (4, 10). However, NF-κB inhibition in skin or liver cells had opposite effects in different models of carcinogenesis. NF-κB inhibition by expression of IκBα-SR in epidermal keratinocytes synergized with oncogenic Ras to induce epidermal cancer (11) or led to spontaneous tumor development (12), while IKK2 ablation in melanocytes protected mice from oncogenic Ras–induced melanoma development (2). Moreover, NF-κB blockade by IκBα-SR expression in hepatocytes inhibited inflammation-associated liver cancer development in the Mdr2-deficient mouse model (3), while IKK2 ablation in hepatocytes sensitized mice to chemical hepatocarcinogenesis induced by diethylnitrosamine (DEN) (13). Finally, liver parenchymal cell–specific knockout of NEMO/IKKγ led to the spontaneous development of hepatocellular carcinomas in mice (14). These findings suggest that the role of IKK/NF-κB signaling within premalignant or tumor cells in carcinogenesis is complex and often depends on the specific tissue studied and the carcinogenic stimulus applied. These results also indicate that NF-κB activation in premalignant or tumor cells is likely to affect different processes that are fundamental for carcinogenesis in addition to its antiapoptotic function.

Conflict of interest: The authors have declared that no conflict of interest exists.
Citation for this article: *J Clin Invest.* 2011;121(7):2781–2793. doi:10.1172/JCI45349.

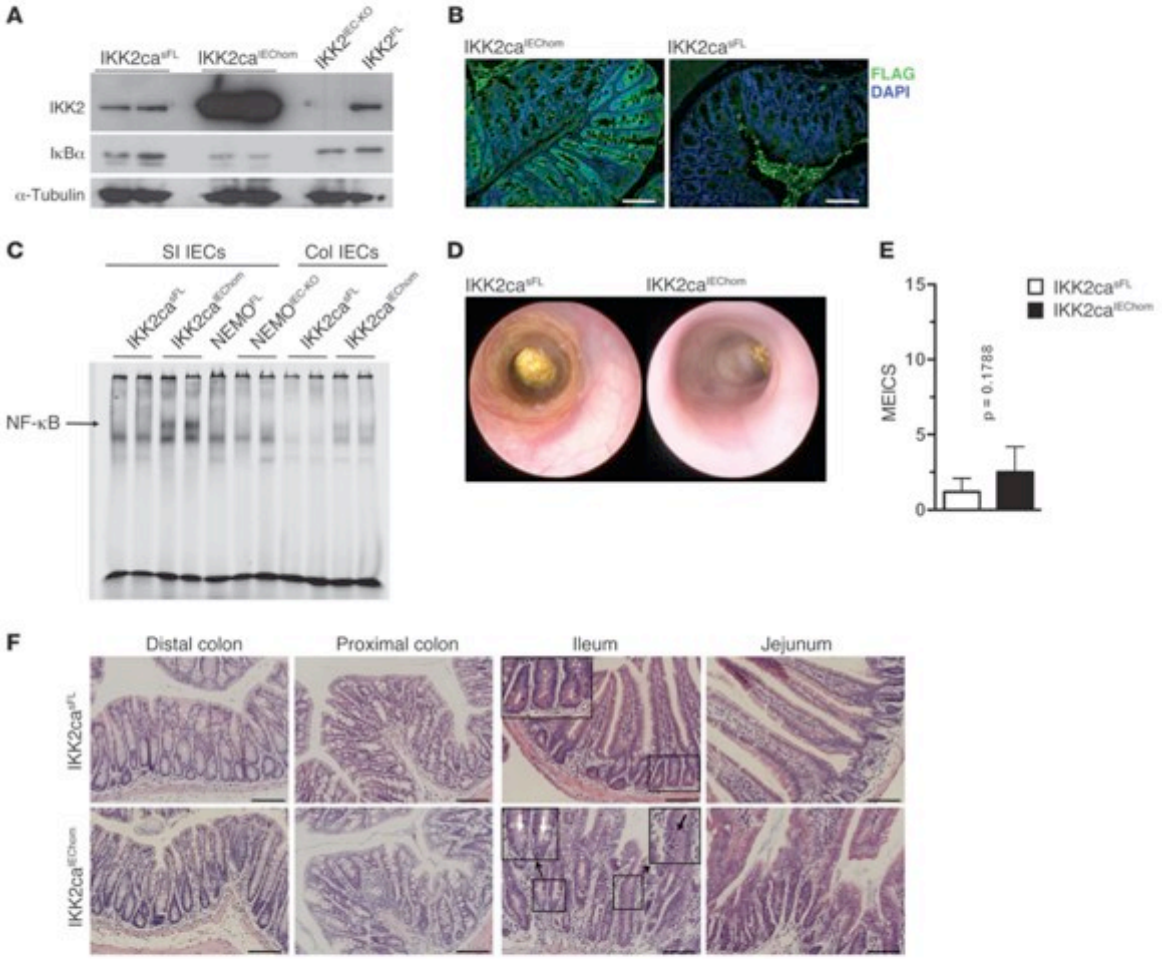

Figure 1

IKK2ca expression in IECs induces NF-κB activation and mild intestinal inflammation. (**A**) Immunoblot reveals increased IKK2 expression and reduced levels of IκBα in SI IECs from IKK2ca^{IEChom} mice compared with IKK2ca^{sFL} littermates. (**B**) Immunofluorescent staining with anti-FLAG antibodies shows IEC-specific expression of FLAG-IKK2ca in IKK2ca^{IEChom} colon sections. Background staining in the lumen of the IKK2ca^{sFL} colon results from incomplete removal of luminal contents. (**C**) EMSA reveals increased NF-κB DNA-binding activity in nuclear extracts from IKK2ca^{IEChom} SI and colonic IECs. (**D**) Representative endoscopic images of colons from 8-week-old IKK2ca^{sFL} and IKK2ca^{IEChom} mice. (**E**) Quantification of MEICS showing no significant colonic inflammation in 7- to 9-week-old IKK2ca^{IEChom} (n = 10) mice compared with IKK2ca^{sFL} (n = 5) littermates. Data are presented as mean ± SD. (**F**) H&E-stained sections show crypt elongation and increased immune cell infiltration in the SI and colon of IKK2ca^{IEChom} compared with IKK2ca^{sFL} mice. Note the lack of Paneth cells in ileal crypts in IKK2ca^{IEChom} mice (indicated by white arrows in inset). The black arrow indicates a mislocalized Paneth cell. Scale bars: 50 μm.

Mutations leading to constitutive NF-κB activation have been found in several cancers (1, 15–17), suggesting that persistent activation of NF-κB could be a critical step in tumor development, although the mechanisms by which cell-intrinsic NF-κB activation promotes tumorigenesis remain incompletely understood. Most importantly, it remains unclear whether constitutive NF-κB activation is sufficient to induce spontaneous tumor development in vivo. Here we used a transgenic mouse model expressing constitutively active IKK2 specifically in intestinal epithelial cells (IECs) to study the mechanisms by which constitutively increased NF-κB activation affects intestinal tumorigenesis. Our results show that persistent NF-κB activation strongly synergizes with chemical and genetic models of intestinal carcinogenesis to induce tumors in both the colon and the small intestine (SI). Most importantly, mice expressing constitutively active IKK2 in IECs spontaneously developed tumors in the colon and the SI, demonstrating that persistent activation of IKK2/NF-κB signaling in IECs is sufficient to induce intestinal tumorigenesis.

Results

Constitutive IKK2/NF-κB activation in IECs induced mild inflammation in the colon and SI. To study in vivo the epithelial-intrinsic role of NF-κB in intestinal tumorigenesis, we generated mice expressing

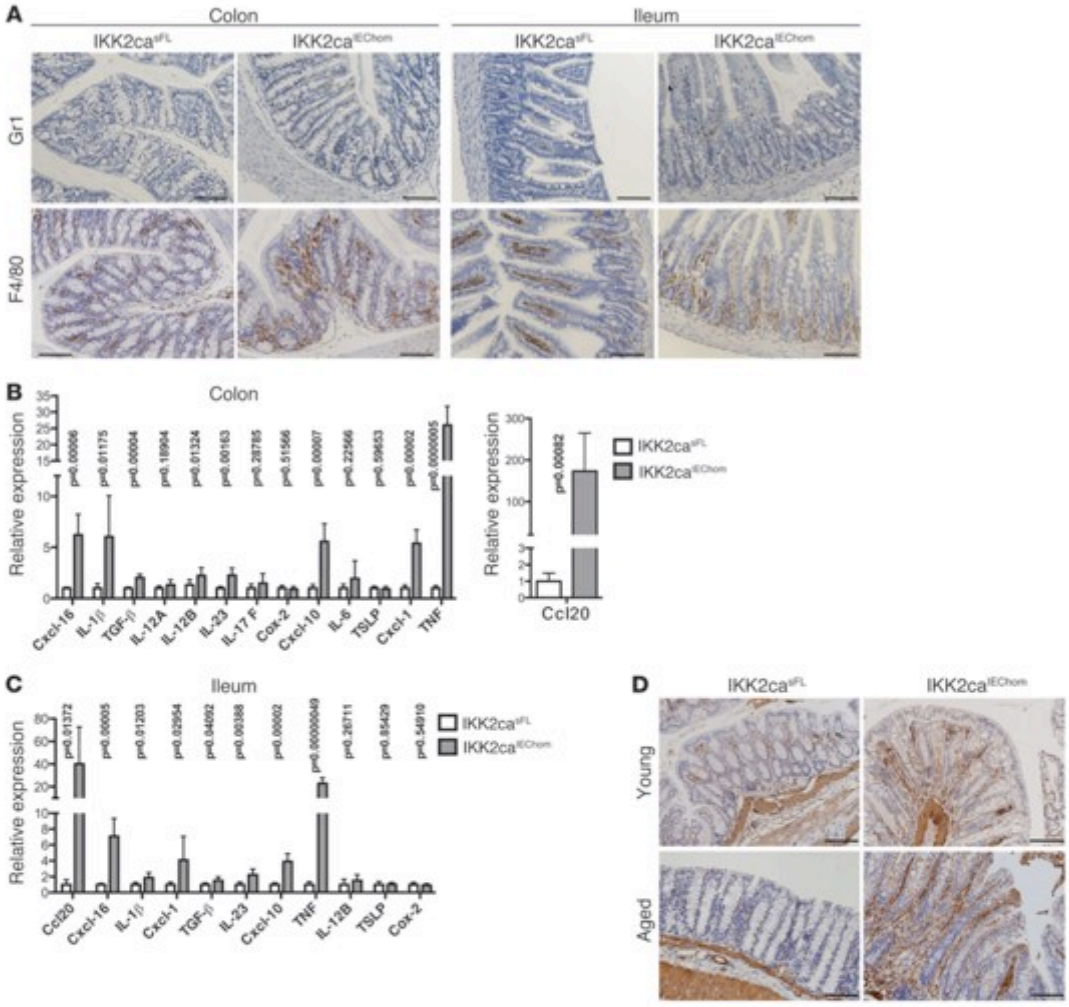

Figure 2

Immune cell infiltration and increased cytokine and chemokine expression in the gut of IKK2ca^{IEChom} mice. (**A**) Immunohistochemical staining for Gr1 and F4/80 reveals increased numbers of granulocytes and macrophages, respectively, in colonic and SI cross sections of 6-week-old IKK2ca^{IEChom} mice. In the SI of IKK2ca^{IEChom} mice, F4/80-positive cells accumulated around the crypts, while in control mice, macrophages were mainly found in the villi. (**B** and **C**) qRT-PCR analysis shows enhanced expression of a subset of proinflammatory genes in the colon (**B**) and the ileum (**C**) of 7- to 8-week-old IKK2ca^{IEChom} mice ($n \geq 6$ for each genotype; mRNA levels are presented as mean ± SD). (**D**) Immunohistochemical staining with antibodies recognizing α-SMA revealed the presence of increased numbers of activated myofibroblasts in colons of young (10 week old) and aged (1 year old) IKK2ca^{IEChom} mice compared with IKK2ca^{fFL} littermates. Scale bars: 50 μm.

constitutively active IKK2 (IKK2ca) specifically in IECs by crossing mice carrying the R26-StopFLIkk2ca (IKK2ca^{fFL}) allele (18) with villin-Cre transgenics (19). Homozygous mice expressing 2 copies of the R26-StopFLIkk2ca allele (IKK2ca^{IEChom}) expressed high levels of IKK2ca specifically in IECs (Figure 1, A and B; Supplemental Figure 1A and Supplemental Figure 2A; supplemental material available online with this article; doi:10.1172/JCI45349DS1) and showed increased NF-κB activation, as assessed by IκBα immunoblot of total protein extracts and by EMSA on nuclear extracts from colonic and SI primary epithelial cells (Figure 1, A and C, and Supplemental Figure 1B). Heterozygous mice carrying 1 copy of the R26-StopFLIkk2ca allele (IKK2ca^{IEChet}) expressed about half the levels of IKK2ca and also showed elevated NF-κB activation in IECs (Supplemental Figure 1). IKK2ca-expressing IECs showed normal levels of IKK1, NEMO, and p65, but increased expression of p100 and RelB, which are produced by NF-κB–regulated genes (Supplemental Figure 1A) (20, 21). IKK2ca^{IEChom} mice showed moderately reduced body weight (Supplemental Figure 2B), prompting us to assess whether they developed spontaneous intestinal disease. Endoscopic analysis of 7- to 9-week-old animals did not reveal signs of inflammation in the distal colon of IKK2ca^{IEChom} mice compared with littermate controls (Figure 1, D and E). Colon length did not

differ; however, the SIs of IKK2ca^{IEChom} mice were markedly elongated compared with those of littermate controls (Supplemental Figure 2, C–E). Histological examination of colon and SI cross sections revealed the presence of scattered areas showing signs of mild focal inflammation, with small numbers of immune cells infiltrating the colonic mucosa and the area around the crypts in the SI (Figure 1F). The epithelium adjacent to these inflammatory infiltrates showed slightly altered morphology with moderately elongated crypts, particularly in the enlarged SI (Figure 1F). Goblet cell numbers in the colon and SI did not differ between IKK2ca^{IEChom} and control mice. However, we detected decreased numbers of Paneth cells in SI crypt bases, while sometimes mislocalized Paneth cells were found higher up toward the luminal side in elongated crypts (Figure 1F), suggesting that increased IKK2/NF-κB activity in IECs alters Paneth cell differentiation or localization.

To characterize the inflammatory infiltrates in the intestinal mucosa of IKK2ca^{IEChom} mice, we performed immunohistochemical staining with specific antibodies recognizing macrophages, granulocytes, T cells, and B cells. F4/80 staining revealed areas showing moderately increased numbers of macrophages in sections from the colon but also from the SI of IKK2ca^{IEChom} mice, where they appeared to accumulate around the base of the crypts (Figure 2A). In addition, small numbers of Gr1^{+} granulocytes were detected in the ileum and to a lesser extent in the colon of IKK2ca^{IEChom} but not in control mice (Figure 2A). B and T cell numbers in the gut did not differ considerably between IKK2ca^{IEChom} and control mice (data not shown). Quantitative RT-PCR (qRT-PCR) analysis on mRNA from colon and ileum revealed increased expression of several proinflammatory cytokines and chemokines including TNF, IL-1β, Ccl20, Cxcl-1, Cxcl-10, and Cxcl-16 in IKK2ca^{IEChom} mice (Figure 2, B and C). Immunoblot analysis also revealed increased IL-1β protein levels in the colon and SI of IKK2ca^{IEChom} mice (Supplemental Figure 3, C and D). TNF, IL-1β, Ccl20, Cxcl-10, and Cxcl-16 were also upregulated in primary colonic and SI IECs (Supplemental Figure 3, A and B), suggesting that they are directly induced by IKK2ca expression in epithelial cells. Immunohistochemical staining with antibodies recognizing α-SMA, a marker of activated myofibroblasts (9), revealed increased activation of stromal fibroblasts in the intestinal mucosa of aged but also young IKK2ca^{IEChom} mice (Figure 2D). Thus, IKK2ca expression in IECs results in increased cytokine and chemokine expression, recruitment of myeloid cells, and activation of stromal fibroblasts in the intestinal mucosa.

Expression of IKK2ca in IECs strongly enhanced chemical carcinogen–induced intestinal tumor development. Because partial inhibition of canonical NF-κB signaling by IEC-specific knockout of IKK2 or p65 sensitized mice to DSS-induced colitis (5, 22), we reasoned that increased IKK2ca-mediated NF-κB activation in epithelial cells might protect mice from DSS-induced intestinal injury. Surprisingly, IKK2ca^{IEChom} mice developed more severe colitis manifesting with pronounced weight loss, intestinal bleeding, and diarrhea after DSS treatment (Figure 3A and data not shown). Histological examination revealed tissue damage with extended loss of crypt structures and increased inflammatory cell infiltration in colons from IKK2ca^{IEChom} compared with IKK2ca^{fFL} mice (Figure 3B). In addition, colons from DSS-treated IKK2ca^{IEChom} mice showed increased expression of proinflammatory cytokines and chemokines including TNF, IL-1β, Cxcl-1, and MCP-1 (Figure 3C). Thus, constitutive NF-κB activation in IECs exacerbated colitis development in response to DSS-induced epithelial injury.

To determine whether constitutive NF-κB activation in IECs affects inflammation-associated colon cancer, we assessed AOM/DSS-induced carcinogenesis in IKK2ca^{IEChom} and control mice (Figure 4A). Since IKK2ca^{IEChom} mice were very sensitive to DSS treatment, we applied a modified protocol including only 1 short cycle of treatment with low DSS concentration (1.5% DSS for 3 days). This treatment induced severe weight loss associated with intestinal bleeding and diarrhea in IKK2ca^{IEChom} but not in control mice (Figure 4A and data not shown). Moreover, endoscopic analysis performed 26 days after AOM injection revealed signs of severe colitis in IKK2ca^{IEChom} but not in IKK2ca^{fFL} mice (Figure 4B). Endoscopy on day 65 revealed that all IKK2ca^{IEChom}, but none of their IKK2ca^{fFL} littermates, had developed multiple tumors in the distal colon (Figure 4C), which displayed histological characteristics typical of mucus-producing adenomas with advanced dysplasia (Figure 4D) and in some cases progressed to adenocarcinomas invading the submucosa (Figure 4E). Thus, IEC-specific expression of IKK2ca had a strong protumorigenic effect resulting in the development of multiple broad-based colonic adenomas even under a very mild AOM/DSS protocol that was not sufficient to induce tumors in control mice. The extreme sensitivity of IKK2ca^{IEChom} mice to DSS-induced colon inflammation most likely contributed to the strongly enhanced tumorigenesis observed in these animals upon AOM/DSS treatment. Greten et al. showed previously that epithelial-specific ablation of IKK2 also sensitized mice to DSS-induced injury resulting in increased colon inflammation; however, these mice showed reduced AOM/DSS-induced tumor development (5). Therefore, while both inhibition and increased activation of IKK2 in the intestinal epithelium sensitized mice to DSS, resulting in increased colon inflammation, they differentially affected AOM/DSS-induced colon cancer development, suggesting that IKK2 exerts important cell-intrinsic functions in IECs that are critical for tumorigenesis.

To uncouple the potential epithelial intrinsic protumorigenic functions of IKK2ca from its effects in DSS-induced colitis, we investigated whether constitutive IKK2/NF-κB activity also affects carcinogenesis induced by repeated AOM injections in the absence of DSS, a model of carcinogen-induced colon cancer that does not depend on inflammation-mediated tumor promotion (23, 24). IKK2ca^{IEChom} and IKK2ca^{fFL} littermates received 5 weekly injections of AOM, and colon cancer development was evaluated 13 weeks after the first injection. Whereas IKK2ca^{fFL} controls did not develop intestinal tumors with this protocol, all IKK2ca^{IEChom} mice developed multiple broad-based adenomas with hyperplasia and early dysplasia in the colon, but also showed hyperplastic crypts with shortened villus structures in the SI (Figure 4F). Thus, constitutively increased IKK2 activity in IECs strongly synergized with AOM-induced mutagenesis to induce intestinal tumorigenesis.

Constitutive IKK2/NF-κB activation strongly synergized with Wnt signaling to promote intestinal tumorigenesis. Most intestinal cancers display increased activation of the Wnt signaling pathway, and mutations activating Wnt signaling cause intestinal tumors in humans and mice (25). The adenomatous polyposis coli gene encoding the APC tumor suppressor, an essential component of the multiprotein complex negatively regulating β-catenin activation, is frequently mutated in human intestinal cancers, and APC mutations cause intestinal tumors in mice (25–28). To assess whether constitutive IKK2/NF-κB activity in IECs affects APC mutation–induced tumorigenesis, we crossed the IKK2ca^{IEC} mice with Apc1638N mice, which bear a truncated Apc allele and spontaneously develop adenomatous polyps in the proximal part of the SI at an age of 6 to 9 months (29).

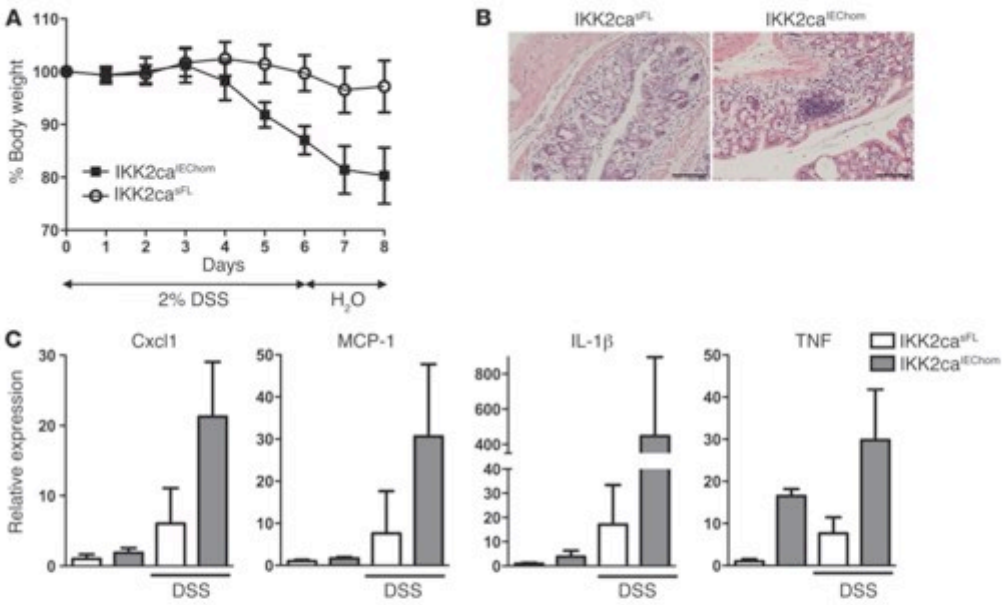

Figure 3

IKK2ca^{IEChom} mice exhibit increased sensitivity to DSS-induced colitis. (**A**) IKK2ca^{IEChom} mice showed more severe weight loss compared with littermate controls in response to administration of 2% DSS ($n \geq 10$ per genotype; data represent mean ± SD). (**B**) Histological cross sections of the distal colon of mice sacrificed on day 8 showed moderate epithelial damage and inflammation in IKK2ca^{sFL} animals, while IKK2ca^{IEChom} mice showed strong inflammation and extended tissue damage in the colonic mucosa. (**C**) qRT-PCR demonstrating increased expression of proinflammatory factors in distal colons of DSS-treated IKK2ca^{IEChom} mice compared with IKK2ca^{sFL} controls (naive mice, $n = 5$ per genotype; DSS-treated mice, $n = 10$ per genotype; mRNA levels are presented as mean ± SD). Scale bars: 50 μm.

Endoscopic and macroscopic analysis of intestines from 4-month-old animals revealed the presence of multiple polyps in both the colon and the proximal half of the SI of Apc1638N/IKK2ca^{IEChet} mice (Figure 5A and data not shown). In contrast, only 2 out of 6 Apc1638N mice harbored 1 to 2 small polyps in the proximal SI, while none of the IKK2ca^{sFL} or IKK2ca^{IEChet} littermate controls showed intestinal tumors (Figure 5A). Histological analysis of colon sections revealed the presence of adenomas containing dysplastic crypts with undifferentiated multilayered epithelium in Apc1638N/IKK2ca^{IEChet} mice (Figure 5B). In addition, SI sections showed the presence of adenomatous polyps containing aberrantly shaped dysplastic crypts with stratified undifferentiated epithelium in Apc1638N/IKK2ca^{IEChet} mice (Figure 5B). Tumors in the colon and SI from Apc1638N/IKK2ca^{IEChet} mice showed strongly increased proliferation as assessed by Ki67 immunohistochemistry (IHC) (Figure 5C). In addition, all epithelial cells in dysplastic crypts from Apc1638N/IKK2ca^{IEChet} mice showed strong nuclear staining for the transcription factor Sox9, a β-catenin/TCF4-target gene that is normally highly expressed in crypt stem cells and at lower levels in transit amplifying (TA) cells, Paneth cells, and enteroendocrine cells, but is absent from differentiated absorptive enterocytes (refs. 30, 31, and Figure 5D). In contrast, epithelial cells in Apc1638N or IKK2ca^{IEChet} mice did not show increased proliferation or Sox9 expression compared with those in control animals (Figure 5D and Supplemental Figure 4). Thus, constitutive IKK2 activation in IECs strongly synergized with the Apc1638N mutation to enhance tumorigenesis, resulting in early development of highly proliferative dysplastic adenomatous lesions displaying increased β-catenin activation in Apc1638N/IKK2ca^{IEChet} mice.

Spontaneous tumor development in the colon and SI of aged IKK2ca^{IEChom} mice. Our results showed that epithelial-specific expression of IKK2ca strongly enhanced tumorigenesis in different inflammation-dependent, carcinogen-induced, and genetic models of intestinal cancer, suggesting that constitutively increased IKK2 activity in IECs promotes tumor development by affecting fundamental cellular processes important for intestinal carcinogenesis. To address whether constitutively increased IKK2 activity was sufficient to induce the spontaneous development of intestinal tumors, we followed a cohort of IKK2ca^{IEChom} and littermate control mice over a period of 12 months and assessed tumor development by endoscopy and postmortem macroscopic and histological examination. During the course of this experiment, we noticed that a fraction of the aging IKK2ca^{IEChom} animals showed pronounced weight loss and diarrhea, occasionally accompanied by rectal prolapse and bleeding, and were sacrificed before the age of 12 months. Histopathological analysis of tissues from these IKK2ca^{IEChom} animals showed thickening of the bowel wall in both the SI and colon and revealed the presence of hyperplastic and sometimes dysplastic crypts, indicating that IKK2ca expression induces intestinal tumors (data not shown). Endoscopic analysis revealed colon inflammation in nearly all IKK2ca^{IEChom} mice that reached 1 year of age and the presence of large tumors in the distal colon in about 50% of these animals (Figure 6, A and B). Histologically, these tumors showed a thickened inflamed mucosa with hyperplastic aberrant crypt growth and in some cases also dysplastic crypts characterized by loss of differentiation and epithelial

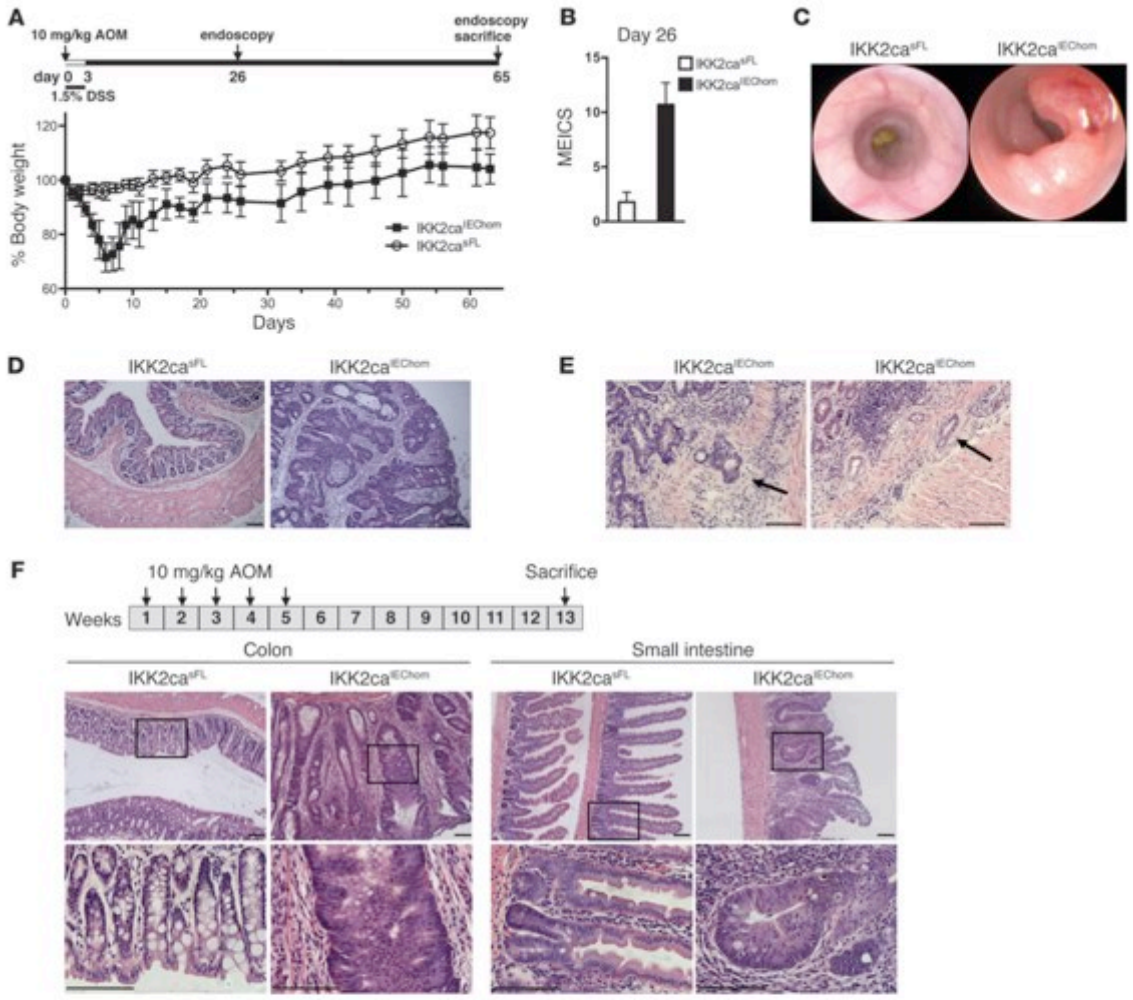

Figure 4

IKK2ca^{IEChom} mice display strongly enhanced tumorigenesis in response to AOM treatments. (**A**) IKK2ca^{IEChom} and IKK2ca^{sFL} mice were injected with 10 mg/kg AOM and given 1.5% DSS in drinking water for 3 days followed by regular drinking water ($n \geq 9$ per genotype; data shown as mean ± SD). (**B**) MEICS determined on day 26 revealed severe colon inflammation in IKK2ca^{IEChom} but not in IKK2ca^{sFL} mice ($n \geq 6$ per genotype; data shown as mean ± SD). (**C**) Endoscopic analysis on day 65 revealed pronounced tumor formation in the distal colons of IKK2ca^{IEChom} but not in IKK2ca^{sFL} mice. (**D**) Histological analysis of colon cross sections revealed the presence of advanced adenomas showing loss of epithelial cell differentiation and epithelial stratification in IKK2ca^{IEChom} mice. In contrast, the colonic mucosa of IKK2ca^{sFL} mice appeared normal. (**E**) Histological tissue sections from AOM/DSS-treated IKK2ca^{IEChom} mice showing colonic adenocarcinomas as identified by invasion of epithelial tissue into the submucosa (indicated by arrows). (**F**) IKK2ca^{IEChom} and IKK2ca^{sFL} mice ($n \geq 8$) received 5 weekly injections of 10 mg/kg AOM and were sacrificed 13 weeks after the first injection. Histological cross sections revealed the presence of tumors displaying pronounced epithelial hyperplasia and early dysplastic lesions in both colon and SI of IKK2ca^{IEChom} but not IKK2ca^{sFL} mice. Scale bars: 50 μm.

stratification (Figure 6C). From 17 IKK2ca^{IEChom} mice examined at the age of 1 year, we found early hyperplastic adenomas in 10 animals and in 6 of those we detected also more advanced adenomatous lesions with epithelial dysplasia. Histological analysis of the SI revealed lesions with abnormal crypt architecture and increased crypt numbers indicating epithelial hyperproliferation in 7 out of 14 IKK2ca^{IEChom} mice, 4 of which also showed the growth of adenomatous polyps with signs of early dysplasia (Figure 6C). Ki67 staining revealed strong hyperproliferation of epithelial cells in tumors from the colon and SI of IKK2ca^{IEChom} mice (Figure 6D). In addition, all epithelial cells in dysplastic crypts showed strong expression of Sox9, indicating activation of β-catenin in these cells (Figure 6D). Collectively, these results demonstrate that constitutively increased IKK2 activity in premalignant IECs was sufficient to induce the spontaneous development of tumors displaying increased proliferation and β-catenin activation in the colon and to a lesser extent also in the SI of IKK2ca^{IEChom} mice.

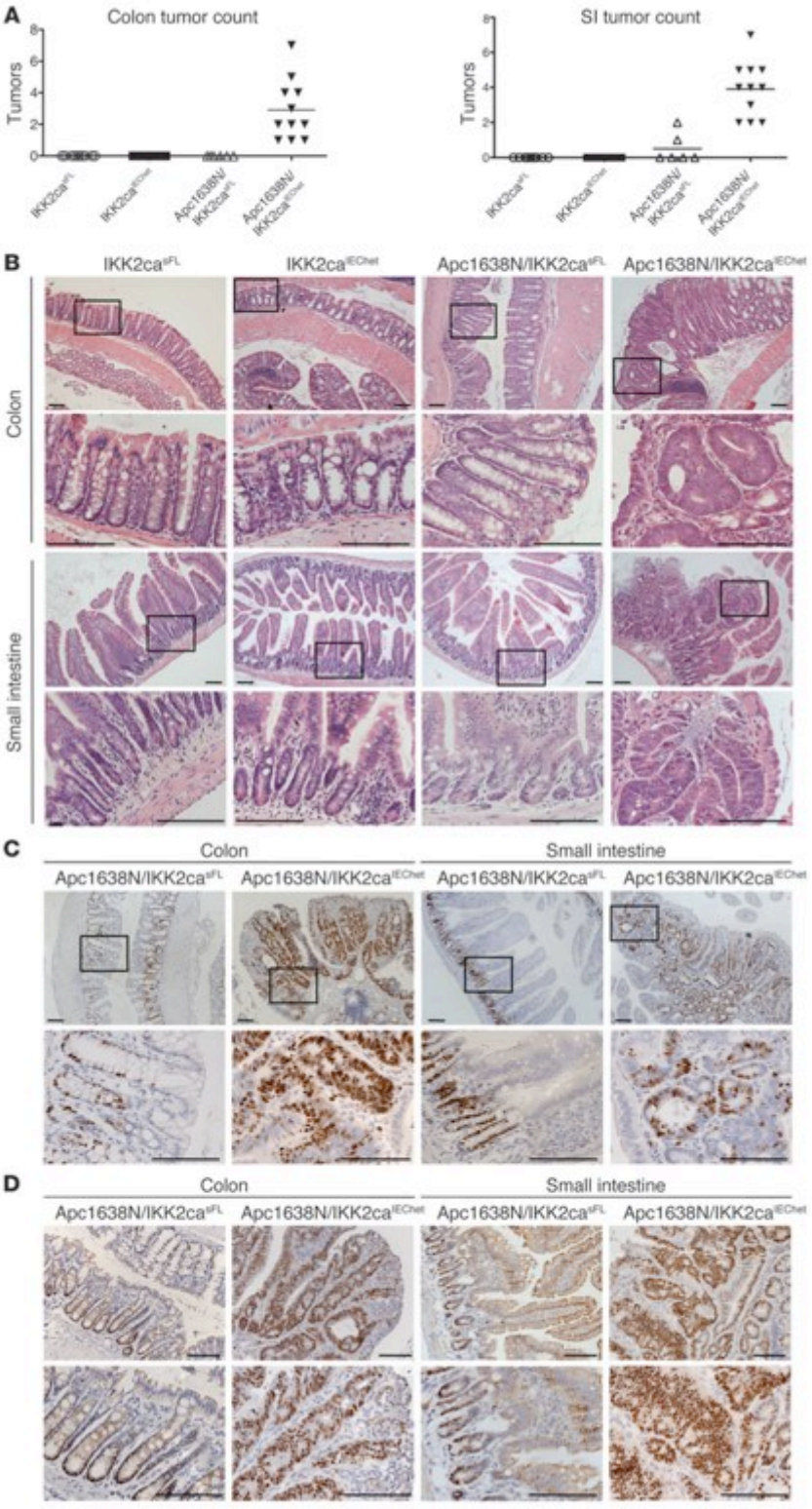

Figure 5

Heterozygous IKK2ca expression in IECs strongly enhances tumorigenesis in Apc1638N mice and results in early tumor formation in the colon and the SI. (**A**) Macroscopic analysis of intestines from 4-month-old mice showed that all Apc1638N/IKK2ca^{IEChet} mice examined (n = 11) had developed at least 1 macroscopically visible tumor in the colon and also multiple clearly identifiable polyps in the proximal half of the SI. Littermate Apc1638N/IKK2ca^{sFL} mice (n = 6) did not show colon tumors, while only 2 out of 6 animals examined bore 1 or 2 small polyps in the pyloric region of the SI. IKK2ca^{sFL} (n = 9) and IKK2ca^{IEChet} (n = 11) mice did not show tumors in either the colon or the SI. (**B**) Histological analysis of colon sections from Apc1638N/IKK2ca^{IEChet} mice revealed the presence of tumors showing hyperplastic and dysplastic crypts with multilayered undifferentiated epithelium. Histological analysis of proximal SI sections from Apc1638N/IKK2ca^{IEChet} mice revealed the growth of polyps that harbored aberrantly shaped, dysplastic crypts showing epithelial stratification and lack of differentiation. Histological analysis of colon and SI sections from IKK2ca^{IEChet} and IKK2ca^{sFL} littermates did not reveal the presence of tumors. (**C**) Immunostaining for Ki67 revealed increased proliferation of epithelial cells in adenomas from the colon and SI of Apc1638N/IKK2ca^{IEChet} mice, whereas Apc1638N/IKK2ca^{sFL} mice showed a normal Ki67 staining pattern. (**D**) Immunohistochemical analysis revealed strong Sox9 expression in all epithelial cells in colonic and SI tumors in Apc1638N/IKK2ca^{IEChet} mice. In contrast, Apc1638N/IKK2ca^{sFL} mice showed normal Sox9 staining, with Sox9-positive IECs in the base of the crypts and the transit-amplifying compartment in both tissues. Scale bars: 50 μm.

Increased β-catenin activity and perturbation of the stem cell compartment in the intestine of IKK2ca^{IEChom} mice. To investigate the early mechanisms by which IKK2ca expression drives intestinal tumorigenesis, we examined colonic and SI tissue from 8-week-old IKK2ca^{IEChom} animals for activation of the β-catenin pathway. Immunohistochemical analysis of β-catenin revealed increased presence of active β-catenin in both cytoplasmic and nuclear extracts from colonic IECs from IKK2ca^{IEChom} mice (Figure 7A). Consistent with the increased β-catenin activation, immunostaining for Ki67 revealed increased epithelial cell proliferation in transgenic colonic crypts with an extension of the Ki67-positive nuclei toward the lumen indicative for an expanded TA cell compartment (Figure 7B). Interestingly, all SI crypt epithelial cells were Ki67^{+} in IKK2ca^{IEChom} mice, in contrast to the well-defined proliferation pattern of control crypts where Ki67 stained TA cells and only occasionally cells in the base of the crypts, where Paneth cells and the rarely dividing intestinal epithelial stem cells are located (32, 33). In line with this observation, crypts in the SI and colon of IKK2ca^{IEChom} mice showed an expansion of the Sox9-expressing epithelial cell compartment, suggesting increased β-catenin transcriptional activity (Figure 7C). Despite the increased epithelial proliferation, the Wnt-regulated c-myc and cyclin D1 genes were not upregulated in IKK2ca-expressing IECs (Supplemental Figure 5C). However, MMP7, also known to be transcriptionally regulated by β-catenin (34), was expressed at higher levels in epithelial cells from IKK2ca^{IEChom} mice (Supplemental Figure 5C). Therefore, some but not all β-catenin target genes were induced in IKK2ca-expressing IECs. Sox9 negatively regulates Wnt-induced expression of c-myc and cyclin D1 (35); therefore, increased Sox9 expression might be responsible for the fact these genes are not upregulated in IKK2ca-expressing IECs.

SI crypts in IKK2ca^{fFL} mice showed the expected Sox9 expression pattern with stem cells, identified as cells located at the bottom of the crypt characterized by a slim cytoplasmic rim and elongated triangular nuclei, and Paneth cells, identified by their small round nuclei and large cytoplasm, strongly stained with anti-Sox9 antibodies (36). In contrast, the Sox9 staining pattern in the SI from IKK2ca^{IEChom} mice did not allow the clear identification of Paneth cells or stem cells in crypt bases (Figure 7C). Furthermore, crypt fission events, which are thought to occur only upon stem cell duplication, were regularly observed in IKK2ca^{IEChom} but not in control mice. These observations indicated that the differentiation or proliferation status of crypt stem cells, which have been identified as the cells of origin of intestinal cancer (37), might be altered already in premalignant intestinal crypts of IKK2ca^{IEChom} mice. Indeed, analysis of genes known to be expressed in intestinal epithelial stem cells (31) showed strong upregulation of Ascl2 and Olfm4 and moderate increase in CD44 and TnfRsF19 expression in the colon from 7- to 8-week-old IKK2ca^{IEChom} mice (Figure 7D). Ascl2, CD44, and Bmi-1 were also upregulated in the SI from these animals (Figure 7E). Olfm4, Bmi-1, and CD44 were previously shown to be regulated by NF-κB (38–40), and we also found that the promoter of Ascl2 contains a consensus NF-κB site (data not shown), suggesting that constitutively increased IKK2/NF-κB activity might directly regulate the intestinal stem cell compartment by inducing the expression of NF-κB target genes encoding stem cell–associated factors. The expression of DLK1 (also called Pref1), a protein that is best known for its role in preventing progenitor cell differentiation in different tissues (41) and has been implicated in colon carcinogenesis (42), was also strongly upregulated in both the colon and SI from IKK2ca^{IEChom} mice (Figure 7F). Thus, several stem cell–associated factors are upregulated in the intestine of IKK2ca^{IEChom} mice and could be implicated in the development of spontaneous tumors in this model.

Discussion

Many cancers display constitutive activation of NF-κB signaling, indicating that NF-κB activation is an important event during tumor development affecting fundamental cellular processes that are critical for carcinogenesis. NF-κB activation in early initiated or malignant tumor cells is believed to perform mainly antiapoptotic functions (17). However, it remains unclear whether constitutive NF-κB activation in premalignant cells performs additional protumorigenic functions that are critical for carcinogenesis. In this context, it is not known whether cell-intrinsic NF-κB activation is sufficient to induce spontaneous tumor development.

Here we show that expression of constitutively active IKK2 in IECs not only strongly synergizes with chemical and genetic models of intestinal carcinogenesis, but also is sufficient to induce the spontaneous development of tumors in both the colon and the SI. Our studies suggest that sustained IKK2 activation in IECs drives intestinal tumorigenesis by exerting both cell-intrinsic and paracrine functions. IKK2 activation in epithelial cells induced the expression of several proinflammatory cytokines and chemokines that are important for intestinal carcinogenesis. It is noteworthy that although IKK2ca expression strongly activated NF-κB signaling in IECs, only a subset of the known NF-κB–regulated cytokines and chemokines were upregulated. For example, IL-6, a well-known NF-κB–inducible cytokine that has been implicated in colorectal carcinogenesis (43–45), was not upregulated in IKK2ca^{IEChom} mice. In contrast, TNF and IL-1β were upregulated in both the SI and colon of IKK2ca^{IEChom} mice, and given their important function in the regulation of intestinal inflammation and carcinogenesis (46, 47), they are likely to be implicated in IKK2ca-mediated intestinal tumor development. The most highly upregulated gene in IKK2ca-expressing IECs was CCL20, a chemokine that has been reported to induce tumor cell growth and migration in human colorectal cancer (48). Another chemokine that was highly induced in the intestine of IKK2ca^{IEChom} mice is Cxcl-16, which together with its receptor Cxcr6 has been suggested to promote inflammation-associated tumor development (49). Therefore, IKK2ca expression in IECs induces the expression of specific cytokines and chemokines with important protumorigenic activities.

Increased numbers of macrophages and granulocytes, but not T or B lymphocytes, were detected in the mucosa of young mice, suggesting that increased cytokine and chemokine expression by IECs initiated an innate immune response driven by myeloid cells. Infiltrating macrophages were found mainly surrounding the base of the crypts in the colon and SI of IKK2ca^{IEChom} mice. Since intestinal tumors originate from crypt stem cells, increased myeloid cell infiltration in this area is likely to contribute to the spontaneous development of intestinal tumors in IKK2ca^{IEChom} mice by creating a microenvironment supporting tumor growth. In addition to immune cells, stromal fibroblasts that are activated to become myofibroblasts constitute an important component of the tumor-supporting microenvironment (50). We detected the presence of increased numbers of α-SMA–expressing activated myofibroblasts in close proximity with the IECs of both aged and young IKK2ca^{IEChom} mice, suggesting that stromal fibroblasts are activated already at a

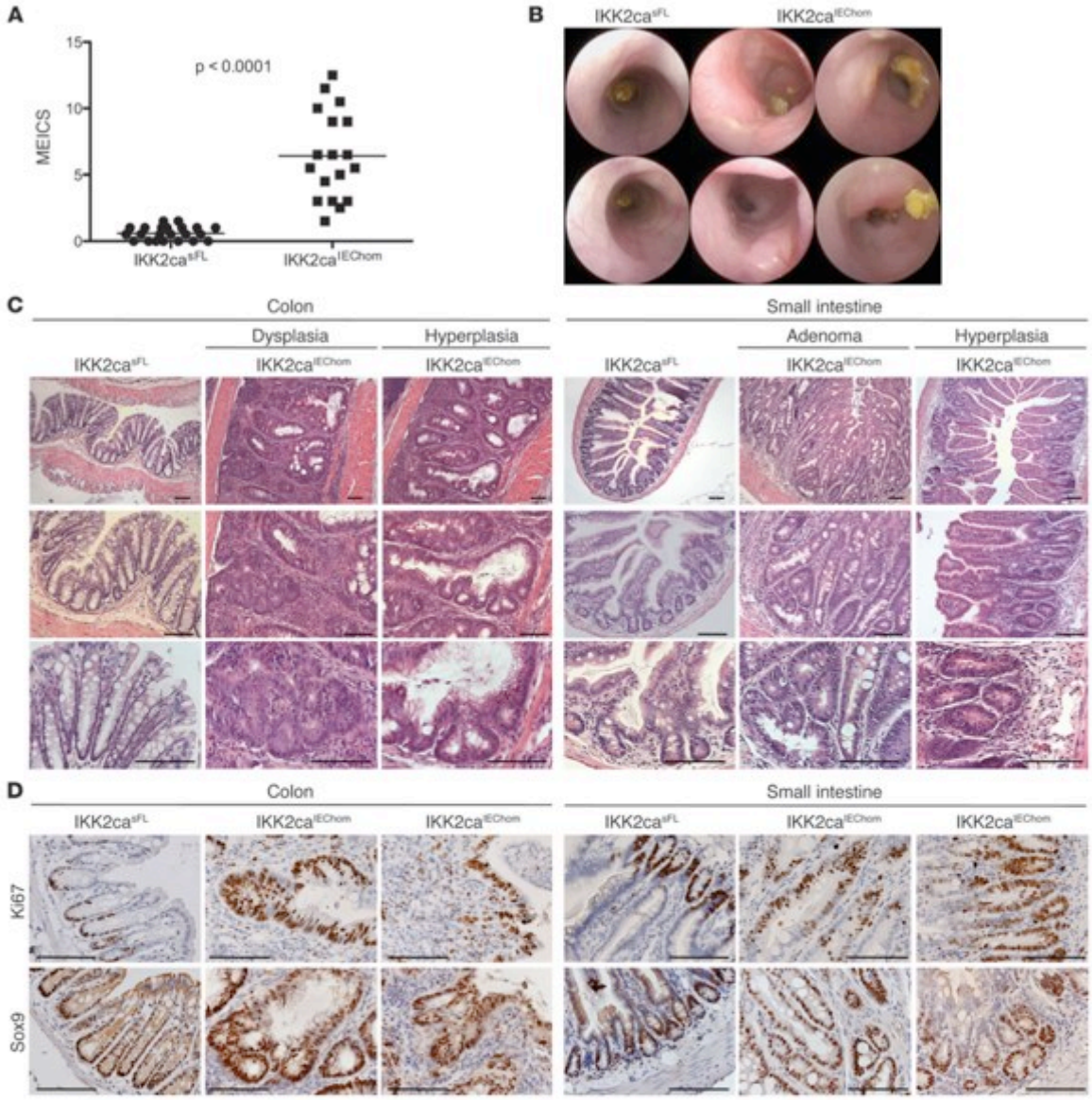

Figure 6

IKK2ca^{IEChom} mice spontaneously develop intestinal tumors. (**A**) Aged (≥48 week old) IKK2ca^{IEChom} mice showed endoscopically detectable colon inflammation, reflected by a heightened MEICS. (**B**) Representative endoscopic pictures of 1-year-old IKK2ca^{IEChom} mice, showing the presence of tumors exhibiting pronounced vascularization in the distal colon. IKK2ca^{fFL} littermates did not show colon inflammation or tumors. (**C**) Histological analysis of colon cross sections showed the presence of tumors in 10 out of 17 animals examined, characterized by thickening of the mucosa, epithelial hyperplasia, aberrantly formed crypts, and inflammation. (**D**) Immunostaining for Ki67 showed strongly increased proliferation of epithelial cells in dysplastic and hyperplastic lesions in the colon and SI from IKK2ca^{IEChom} mice. Immunostaining for Sox9 also revealed strongly increased Sox9 expression in epithelial cells in colonic and SI tumors. IKK2ca^{fFL} littermates showed normal Ki67 and Sox9 staining in the colon and SI. Scale bars: 50 μm.

very early stage and could contribute to intestinal tumor initiation and progression in this model. Cytokines secreted by IKK2ca-expressing IECs are likely to induce the differentiation of stromal fibroblasts to tumor-supporting myofibroblasts. Indeed, proinflammatory cytokines such as IL-1β were previously shown to activate stromal fibroblasts to support tumor initiation and growth (9). Therefore, constitutive activation of IKK2/NF-κB signaling in IECs acts in a paracrine manner

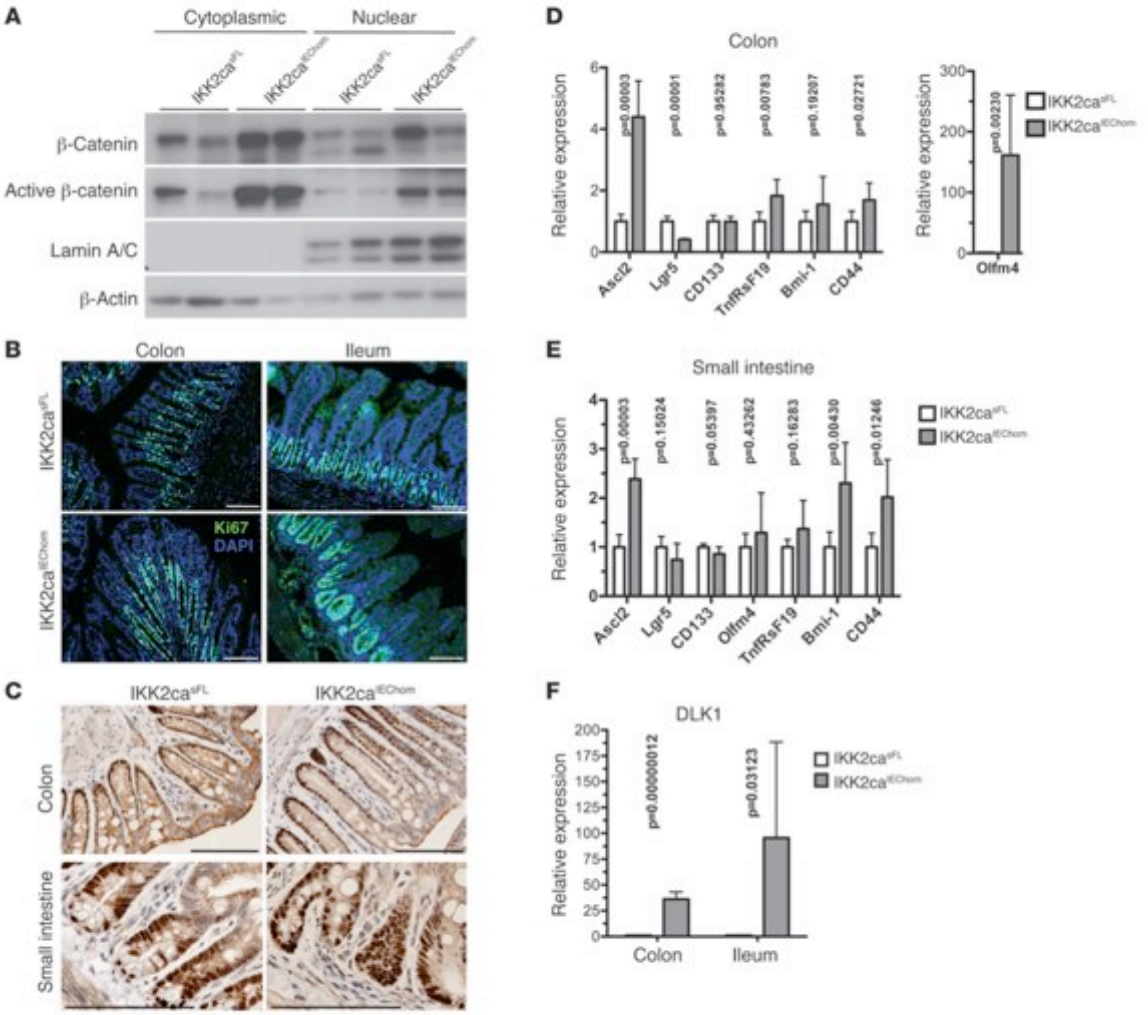

Figure 7

Increased β-catenin activation, hyperproliferation, and elevated stem cell factor expression in IECs from IKK2ca^{IEChom} mice. (**A**) Immunoblot analysis on cytoplasmic and nuclear extracts from colonic IECs showed increased levels of β-catenin and active N terminally nonphosphorylated β-catenin in 8-week-old IKK2ca^{IEChom} compared with IKK2ca^{sFL} mice. (**B**) Immunofluorescent staining for Ki67 reveals increased IEC proliferation in the colon of 10-week-old IKK2ca^{IEChom} mice, where the proliferating cells were extended toward the lumen. Whereas in control ileum, mainly the TA cells showed Ki67 staining, all crypt cells were Ki67$^+$ in the ileum of IKK2ca^{IEChom} mice. (**C**) Immunohistochemical staining revealed increased numbers of Sox9-expressing IECs in the colon and SI of 10-week-old IKK2ca^{IEChom} compared with IKK2ca^{sFL} mice. Paneth cells and stem cells were not identifiable with Sox9 staining in SI crypts from IKK2ca^{IEChom} mice. (**D** and **E**) qRT-PCR analysis showed increased expression of intestinal stem cell factors in the colon (**D**) and in the SI (**E**) of 7- to 8-week-old IKK2ca^{IEChom} mice compared with IKK2ca^{sFL} littermates ($n \geq 6$ per genotype; mRNA levels are presented as mean ± SD). (**F**) qRT-PCR analysis showed increased expression of DLK1 in the colon and in the ileum of 7- to 8-week-old IKK2ca^{IEChom} mice compared with IKK2ca^{sFL} littermates ($n \geq 6$ per genotype; mRNA levels are presented as mean ± SD). Scale bars: 50 μm.

to induce the infiltration of myeloid cells and the activation of stromal fibroblasts, creating a microenvironment supporting tumor growth. However, it is unlikely that IKK2ca expression drives intestinal tumorigenesis only by inducing cytokine expression, as the chronic intestinal inflammation caused by increased TNF expression in a mouse model of severe Crohn disease was not sufficient to induce intestinal tumors (51).

The Wnt signaling pathway controls normal epithelial homeostasis, and mutations activating Wnt signaling cause intestinal tumors in humans and mice (26, 52, 53). We therefore hypothesized that constitutive IKK2 activation in IECs might have an impact on Wnt signaling to induce intestinal tumorigenesis. Indeed, we found that IECs in IKK2ca^{IEChom} mice showed increased expression and activation of β-catenin already in a premalignant state, a surprising

result considering previous studies reporting that IKK2 negatively regulates β-catenin activity (54). Although the precise mechanisms by which constitutive IKK2/NF-κB signaling in IECs induces β-catenin activation are not fully understood at present, overexpression of IKK2ca could increase β-catenin activity by either cell-intrinsic or paracrine functions. β-catenin activation in tumors is not controlled solely by Wnt ligands or mutations activating Wnt signaling, but additional Wnt-independent cues from the microenvironment are also required for full activation of β-catenin signaling (52, 55). Indeed, stromal myofibroblasts were recently shown to regulate β-catenin activation in colon cancer cells via the secretion of factors not related to Wnt ligands (56). In addition, macrophages have been shown to regulate β-catenin activation in tumor cells by secreting cytokines such as TNF and IL-1β (56–59). Macrophage-produced TNF activated Wnt signaling by inducing GSK3β phosphorylation in an NF-κB–independent manner (57). Furthermore, IL-1β activated β-catenin via the NF-κB–dependent induction of PDK1/Akt-mediated phosphorylation of GSK3β (59). IKK activation was also required for GSK3β phosphorylation and β-catenin activation in response to progastrin stimulation (60). Thus, constitutive IKK2 activation in IECs might also activate β-catenin in a cell-intrinsic manner by inducing PDK1/Akt-mediated phosphorylation of GSK3β. In addition, since degradation of both β-catenin and IκB proteins is regulated by the β-TrCP E3 ubiquitin ligase (61), it is possible that high expression levels of constitutively active IKK2 inducing continuous phosphorylation and degradation of IκB proteins, as in the IECs of IKK2ca^{IEChom} mice, reduces β-TrCP availability for β-catenin degradation and in this way indirectly increases β-catenin activity.

The Wnt signaling pathway regulates the fate of intestinal crypt stem cells, which are the cells of origin of intestinal cancers (37, 62). We observed that all cells in the base of SI crypts, which in wild-type mice harbor rarely dividing stem cells and Paneth cells, stained strongly with Ki67 antibodies in IKK2ca^{IEChom} mice, suggesting that the crypt stem cells show increased proliferation in IKK2ca^{IEChom} mice. In addition, gene expression analysis in the intestine of IKK2ca^{IEChom} mice revealed increased expression of a number of stem cell–specific genes including *Ascl2*, *Olfm4*, *CD44*, *TnfRsF19*, and *Bmi-1*. These alterations are likely to be linked with β-catenin activation in IECs from IKK2ca^{IEChom} mice, since *Ascl2*, *TnfRsF19*, and *CD44* are β-catenin target genes (31). However, *Olfm4*, *Bmi-1*, and *CD44* are regulated by NF-κB (38–40). In addition, we found that the gene encoding Ascl2, a transcription factor controlling intestinal stem cell fate (31), contains an NF-κB consensus site in its promoter suggesting that NF-κB activation could also directly induce Ascl2 expression. In addition, DLK1 was strongly upregulated in IECs overexpressing IKK2ca. Although DLK1 has not been directly associated with intestinal crypt stem cells, it is known to prevent preadipocyte differentiation by inducing the expression of Sox9 and is thought to play a more general role in maintaining progenitor cells in different tissues in an undifferentiated state (41). Thus, the observed increase in Sox9 expression in IKK2ca-expressing IECs could be induced cooperatively by β-catenin and DLK1. DLK1 was also implicated in colorectal carcinogenesis (42), suggesting it could be directly implicated in intestinal tumorigenesis in IKK2ca^{IEChom} mice. Alterations in the intestinal stem cell compartment have not been reported in mice with epithelial-specific inhibition of NF-κB (5, 22, 63), suggesting that impairment of NF-κB activity might not be sufficient to alter intestinal stem cell homeostasis. However, constitutively increased NF-κB activation, such as in IKK2ca^{IEChom} mice or upon amplification of the Ikk2 genomic locus in human colorectal cancers (15), could affect the intestinal stem cell compartment and in this way contribute to intestinal tumorigenesis. In our experimental approach, IKK2ca is expressed under the control of the Rosa26 locus that drives strong expression in all cell types of the intestinal epithelium including crypt stem cells (64); therefore, we cannot address the specific contribution of stem cell–intrinsic NF-κB activation in intestinal tumorigenesis. Studies in new mouse models allowing stem cell–specific manipulation of NF-κB activity will be required to address the potential role of NF-κB in intestinal epithelial stem cells.

Taken together, our results presented here show that constitutive IKK2 activation in premalignant epithelial cells is sufficient to initiate and sustain the full spectrum of cell-intrinsic and microenvironmental alterations that are required for intestinal tumorigenesis. While IKK2ca expression strongly activated NF-κB, we cannot exclude that other NF-κB–independent functions induced by IKK2 contributed to intestinal tumorigenesis in this model. In addition to its well-established antiapoptotic function, IKK2 activation rendered tumor cells self-sufficient by providing them with the capacity to alter their microenvironment to support tumor growth. These findings provide experimental evidence that mutations activating IKK2/NF-κB signaling could have a causative role in carcinogenesis, although it remains to be investigated whether constitutive NF-κB activation is sufficient to induce tumor development in tissues other than the intestinal epithelium. However, a recent unbiased large scale genomic analysis of somatic copy number alterations in human cancers revealed that members of the NF-κB signaling pathway, including IKK2, were frequently amplified in different cancer types (15), supporting a fundamental tumor cell–intrinsic role of NF-κB in carcinogenesis.

Methods

Mice. R26IKK2ca^{sFL} (18), villinCre (19), and Apc1638N mice (29) have been described. Unless otherwise indicated, littermates carrying R26IKK2ca^{sFL} alleles, but not the villin-Cre transgene, served as control mice for the described experiments. Animals were housed in individually ventilated cages in a specific pathogen–free mouse facility at the University of Cologne. All animal studies were approved by local governmental authorities (Landesamt für Natur, Umwelt und Verbraucherschutz Nordrhein-Westfalen, Germany).

Mouse experiments. DSS (MP, MW 36000–50000) was provided in the drinking water. AOM was administered via intraperitoneal injections at 10 mg/kg. For endoscopy, mice were anesthetized with ketamine (Ratiopharm)/Rompun (Bayer), and a high-resolution miniendoscope, Coloview (Karl Storz), was used to determine the murine endoscopic index of colitis severity (murine endoscopic inflammatory colitis score [MEICS]) and to assess colonic tumorigenesis as previously described (65).

Histology. Tissues were fixed overnight in 4% paraformaldehyde, embedded in paraffin, and cut into 4-μm sections. H&E-stained sections were scored in a blinded fashion for the amount of inflammation, tissue damage, and/or tumorigenesis. For IHC staining, paraffin sections were rehydrated and heat-induced antigen retrieval was performed either in 10 mM sodium citrate, 0.05% Tween-20, pH 6.0, or in 10 mM Tris; 1 mM EDTA, pH 9.0. Primary antibodies were anti-Ki67 (Dako), anti-FLAG (Sigma-Aldrich), anti-Gr1 (BD Biosciences — Pharmingen), anti-F4/80 (clone A3–1), anti-B220 (clone RA3-6B2), anti-CD3 (Abcam), anti-Sox9 (Millipore), anti–β-catenin (BD Biosciences — BD Transduction Laboratories). Biotinylated secondary antibodies, ABC Kit Vectastain Elite, and DAB substrate (PerkinElmer, Vector, and Dako) were used. Incubation times with DAB were equal for

all samples. For immunofluorescence, Alexa Fluor 488–coupled antibodies (Invitrogen) were used; nuclei were counterstained with DAPI (Roche). Pictures were taken with a fluorescence microscope (DM5500; Leica) at the same exposure and intensity settings for all systems analyzed.

IEC isolation and immunoblotting. IECs were isolated by sequential incubation of intestinal tissue in 1 mM DTT and 1.5 mM EDTA solutions as described previously (66). For total extracts, cells were lysed in high-salt RIPA buffer (20 mM HEPES, pH 7.6; 350 mM NaCl; 20% glycerol; 1 mM $MgCl_2$; 0.5 mM EDTA; 0.1 mM EGTA; 1% NP-40) for 30 minutes on ice. For the preparation of cytoplasmic extracts, cells were lysed in hypotonic lysis buffer (10 mM HEPES, pH 7.6; 10 mM KCl; 2 mM $MgCl_2$; 0.1 mM EDTA) on ice, and the nuclear extract was recovered by lysis under high-salt conditions (50 mM HEPES, pH 7.8; 50 mM KCl; 300 mM NaCl; 0,1 mM EDTA; 10% glycerol). Protease inhibitor cocktail and PhosSTOP (Roche) were added prior to use. Protein extracts were separated by 10% SDS-PAGE and transferred to Immobilon-P PVDF membranes (Millipore). Membranes were probed with primary antibodies anti-IKK2 (rabbit monoclonal; Cell Signaling), anti-IKK1 and anti-p100 (rabbit; Cell Signaling), anti-NEMO (rabbit; made in our laboratory; ref. 14), anti-IκBα (rabbit; Santa Cruz Biotechnology Inc.), anti-p65 and anti-RelB (rabbit; Santa Cruz Biotechnology Inc.), anti-FLAG M2 peroxidase-coupled (mouse; Sigma-Aldrich), anti–α-tubulin (mouse; Sigma-Aldrich), anti–IL-1β (rabbit; Abcam) anti–β-catenin (mouse; BD Biosciences — BD Transduction Laboratories), anti-active β-catenin (mouse; Millipore), anti–β-actin (goat; Santa Cruz Biotechnology Inc.), and anti–lamin A/C (goat; Santa Cruz Biotechnology Inc.). Membranes were then incubated with secondary HRP-coupled antibodies (GE Healthcare and Jackson ImmunoResearch) and developed with chemiluminescent detection substrate (GE Healthcare and Thermo Scientific).

EMSA. Nuclear IEC extracts were prepared as described previously (67). An NF-κB consensus probe (5′-AGTTGAGGGGACTTTCCCAGGC-3′) was 5′-labeled with IR-Dyes (Li-Cor Biosciences) and detected with the Odyssey Infrared System.

qRT-PCR. Total RNA was extracted with Trizol Reagent (Invitrogen) and RNeasy Columns (QIAGEN), and cDNA was prepared with Superscript III cDNA-synthesis Kit (Invitrogen). qRT-PCR was performed with SYBR Green or TaqMan analysis (Applied Biosystems). Gapdh, Villin, and TATA-Box binding protein (TBP) were used as reference genes.

TaqMan probes and primer sequences used for qRT-PCR. TaqMan probes were as follows: Cxcl1, Mm00433859_m1; Cxcl10, Mm00445235_m1; Cxcl-16, Mm00469712_m1; Ccl20, Mm00444228_m1; TNF, Mm00443258_m1; MCP-1, Mm00441242_m1; IL-1β, Mm00434228_m1; IL-6, Mm00446190_m1; IL-12 p35, Mm00434165_m1; IL-12 p40, Mm99999067_m1; IL-23 p19, Mm00518984_m1; IL-17F, Mm00521423_m1; TGF-b1, Mm03024053_m1; Cox2, Mm00478374_m1; TSLP, Mm00498739_m1; Ascl2, Mm01268891_g1; Olfm4, Mm01320260_m1; DLK1, Mm00494477_m1; Lgr5, Mm00438890_m1; CD133, Mm00477115_m1; Gapdh, Mm99999915_g1; TATA box binding protein; and Mm00446973_m1.

Primer sequences for SYBR Green qRT-PCR were obtained from PrimerBank (http://pga.mgh.harvard.edu/primerbank/index.html): Bmi-1 for TATAACTGATGATGAGATAATAAGC, rev ATAAGTGGTTACAGGAAGTC; TnfRsF19 for ATTCTCTTCCTACTCCACCTG, rev CATAGCCGAAGCCACATTC; CD44 for TCTGCCATCTAGCACTAAGAGC, rev GTCTGGGTATTGAAAGGTGTAGC; IKK2 for CTGAAGATCGCCTGTAGCAAA, rev TCCATCTGTAACCAGCTCCAG; IKK1 for GTCAGGACCGTGTTCTCAAGG, rev GCTTCTTTGATGTTACTGAGGGC; c-myc for ATGCCCCTCAACGTGAACTTC, rev CGCAACATAGGATGGAGAGCA; cyclin D1 for GCGTACCCTGACACCAATCTC, rev CTCCTCTTCGCACTTCTGCTC; MMP7 for CTGCCACTGTCCCAGGAAG, rev GGGAGAGTTTTCCAGTCATGG; villin for TCAAAGGCTCTCTCAACATCAC, rev AGCAGTCACCATCGAAGAAGC; Gapdh for CATGTTCCAGTATGACTCCACTC, rev GGCCTCACCCCATTTGATGT.

Statistics. All data shown represent the mean ± SD. Statistical analyses were performed using unpaired 2-tailed Student's *t* tests with unequal variance. $P < 0.05$ was considered significant.

Acknowledgments

We wish to thank C. Uthoff-Hachenberg, J. Pfeiffer, E. Mahlberg, D. Beier, J. Buchholz, B. Huelser, and B. Wolff for excellent technical assistance. We also thank Alan Clarke for valuable discussions. This work was supported by the European Commission FP7 program grant INFLA-CARE (EC contract number 223151) and by grants from the Deutsche Forschungsgemeinschaft to M. Pasparakis.

Received for publication October 7, 2010, and accepted in revised form April 6, 2011.

Address correspondence to: Manolis Pasparakis, Institute for Genetics, University of Cologne, Zülpicher Str. 47a, D-50674 Cologne, Germany. Phone: 49.221.470.1526; Fax: 49.221.470.5163; E-mail: pasparakis@uni-koeln.de.

1. Staudt LM. Oncogenic activation of NF-kappaB. *Cold Spring Harb Perspect Biol.* 2010;2(6):a000109.
2. Yang J, et al. Conditional ablation of Ikkb inhibits melanoma tumor development in mice. *J Clin Invest.* 2010;120(7):2563–2574.
3. Pikarsky E, et al. NF-kappaB functions as a tumour promoter in inflammation-associated cancer. *Nature.* 2004;431(7007):461–466.
4. Meylan E, et al. Requirement for NF-kappaB signalling in a mouse model of lung adenocarcinoma. *Nature.* 2009;462(7269):104–107.
5. Greten FR, et al. IKKbeta links inflammation and tumorigenesis in a mouse model of colitis-associated cancer. *Cell.* 2004;118(3):285–296.
6. Sakamoto K, et al. Inhibitor of kappaB kinase beta regulates gastric carcinogenesis via interleukin-1alpha expression. *Gastroenterology.* 2010; 139(1):226–238.e226.
7. Mantovani A, Allavena P, Sica A, Balkwill F. Cancer-related inflammation. *Nature.* 2008; 454(7203):436–444.
8. Grivennikov SI, Greten FR, Karin M. Immunity, inflammation, and cancer. *Cell.* 2010; 140(6):883–899.
9. Erez N, Truitt M, Olson P, Arron ST, Hanahan D. Cancer-associated fibroblasts are activated in incipient neoplasia to orchestrate tumor-promoting inflammation in an NF-kappaB-dependent manner. *Cancer Cell.* 2010;17(2):135–147.
10. Basseres DS, Ebbs A, Levantini E, Baldwin AS. Requirement of the NF-kappaB subunit p65/RelA for K-Ras-induced lung tumorigenesis. *Cancer Res.* 2010;70(9):3537–3546.
11. Dajee M, et al. NF-kappaB blockade and oncogenic Ras trigger invasive human epidermal neoplasia. *Nature.* 2003;421(6923):639–643.
12. van Hogerlinden M, Rozell BL, Ahrlund-Richter L, ToftgÅrd R. Squamous cell carcinomas and increased apoptosis in skin with inhibited Rel/nuclear factor-kappaB signaling. *Cancer Research.* 1999;59(14):3299–3303.
13. Maeda S, Kamata H, Luo JL, Leffert H, Karin M. IKKbeta couples hepatocyte death to cytokine-driven compensatory proliferation that promotes chemical hepatocarcinogenesis. *Cell.* 2005;121(7):977–990.
14. Luedde T, et al. Deletion of NEMO/IKKgamma in liver parenchymal cells causes steatohepatitis and hepatocellular carcinoma. *Cancer Cell.* 2007;11(2):119–132.
15. Beroukhim R, et al. The landscape of somatic copy-number alteration across human cancers. *Nature.* 2010;463(7283):899–905.
16. Prasad S, Ravindran J, Aggarwal BB. NF-kappaB and cancer: how intimate is this relationship. *Mol Cell Biochem.* 2010;336(1–2):25–37.
17. Karin M. Nuclear factor-kappaB in cancer development and progression. *Nature.* 2006; 441(7092):431–436.
18. Sasaki Y, et al. Canonical NF-kappaB activity, dispensable for B cell development, replaces BAFF-receptor signals and promotes B cell proliferation upon activation. *Immunity.* 2006;24(6):729–739.
19. Madison BB, Dunbar L, Qiao XT, Braunstein K, Braunstein E, Gumucio DL. Cis elements of the villin gene control expression in restricted domains of the vertical (crypt) and horizontal (duodenum, cecum) axes of the intestine. *J Biol Chem.* 2002;277(36):33275–33283.
20. Lombardi L, et al. Structural and functional characterization of the promoter regions of the NFKB2 gene. *Nucleic Acids Res.* 1995;23(12):2328–2336.

21. Bren GD, Solan NJ, Miyoshi H, Pennington KN, Pobst LJ, Paya CV. Transcription of the RelB gene is regulated by NF-kappaB. *Oncogene*. 2001;20(53):7722–7733.
22. Steinbrecher KA, Harmel-Laws E, Sitcheran R, Baldwin AS. Loss of epithelial RelA results in deregulated intestinal proliferative/apoptotic homeostasis and susceptibility to inflammation. *J Immunol*. 2008;180(4):2588–2599.
23. Nambiar PR, Girnun G, Lillo NA, Guda K, Whiteley HE, Rosenberg DW. Preliminary analysis of azoxymethane induced colon tumors in inbred mice commonly used as transgenic/knockout progenitors. *Int J Oncol*. 2003;22(1):145–150.
24. Neufert C, Becker C, Neurath MF. An inducible mouse model of colon carcinogenesis for the analysis of sporadic and inflammation-driven tumor progression. *Nat Protoc*. 2007;2(8):1998–2004.
25. Barker N, Clevers H. Catenins, Wnt signaling and cancer. *Bioessays*. 2000;22(11):961–965.
26. Miyoshi Y, et al. Somatic mutations of the APC gene in colorectal tumors: mutation cluster region in the APC gene. *Hum Mol Genet*. 1992;1(4):229–233.
27. Su LK, et al. Multiple intestinal neoplasia caused by a mutation in the murine homolog of the APC gene. *Science*. 1992;256(5057):668–670.
28. Fodde R. The APC gene in colorectal cancer. *Eur J Cancer*. 2002;38(7):867–871.
29. Fodde R, et al. A targeted chain-termination mutation in the mouse Apc gene results in multiple intestinal tumors. *Proc Natl Acad Sci U S A*. 1994;91(19):8969–8973.
30. Blache P, et al. SOX9 is an intestine crypt transcription factor, is regulated by the Wnt pathway, and represses the CDX2 and MUC2 genes. *J Cell Biol*. 2004;166(1):37–47.
31. van der Flier LG, et al. Transcription factor achaete scute-like 2 controls intestinal stem cell fate. *Cell*. 2009;136(5):903–912.
32. van Es JH, et al. Wnt signalling induces maturation of Paneth cells in intestinal crypts. *Nat Cell Biol*. 2005;7(4):381–386.
33. Barker N, van de Wetering M, Clevers H. The intestinal stem cell. *Genes Dev*. 2008;22(14):1856–1864.
34. Crawford HC, et al. The metalloproteinase matrilysin is a target of beta-catenin transactivation in intestinal tumors. *Oncogene*. 1999;18(18):2883–2891.
35. Bastide P, et al. Sox9 regulates cell proliferation and is required for Paneth cell differentiation in the intestinal epithelium. *J Cell Biol*. 2007;178(4):635–648.
36. Barker N, Clevers H. Leucine-rich repeat-containing G-protein-coupled receptors as markers of adult stem cells. *Gastroenterology*. 2010;138(5):1681–1696.
37. Barker N, et al. Crypt stem cells as the cells-of-origin of intestinal cancer. *Nature*. 2009;457(7229):608–611.
38. Hinz M, et al. Nuclear factor kappaB-dependent gene expression profiling of Hodgkin's disease tumor cells, pathogenetic significance, and link to constitutive signal transducer and activator of transcription 5a activity. *J Exp Med*. 2002;196(5):605–617.
39. Chin KL, et al. The regulation of OLFM4 expression in myeloid precursor cells relies on NF-kappaB transcription factor. *Br J Haematol*. 2008;143(3):421–432.
40. Dutton A, et al. Bmi-1 is induced by the Epstein-Barr virus oncogene LMP1 and regulates the expression of viral target genes in Hodgkin lymphoma cells. *Blood*. 2007;109(6):2597–2603.
41. Sul HS. Minireview: Pref-1: role in adipogenesis and mesenchymal cell fate. *Mol Endocrinol*. 2009;23(11):1717–1725.
42. Dong M, et al. Azoxymethane-induced pre-adipocyte factor 1 (Pref-1) functions as a differentiation inhibitor in colonic epithelial cells. *Carcinogenesis*. 2004;25(11):2239–2246.
43. Becker C, et al. TGF-beta suppresses tumor progression in colon cancer by inhibition of IL-6 transsignaling. *Immunity*. 2004;21(4):491–501.
44. Bollrath J, et al. gp130-mediated Stat3 activation in enterocytes regulates cell survival and cell-cycle progression during colitis-associated tumorigenesis. *Cancer Cell*. 2009;15(2):91–102.
45. Grivennikov S, et al. IL-6 and Stat3 are required for survival of intestinal epithelial cells and development of colitis-associated cancer. *Cancer Cell*. 2009;15(2):103–113.
46. Popivanova BK, et al. Blocking TNF-alpha in mice reduces colorectal carcinogenesis associated with chronic colitis. *J Clin Invest*. 2008;118(2):560–570.
47. Dinarello CA. Why not treat human cancer with interleukin-1 blockade? *Cancer Metastasis Rev*. 2010;29(2):317–329.
48. Ghadjar P, Rubie C, Aebersold DM, Keilholz U. The chemokine CCL20 and its receptor CCR6 in human malignancy with focus on colorectal cancer. *Int J Cancer*. 2009;125(4):741–745.
49. Darash-Yahana M, et al. The chemokine CXCL16 and its receptor, CXCR6, as markers and promoters of inflammation-associated cancers. *PLoS ONE*. 2009;4(8):e6695.
50. Franco OE, Shaw AK, Strand DW, Hayward SW. Cancer associated fibroblasts in cancer pathogenesis. *Semin Cell Dev Biol*. 2010;21(1):33–39.
51. Kontoyiannis D, Pasparakis M, Pizarro TT, Cominelli F, Kollias G. Impaired on/off regulation of TNF biosynthesis in mice lacking TNF AU-rich elements: implications for joint and gut-associated immunopathologies. *Immunity*. 1999;10(3):387–398.
52. Fodde R, Brabletz T. Wnt/beta-catenin signaling in cancer stemness and malignant behavior. *Curr Opin Cell Biol*. 2007;19(2):150–158.
53. Clevers H. Wnt/beta-catenin signaling in development and disease. *Cell*. 2006;127(3):469–480.
54. Lamberti C, et al. Regulation of beta-catenin function by the IkappaB kinases. *J Biol Chem*. 2001;276(45):42276–42286.
55. Brabletz T, et al. Variable beta-catenin expression in colorectal cancers indicates tumor progression driven by the tumor environment. *Proc Natl Acad Sci U S A*. 2001;98(18):10356–10361.
56. Vermeulen L, et al. Wnt activity defines colon cancer stem cells and is regulated by the microenvironment. *Nat Cell Biol*. 2010;12(5):468–476.
57. Oguma K, et al. Activated macrophages promote Wnt signalling through tumour necrosis factor-alpha in gastric tumour cells. *EMBO J*. 2008;27(12):1671–1681.
58. Kaler P, Augenlicht L, Klampfer L. Macrophage-derived IL-1beta stimulates Wnt signaling and growth of colon cancer cells: a crosstalk interrupted by vitamin D3. *Oncogene*. 2009;28(44):3892–3902.
59. Kaler P, Godasi BN, Augenlicht L, Klampfer L. The NF-kappaB/AKT-dependent induction of Wnt signaling in colon cancer cells by macrophages and IL-1beta. *Cancer Microenviron*. 2009;2(1):69–80.
60. Umar S, Sarkar S, Wang Y, Singh P. Functional crosstalk between beta-catenin and NFkappaB signaling pathways in colonic crypts of mice in response to progastrin. *J Biol Chem*. 2009;284(33):22274–22284.
61. Fuchs SY, Spiegelman VS, Kumar KG. The many faces of beta-TrCP E3 ubiquitin ligases: reflections in the magic mirror of cancer. *Oncogene*. 2004;23(11):2028–2036.
62. Li L, Clevers H. Coexistence of quiescent and active adult stem cells in mammals. *Science*. 2010;327(5965):542–545.
63. Nenci A, et al. Epithelial NEMO links innate immunity to chronic intestinal inflammation. *Nature*. 2007;446(7135):557–561.
64. Zhu L, et al. Prominin 1 marks intestinal stem cells that are susceptible to neoplastic transformation. *Nature*. 2009;457(7229):603–607.
65. Becker C, et al. In vivo imaging of colitis and colon cancer development in mice using high resolution chromoendoscopy. *Gut*. 2005;54(7):950–954.
66. Ukena SN, et al. Probiotic Escherichia coli Nissle 1917 inhibits leaky gut by enhancing mucosal integrity. *PLoS ONE*. 2007;2(12):e1308.
67. Schmidt-Supprian M, et al. NEMO/IKK gamma-deficient mice model incontinentia pigmenti. *Mol Cell*. 2000;5(6):981–992.

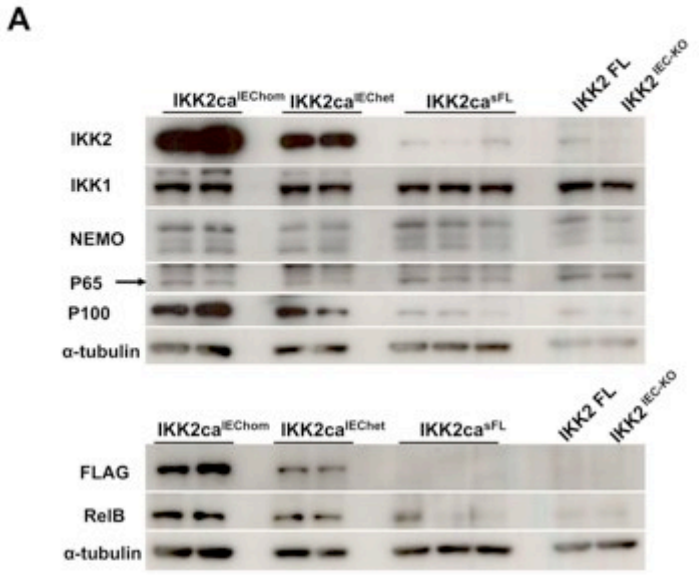

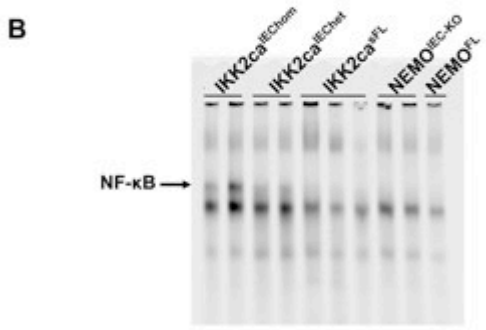

Supplementary Figure 1
Comparison of expression levels of IKK2 and NF-κB pathway components in IECs from IKK2ca^{IEChom} and IKK2ca^{IEChet} mice
A. WB analysis of protein extracts from small intestinal IECs depict IKK2 and IKK2ca only (anti-FLAG) in IKK2ca^{IEChom} and IKK2ca^{IEChet} mice. No difference in IKK1 or NEMO protein were detectable between genotypes. The protein abundance of RelB and p100, both targets of NF-κB regulated transcription, was elevated in both IKK2ca^{IEChom} and IKK2ca^{IEChet} mice.
B. EMSA performed with nuclear extracts from small intestinal IECs reveals increased NF-κB DNA-binding activity in IECs from IKK2ca^{IEChom} and IKK2ca^{IEChet} mice, as indicated by a shift in the NF-κB probe (marked by an arrow).

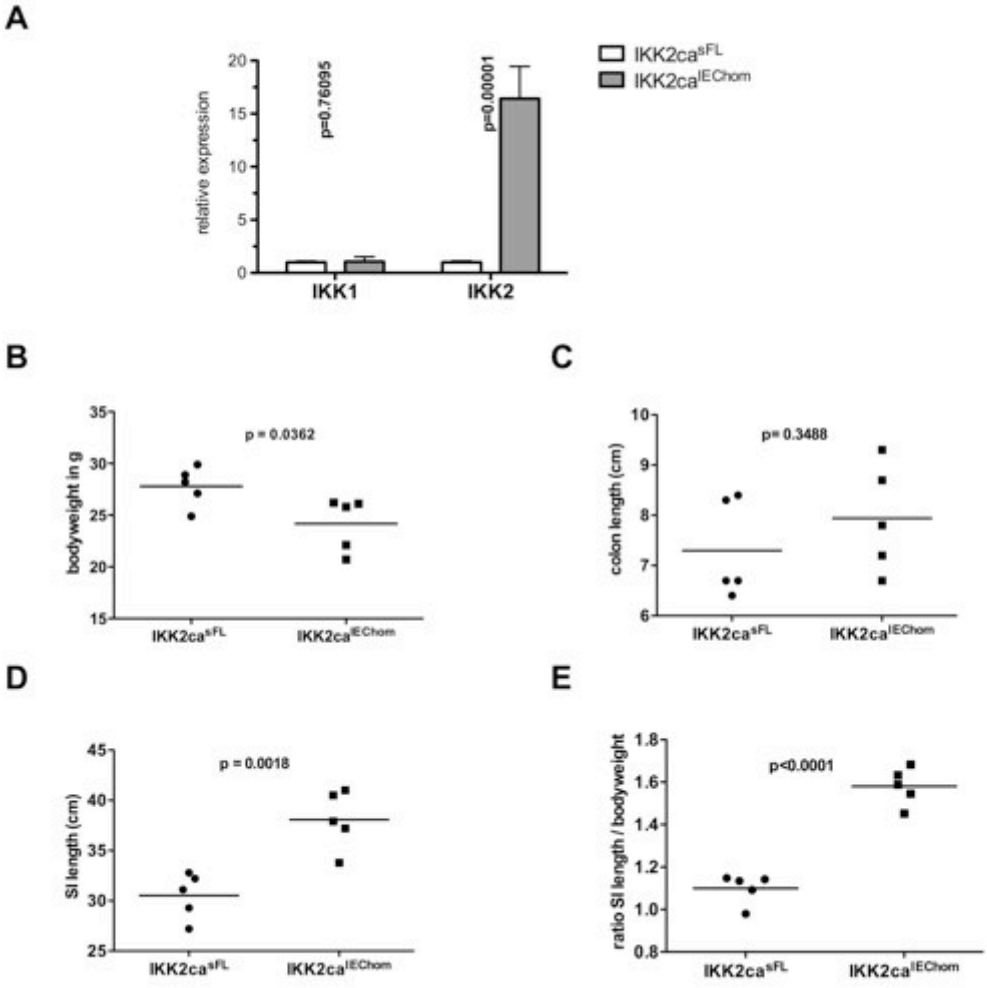

Supplementary Figure 2
Expression of IKK2, body weight and intestinal length of IKK2ca^{IEChom} mice
A. Quantitative RT-PCR showing elevated expression of IKK2 in colon IECs of IKK2ca^{IEChom} mice whereas IKK1 was not differentially expressed between genotypes (n = 5 per genotype; mRNA levels are presented as mean values ± SD).
B. Reduced body weight of male IKK2ca^{IEChom} mice at 10 weeks of age (n = 5 per genotype; horizontal line represents mean value).
C. No statistically significant difference in colon lengths was observed between IKK2ca^{sFL} and IKK2ca^{IEChom} male mice at 10 weeks of age (n = 5 per genotype; horizontal line represents mean value).
D. The length of the small intestine was significantly longer in the same 10 week old male IKK2ca^{IEChom} mice when compared to IKK2ca^{sFL} animals (n = 5 per genotype; horizontal line represents mean value).
E. The relative length of the small intestine compared to the body weight of each mouse was significantly higher in IKK2ca^{IEChom} mice (n = 5 per genotype; horizontal line represents mean value)

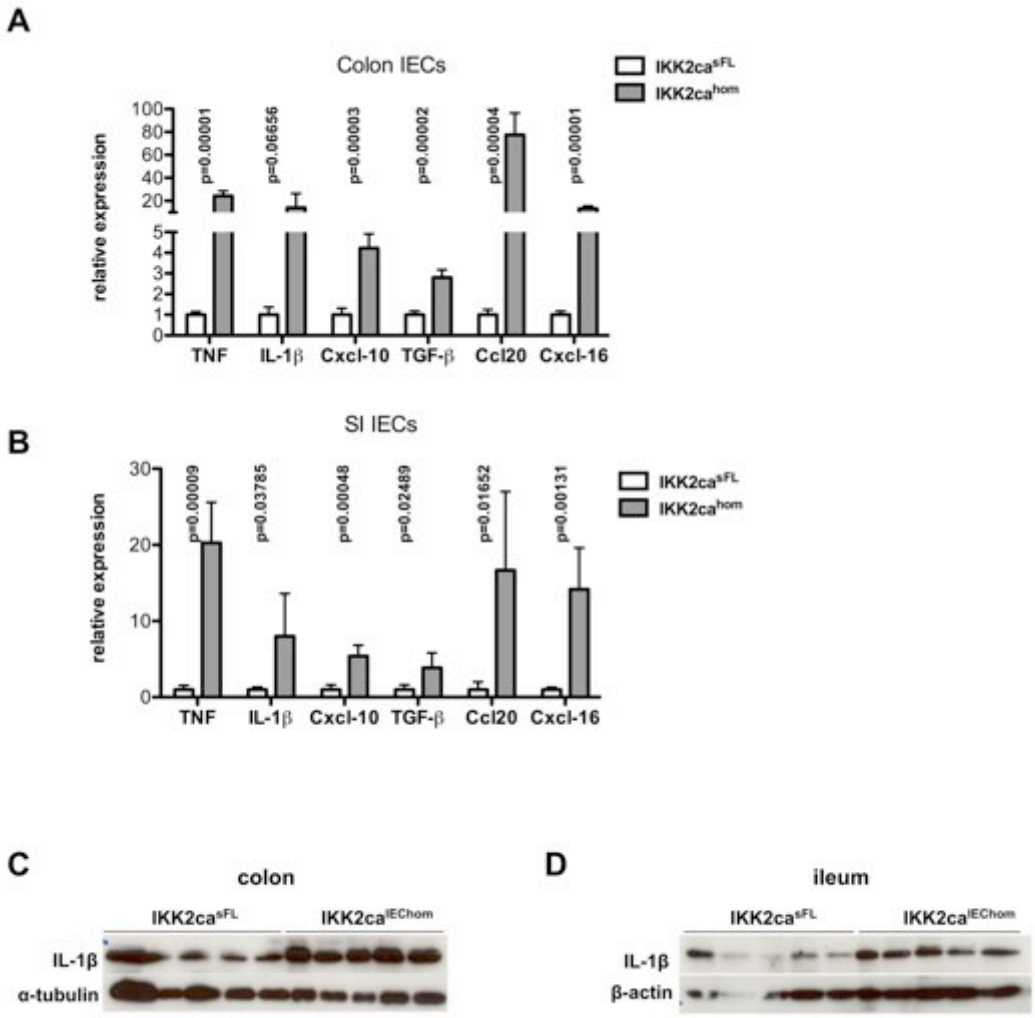

Supplementary Figure 3
Production of inflammatory mediators by intestinal epithelial cells of IKK2ca^{IEChom} mice
A. Quantitative RT-PCR analysis shows significantly elevated expression levels of inflammatory mediators in colonic IECs from 8-week-old IKK2ca^{IEChom} animals. (n=5 per genotype; mRNA levels are presented as mean ± SD)
B. Inflammatory molecules are expressed at higher levels in primary small intestinal IECs derived from IKK2ca^{IEChom} mice when compared SI IECs from IKK2ca^{sFL} control animals. (n=5 per genotype; mRNA levels are presented as mean ± SD)
C. WB analysis for IL-1β on whole colon tissue extracts indicating an increased abundance of IL-1β protein in the colon of IKK2ca^{IEChom} mice.
D. Increased amount of IL-1β protein in ileal extracts derived from IKK2ca^{IEChom} mice as assessed by WB analysis.

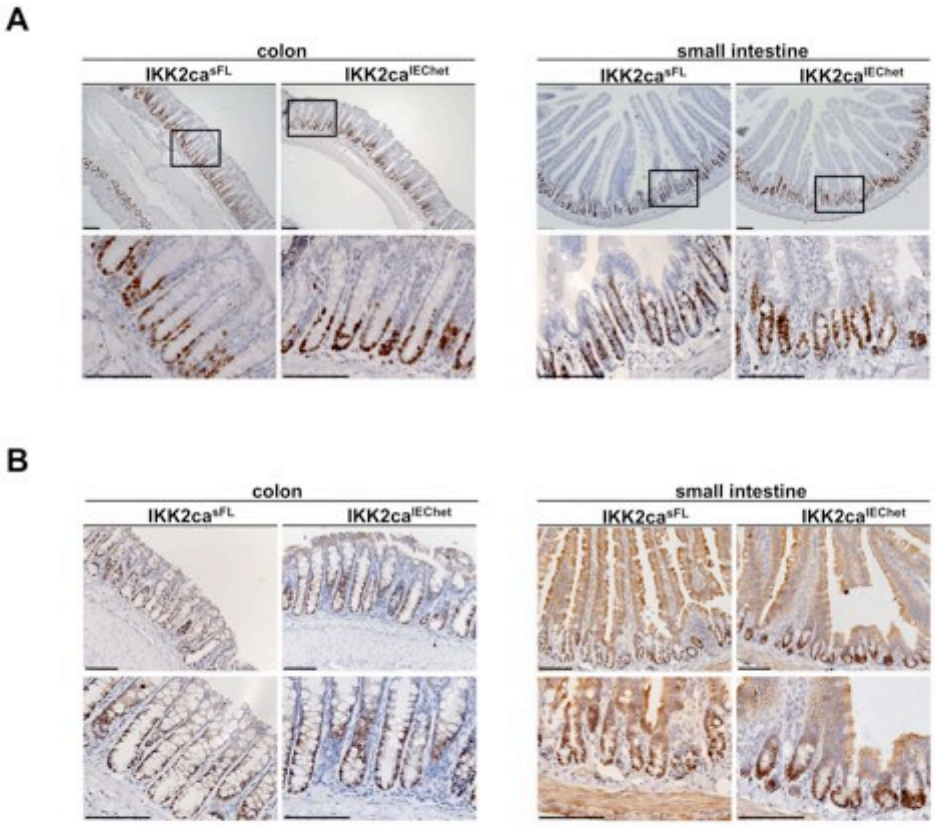

Supplementary Figure 4
No differences in Ki67 and Sox9 expression in IECs between IKK2ca^{sFL} and IKK2ca^{IEChet} mice

A. Ki67 immunohistochemical staining of sections from the colon and SI of 4-month-old animals did not reveal considerable differences between IKK2ca^{IEChet} and IKK2ca^{sFL} mice, consistent with the normal histology of these tissues as shown in figure 5B.

B. Sox9 immunohistochemical staining of sections from the colon and SI of 4-month-old animals did not reveal considerable differences between IKK2ca^{IEChet} and IKK2ca^{sFL} mice, consistent with the normal histology of these tissues as shown in figure 5B.

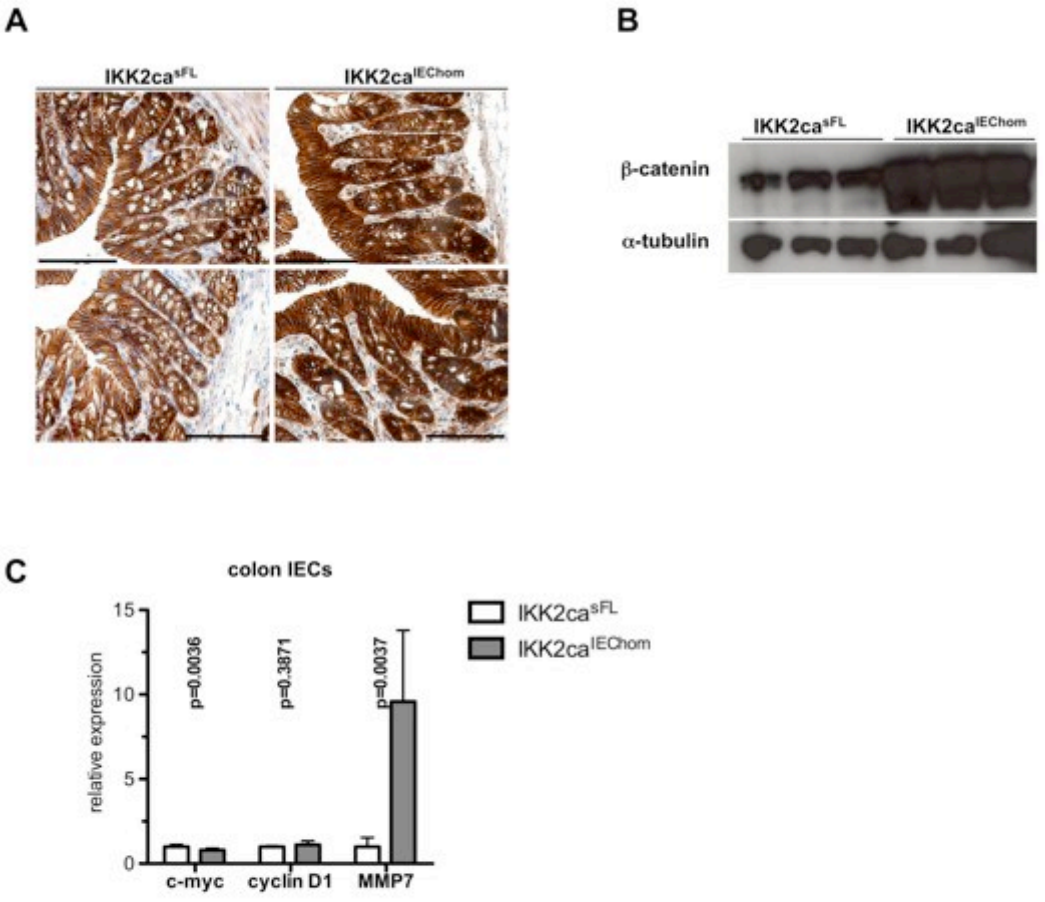

Supplementary Figure 5
Increased β-catenin levels in IKK2ca^{IEChom} mice
A. Immunohistochemical staining showing increased abundance of β-catenin protein in the colonic epithelium of 9-week-old IKK2ca^{IEChom} mice when compared to IKK2ca^{sFL} littermates. Pictures shown were taken from sections of IKK2ca^{sFL} and IKK2ca^{IEChom} colons that were cut at the same thickness and were placed on the same glass slides to make sure identical conditions were used for the staining.
B. Immunoblot analysis of protein extracts from small intestinal IECs from IKK2ca^{IEChom} mice revealed higher levels of β-catenin compared to IKK2ca^{sFL} IECs.
C. Quantitative RT-PCR analysis of selected Wnt target genes in colon IECs from IKK2ca^{sFL} and IKK2ca^{IEChom} mice. (mRNA levels are presented as mean ± SD; n=5 per genotype).
All scale bars represent 50 μm.